

Electrophilic ‘Umpolung’ Cyclizations of Alkynes
in the
Synthesis of Polycyclic Aromatic Hydrocarbons

by
Liam Britt

A thesis
presented to the University of Waterloo
in fulfillment of the
thesis requirements for the degree of
Master of Science
in
Chemistry

Waterloo, Ontario, Canada, 2021

© Liam Britt 2021

Author's Declaration

I hereby declare that I am the sole author of this thesis.

This is a true copy of the thesis, including any required final revisions, as accepted by my examiners.

I understand that my thesis may be made electronically available to the public.

Abstract

Polycyclic aromatic hydrocarbons (PAHs), such as acenes and phenacenes, are important structural motifs which have found great utility in the future of electronics as organic semi-conducting materials. Reliable methods of synthesizing PAHs, particularly the phenacene type, are limited; and modern techniques employ expensive transition metal catalysts. A less explored but potentially superior strategy involves utilizing hypervalent iodine methodology, avoiding the need for transition metal catalysts. In recent studies, a reaction was developed that could couple *ortho*-biphenylstyrenes intramolecularly in the synthesis of phenanthrenes using only a catalytic amount of iodotoluene, and *m*-CPBA as an oxidant. In this thesis, we investigate the mechanism of the rearrangement observed in this recently uncovered reaction, and further apply what we have learned toward a novel strategy for electrophilic ‘umpolung’ cyclizations of alkynes in the synthesis of fluorinated PAHs.

Acknowledgements

I would first like to extend my deepest gratitude to my supervisor, Dr. Graham Murphy, for all of his guidance and support, as well as patience and understanding throughout my time in Waterloo. His love for chemistry, creative spirit, and willingness to foster that in others has kept the fire burning in my spirit.

I would like to thank my committee members, Dr. Mike Chong and Dr. Eric Fillion for their continued guidance and commitment to excellence within the field. I would like to further extend my gratitude to Dr. Mike Chong who helped me find my path toward excellence, with lessons I will continue to learn for the rest of my life.

I would also like to thank my fellow colleagues in the Murphy lab, both past and present, from whom I have learned so much through endless discussions of chemistry and all else. In particular, I would like to thank those for the continued support in the writing, reviewing, and editing of my thesis: Avery To, Tristan Chidley, and Islam Jameel.

A special thanks to Dr. Zhensheng Zhao for his early work¹ and assistance in the lab during my first year on campus. I would also like to acknowledge the important work and assistance provided by Jalil Assoud with my X-ray crystallography samples. Furthermore, I would like to extend my sincere gratitude to Janet Venne for all her assistance at the NMR.

Lastly, I want to express my sincerest thanks and gratitude to the entire University of Waterloo and its Department of Chemistry for granting me the opportunity to complete my graduate studies, and for all their support and resources provided to me over the past few years.

Table of Contents

Author's Declaration	ii
Abstract	iii
Acknowledgements	iv
List of Figures	vii
List of Tables	viii
List of Abbreviations	ix
List of Schemes	x
Chapter 1: Introduction	1
1.1 Polycyclic Aromatic Hydrocarbons	1
1.2 Hypervalent Iodine	2
1.3 Iodonium Salts	7
1.4 Catalytic Synthesis of Phenanthrene using Hypervalent Iodine Reagents	10
Chapter 2: Mechanistic Studies	13
2.1 Background: Vinylene Phenonium Cation	13
2.2 Mechanistic Studies of the HVI Catalyzed Reaction	16
2.3 Synthesis of Styrenes and Epoxide Control Reactions	24
2.4 Synthesis of <i>cis</i> - and <i>trans</i> - β -methyl Styrene Isomers	27
2.5 Vinyl (aryl)iodonium Salts	30
2.6 Discussion	35
2.7 Experimental Procedures for Chapter 2	41
2.7.1 Synthesis of 2-(4-methylphenyl)benzaldehyde (46)	42
2.7.2 Synthesis of 4'-methyl-2-(prop-1-en-1-yl)-1,1'-biphenyl	43
2.7.3 Synthesis of epoxide: 2-methyl-3-(4'-methyl-[1,1'-biphenyl]-2-yl)oxirane	44
2.7.4 Synthesis of 2-ethynyl-4'-methyl-1,1'-biphenyl (49)	45
2.7.5 Alternate synthesis of 2-ethynyl-4'-methyl-1,1'-biphenyl (49)	46
2.7.6 General procedure for phenanthrene synthesis	47
2.7.7 General procedure for control reactions with epoxide	48
2.7.8 Synthesis of <i>cis</i> -4'-methyl-2-(prop-1-en-1-yl)-1,1'-biphenyl	48
2.7.9 Synthesis of <i>trans</i> -4'-methyl-2-(prop-1-en-1-yl)-1,1'-biphenyl	50
2.7.10 Synthesis of 2-bromo-4'-methyl-1,1'-biphenyl	50

2.7.11	Synthesis of (<i>Z</i>)-4,4,5,5-tetramethyl-2-(2-(4'-methyl-[1,1'-biphenyl]-2-yl)prop-1-en-1-yl)-1,3,2-dioxaborolane (Z-53).....	51
2.7.12	Synthesis of (<i>E</i>)-4,4,5,5-tetramethyl-2-(2-(4'-methyl-[1,1'-biphenyl]-2-yl)prop-1-en-1-yl)-1,3,2-dioxaborolane.....	52
2.7.13	General procedure for preparation and reaction of <i>E</i> - and <i>Z</i> - iodonium salts	53
2..14	Synthesis of (<i>E</i>)-(2-(4'-methyl-[1,1'-biphenyl]-2-yl)vinyl-1-D)(<i>p</i> -tolyl)iodonium tetrafluoroborate (E-33).....	54
Chapter 3: Umpolung Electrophilic Cyclizations		57
3.1	Background: Phenacenes.....	57
3.2	Fluorovinyl (aryl)iodonium salts.....	60
3.3	Results	64
3.4	Discussion	75
3.5	Future directions.....	81
3.6	Experimental Procedures for Chapter 3	86
3.6.1	Synthesis of (2-bromophenyl)ethynyl) trimethylsilane	86
3.6.2	Synthesis of (4'-methyl-[1,1'-biphenyl]-2-yl)ethynyl) trimethylsilane.....	87
3.6.3	Synthesis of alkynyl trifluoroborate (88).....	88
3.6.4	General procedure for synthesis of (<i>Z</i>)-(2-fluoro-2-(4'-methyl-[1,1'-biphenyl]-2-yl)vinyl)-(p-tolyl) iodonium tetrafluoroborate (Z-90) from alkynyl trifluoroborate (88)	89
3.6.5	General procedure for conversion of vinyl iodonium salt to phenanthrene (91a)..	90
3.6.6	Synthesis of (4'-methyl-[1,1'-biphenyl]-2-yl)ethynyl)(p-tolyl)iodonium tetrafluoroborate (89).....	91
References.....		93
Appendix I – X Ray Crystal Structures		96
3.6.7	Vinyl (aryl)iodonium trifluoroacetate (92)	96
3.6.8	Fluorovinyl (aryl)iodonium tetrafluoroborate (Z-90)	111

List of Figures

Figure 1.1: Polycyclic aromatic hydrocarbons (PAHs)	1
Figure 1.2: Basic geometry of aryl- λ^3 -iodanes.....	3
Figure 1.3: Examples of common hypervalent iodine (III) compounds.	4
Figure 1.4: 3-center-4-electron bonding model in hypervalent iodine (III) compounds	5
Figure 1.5: Common hypervalent iodine reagents and aryl iodonium salts.	8
Figure 3.1: X-ray diffraction crystal structure model of 92 as a dimer.	66
Figure 3.2: X-ray diffraction crystal structure of Z-90	74

List of Tables

Table 2.1: Probing the reactivity of epoxide (47) in the HVI catalyzed reaction.	26
Table 2.2: Screening of <i>cis/trans</i> isomers under the reaction conditions	29
Table 2.3: Screening of <i>E</i> - and <i>Z</i> -iodonium salts in reaction conditions.....	35
Table 3.1: Attempted fluorination of 92	67
Table 3.2: Fluorination of alkynyl iodonium BF ₄ derived from alkynyl-TMS.	69
Table 3.3: Optimization of <i>Z</i> - 90 from alkynyl trifluoroborate (88) starting material.	71
Table 3.4: Further optimization of <i>Z</i> - 90 synthesis.....	72
Table 3.5: Solvent and temperature screening in thermal decomposition of <i>Z</i> - 90	75

List of Abbreviations

Ar	Aromatic ring
DCE	Dichloroethane
DCM	Dichloromethane
DME	Dimethoxyethane
DMF	Dimethylformamide
DMSO	Dimethylsulfoxide
EAS	Electrophilic aromatic substitution
ESI	Electrospray ionization
Eq.	Molar equivalent
HOMO	Highest occupied molecular orbital
HRMS	High resolution mass spectrometry
HVI	Hypervalent iodine
IR	Infrared spectroscopy
IUPAC	International Union of Pure and Applied Chemistry
L	Ligand
LG	Leaving group
<i>m</i> -CPBA	meta-chloroperoxybenzoic acid
m.p.	Melting point
m/z	Mass-to-charge ratio
MS	Mass spectrometry
Me	Methyl
NMR	Nuclear magnetic resonance
NR	No reaction
<i>p</i> -Toll	para-iodotoluene
PAHs	Polycyclic aromatic hydrocarbons
PFA	Perfluoroalkoxy alkanes
PIFA	Phenyliodine bis(trifluoroacetate)
PTFE	Polytetrafluoroethylene
PhI	Iodobenzene
PhIO	Iodosyl benzene
RT	Room temperature
SN	Nucleophilic substitution
THF	Tetrahydrofuran
TLC	Thin layer chromatography
TolIF2	Iodotoluene difluoride
Wt %	Weight percent

List of Schemes

Scheme 1.1: Ligand exchange pathway of λ^3 -iodane, associative -ate complex.....	6
Scheme 1.2: Mechanisms of λ^3 -iodane reactivity	7
Scheme 1.3: Arylation of silyl enol ether in the total synthesis of (\pm)-tabersonine.....	8
Scheme 1.4: Preparation of vinyl (aryl)iodonium salts from vinyl boronic acids, stannanes, and silanes.....	9
Scheme 1.5: Examples of aromatic C-C bond couplings mediated by PIFA.	10
Scheme 1.6: Catalytic oxidative alkene coupling of arenes in the synthesis of phenanthrenes. ..	11
Scheme 1.7: Coupling of arenes with electron donating substituents and electron-withdrawing substituents.....	11
Scheme 1.8: Differences in yield of <i>cis</i> - and <i>trans</i> -isomers.	12
Scheme 1.9: α -methyl styrene substrate producing a mixture of regioisomers.	12
Scheme 2.1: Synthesis of phenanthrene by decomposition of vinyl (aryl)iodonium salt (20).	13
Scheme 2.2: Solvolysis of <i>E</i> - 22 produced an equal mixture of regioisomers 24a and 24b	14
Scheme 2.3: Rearrangement products of <i>E</i> - 25 and <i>Z</i> - 25 iodonium salt.	15
Scheme 2.4: Mixture of isomers A and B in β -methyl styrene substrate.	16
Scheme 2.5: Proposed vinylene phenonium intermediate in phenanthrene synthesis.....	17
Scheme 2.6: Umpolung electrophilic addition reactions of styrenes and iodine(III) reagents to give 1,2-disubstituted alkanes.	17
Scheme 2.7: Elimination to form vinyl iodonium salt.....	18
Scheme 2.8: Proposed reaction with deuterated <i>E</i> - 33	20
Scheme 2.9: Proposed reactions with methyl isomers <i>E</i> - 32 and <i>Z</i> - 32	20
Scheme 2.10: Out-of-plane vinylic S_N2 with retention of configuration.....	21
Scheme 2.11: Intermolecular vinylic S_N2 reaction with halides and vinyl (aryl)iodonium salts, inversion of stereoconfiguration.	22
Scheme 2.12: Nucleophilic addition-elimination mechanism with sulfonyl substituted vinyl (aryl)iodonium salt. Retention of stereoconfiguration.....	22
Scheme 2.13: Double substitution of chlorovinyl (aryl)iodonium salt with sulfonate through double Ad_N -E mechanism.	23
Scheme 2.14: Synthesis of β -methyl styrene (31) and epoxide (47) as a <i>cis/trans</i> mixture.	25
Scheme 2.15: Preparation of terminal alkyne (49)	28
Scheme 2.16: Unsuccessful semi-reduction of alkyne.	28
Scheme 2.17: Synthesis of <i>cis</i> - 31 by semi-reduction of 50 using P2-nickel.	28
Scheme 2.18: Palladium(II) catalyzed isomerization of styrenes to obtain <i>trans</i> - 31	29
Scheme 2.19: Retrosynthesis of iodonium salts <i>E</i> - 53 and <i>Z</i> - 53	31
Scheme 2.20: Preparation of <i>Z</i> - 53 and associated precursors.....	32
Scheme 2.21: Preparation of 2-bromobiaryl (50)	33
Scheme 2.22: Attempts at bromoboration of alkyne (49).....	33
Scheme 2.23: Copper(I) catalyzed carboborylation in production of <i>E</i> - 53	33
Scheme 2.24: Proposed vinylene phenonium intermediate 32-I produced from <i>E</i> - 32	36

Scheme 2.25: Out-of-plane vinylic S _N 2 with retention of configuration.....	37
Scheme 2.26: Complete reaction with catalytic cycle and suggested mechanism for alkene-arene coupling reaction.....	38
Scheme 2.27: Synthesis of deuterated vinyl (aryl)iodonium salt <i>E</i> - 33	39
Scheme 2.28: Decomposition of <i>E</i> - 33 to yield ² H- B as a single isomer.	40
Scheme 2.29: HRMS of the iodonium salt water adduct 33-I and fragment vinyl cation in MS/MS mode.....	40
Scheme 2.30: Out-of-plane vinylic S _N 2 with retention of stereochemistry.....	41
Scheme 3.1: Synthesis of acene (67) by Elb's reaction.....	57
Scheme 3.2: Synthesis of phenacene (65) via ruthenium catalyzed <i>o</i> -directed C-H coupling.....	58
Scheme 3.3: Synthesis of picene and dibenzo[a,h]anthracene by alkene arene coupling.	59
Scheme 3.4: Synthesis of fluorinated phenacene (72) via a palladium catalyzed cyclization.....	60
Scheme 3.5: Preparation of triflyl vinyl iodonium triflates and fluorovinyl iodonium tetrafluoroborates from alkynes.....	61
Scheme 3.6: Umpolung electrophilic cyclization of alkynes in the synthesis of phenanthrenes. 61	
Scheme 3.7: A potential one-pot synthesis of monofluorinated picene (62) by iodonium salt mediated alkene arene ring closure.....	62
Scheme 3.8: Known synthetic methods to <i>Z</i> - and <i>E</i> -2-fluoro vinyl(phenyl)iodonium salts.	63
Scheme 3.9: Proposed synthesis of fluorophenanthrenes from tetrafluoroborate salt (88).....	64
Scheme 3.10: Proposed synthesis of fluorophenanthrenes from alkyne (49) and TolIF ₂	64
Scheme 3.11: Attempted syntheses of <i>Z</i> - 90 from terminal alkyne (49) with TolIF ₂	65
Scheme 3.12: Attempted synthesis of alkynyl (phenyl)iodonium salt (89) from 49	65
Scheme 3.13: Synthesis of alkynyl (phenyl)iodonium trifluoroacetate (92).....	66
Scheme 3.14: Preparation of alkynyl silane (95) in fast 2-step process.	68
Scheme 3.15: Synthesis of alkynyl trifluoroborate (88) from alkyne 95	70
Scheme 3.16: HRMS of <i>Z</i> - 90 and fragment ions detected in MS-MS mode.....	73
Scheme 3.17: Deprotonation of vinyl (aryl)iodonium salt (75) and α -elimination for generation of vinylidene carbene (76).....	76
Scheme 3.18: α -elimination in reaction with vinyl iodonium and TBAF to produce alkyne.....	77
Scheme 3.19: Decompositions of vinyl (aryl)iodonium salts which lead to a single isomer.	78
Scheme 3.20: Resonance stabilization by fluorine in carbene and carbocations.....	79
Scheme 3.21: Iodonium ylide resonance structures of <i>Z</i> - 90	80
Scheme 3.22: Electronic structure and reactivity of <i>Z</i> - 90 2-fluorovinyl (aryl)iodonium salt.	81
Scheme 3.23: Role of H-F hydrogen bonding in Et ₃ N•5HF for the synthesis of <i>E</i> - 90 from 49 ... 83	
Scheme 3.24: Preliminary result in the direct synthesis of <i>E</i> - 90 from 49	84
Scheme 3.25: Demonstration of one-pot synthesis of 91a using <i>in situ</i> generated TolIF ₂	85
Scheme 3.26: Proposed scalable process for the synthesis of 91a	85

Chapter 1: Introduction

1.1 Polycyclic Aromatic Hydrocarbons

Polycyclic aromatic hydrocarbons (PAHs) (Figure 1.1) are a widespread and ubiquitous structure in nature. In fact, up to 20% of the carbon in the universe may be associated with PAHs.² Phenanthrene type PAHs are found in natural products and alkaloids,³ while acene and phenacene type PAHs have recently been shown to be ideal molecules for organic electronics, especially in organic field-effect transistors⁴ (OFETs), light emitting diodes⁵ (OLEDs), and as superconductors.⁶

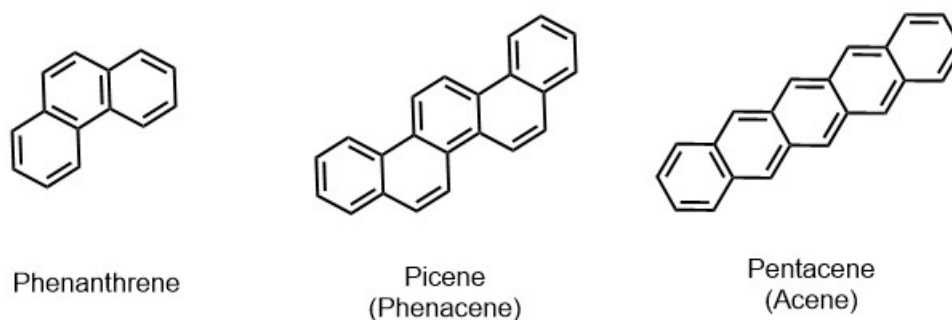


Figure 1.1: Polycyclic aromatic hydrocarbons (PAHs)

Many methods have been developed toward the synthesis of the phenanthrene scaffold. Traditional approaches of phenanthrene synthesis include metal catalyzed⁷ or photocyclic biaryl coupling of *cis*-stilbenes,⁸ or olefination of biphenyl styrenes by McMurry coupling,⁹ both of which are restricted by the need of stoichiometric reagents or a limited substrate scope. Many more methods have been developed using transition metal catalysts. These methods employ metals such as ruthenium, rhodium, and many others to perform carbonyl olefin metathesis,¹⁰ alkyne annulation,¹¹ cycloisomerization,¹² carbene dimerization,¹³ or Grubbs ring-closing metathesis.¹⁴

These transition metals form highly effective catalysts¹⁵ but are often expensive, difficult to recover for reuse, or are prepared from rare minerals.

In this thesis, novel hypervalent iodine mediated reactivity in the synthesis of phenanthrenes will be explored. We will probe the mechanism of this reactivity and extend it to the synthesis of functionally useful heteroatom substituted PAHs. With further development, this reactivity could provide a simple, scalable, metal-free reaction to access synthetically challenging PAHs.

1.2 Hypervalent Iodine

Hypervalent iodine (HVI) reagents have recently drawn significant interest¹⁶ as cheaply produced reagents with a wide range of reactivity in mild conditions, in some ways mimicking the reactivity of late transition metal catalysts. At the most basic level, HVI most closely mimics the mild oxidizing heavy metals, replacing mercury and lead salts. However with a wide diversity of structure and reactivity of HVI compounds, their reactivity extends far beyond these metals and consequently have extensive use, especially in total synthesis.¹⁷

The first HVI compound reported was phenyliodine(III) dichloride (PhICl_2), discovered by Willgerodt in 1886 after passing chlorine gas through a solution of iodobenzene in chloroform.¹⁸ After the publication of PhICl_2 , it remained an obscure compound and little progress was made in the area of HVI chemistry. Nearly 100 years later, the 1980's saw a surge of interest in HVI chemistry with the development of many new HVI compounds. This resurgence was attributed to their remarkable properties as synthetic reagents, displaying a wide range of chemical reactivity, mild reaction conditions, and ease of handling. HVI reagents are cheap to manufacture and the by-products are often recyclable or environmentally benign, which is a highly desirable attribute in

the chemical industry. Marking this progress, the first review of HVI reagents for carbon-carbon bond formation was written by Moriarty in 1990.¹⁹

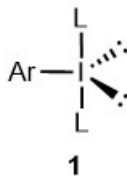


Figure 1.2: Basic geometry of aryl- λ^3 -iodanes

HVI compounds are referred to as iodanes, and use a λ^n notation for naming, where n describes the oxidation state of the central iodine atom. Aryl- λ^3 -iodanes are the most common type of aryl- λ^3 -iodane used in organic synthesis. The aryl- λ^3 -iodanes consist of an aryl iodide with an iodine(III) oxidation state, where the iodine is bonded with a heteroatom ligand(s). Aryl- λ^3 -iodanes have a T-shaped geometry with the arene and lone pairs occupying the equatorial positions. The two heteroatoms sit in the apical positions to form the linear hypervalent L-I-L bond (Figure 1.2, **1**). These compounds are relatively stable reagents and can usually be stored at room temperature or in the freezer. Alkyl- λ^3 -iodanes are unstable, and typically only exist as transient intermediates or at cryogenic temperatures.¹⁶ Iodanes require ligands with high electronegativity participating in the hypervalent L-I-L bond to allow stability at room temperature. Other examples of common aryl- λ^3 -iodane reagents include phenyliodine(III) diacetate²⁰ (PIDA) (Figure 1.3, **3**), which serves as an acetoxylation reagent; phenyliodine(III) bis(trifluoroacetate) (PIFA), (**4**) which is a more reactive version of PIDA typically used as an oxidant in HVI mediated transformations; iodotoluene difluoride (TolIF₂), (**5**) which serves as an electrophilic fluorinating agent and a bench stable surrogate of elemental fluorine; iodosobenzene (PhIO), (**6**) which is an aryl- λ^3 -iodane with only one heteroatom substituent, as oxygen can carry

a second charge providing an ylide. Consequently, iodosobenzene forms polymeric units which are insoluble in common organic solvents like dichloromethane, chloroform and diethyl ether.

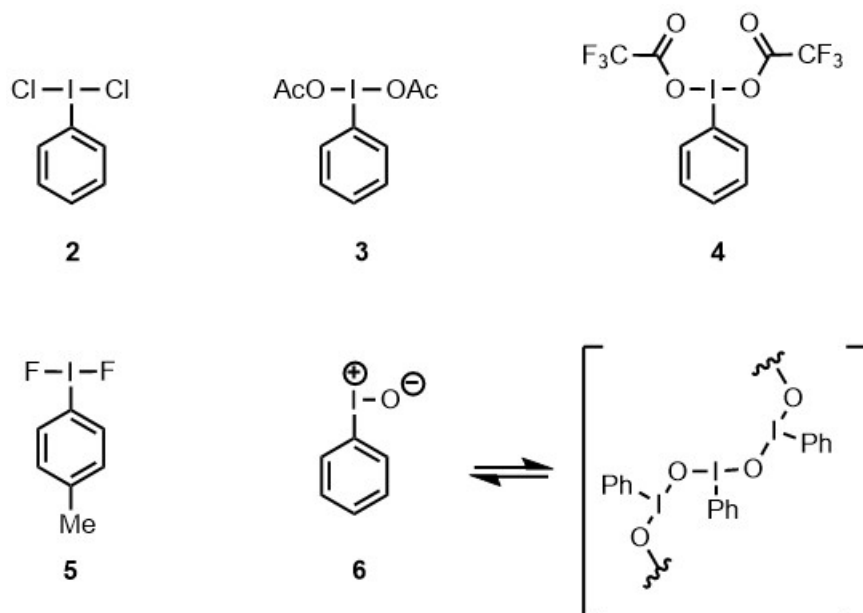


Figure 1.3: Examples of common hypervalent iodine (III) compounds

The reactivity of aryl- λ^3 -iodanes and other hypervalent iodine compounds can be best explained in relation to the late transition metals. Transition metal reactivity is in part due to their properties as large electrophilic atoms with weakly bound electrons, which allow them to move between oxidation states with relatively low energy requirements. Transition metals often form coordination complexes by interaction with donor ligands or solvent, forming dative bonds by accepting a pair of electrons into an empty orbital of the metal. Next to xenon, iodine is the heaviest stable non-metal element in the p-block. While considered a non-metal, it displays some metalloid-like properties and can form charge-transfer complexes.

Iodine is highly polarizable; its valence electrons rest in high energy orbitals and have a dispersed electron cloud due to the shielding effect of the core electrons. As a result, iodine has a relatively low electronegativity (2.66) (Pauling) compared to other halogens, such as bromine

(2.96). It is more comparable to that of gold (2.54) and carbon (2.55). With these attributes, certain alkyl and aryl iodides are capable of being oxidized under mild conditions and forming a stable hypervalent bond, which significantly alters the properties of the central iodine atom. In terms of molecular orbital theory, the hypervalent bond is modelled as a 3-center-4-electron bond.²¹ Iodine contributes two electrons from one of its lone pairs, while the other two electrons come from the external ligands or oxidant. The highest occupied molecular orbital (HOMO) of this bond is a non-bonding orbital, this results in a highly polarized bonding mode where the electron density is concentrated on the ligands and minimized on the central iodine atom (Figure 1.4). This bond polarization is comparable to the common metal-ligand interaction and can be functionally viewed as a form of dative bonding. It differs in that the system has a bond order of one shared across the 3-atom system. The hypervalent bonds are significantly longer and weaker compared to the valence bonds and require ligands capable of stabilizing a negative charge. The bond can also be shared unequally if a combination of ligands is used.

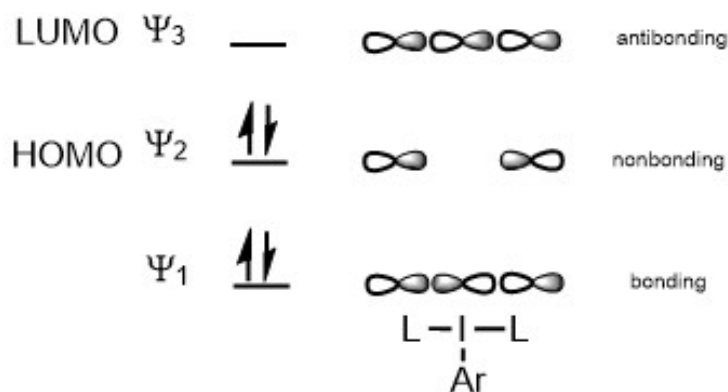
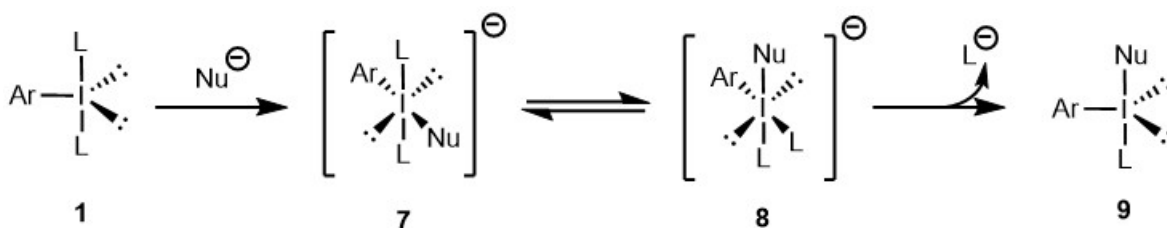


Figure 1.4: 3-center-4-electron bonding model in hypervalent iodine (III) compounds

The two fundamental transformations associated with λ^3 -iodanes are that of ligand exchange and reductive elimination. Ligand exchange occurs by an associative pathway with negatively charged ligands or nucleophiles that coordinate around the electrophilic iodine center

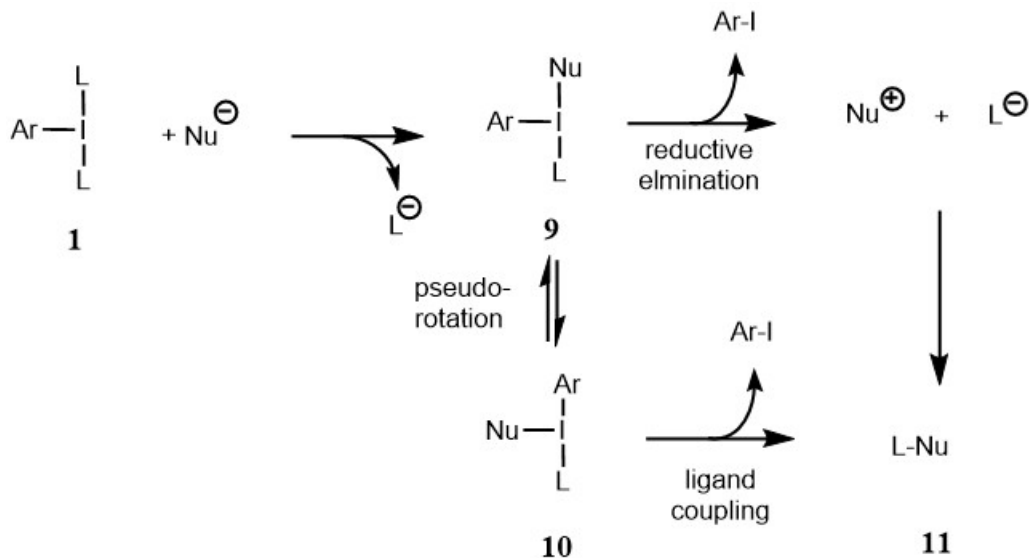
to generate a transitory square-planar charge complex (Scheme 1.1, **7**) comparable to the ligand sphere of transition metal chemistry. However, these proposed ‘-ate complexes’ are unstable and have not been isolated. The complex is able to undergo a pseudo-rotation (**8**) and ligand dissociation to give the new λ^3 -iodane (**9**).



Scheme 1.1: Ligand exchange pathway of λ^3 -iodane, associative -ate complex

The new λ^3 -iodane complex **9** is able to undergo reductive elimination and return to its ground state while creating a new covalent bond between the nucleophile and ligand (Scheme 1.2, **11**). The reaction is driven forward if **9** is unstable compared to **1** (Scheme 1.1). The precise mechanism of the ligand coupling is not clear. The λ^3 -iodane **9** may undergo another pseudo-rotation so that it brings the ligands close in space (90°) (**10**) during the bond breaking and bond forming process, or it may eliminate directly to give the aryl iodide and create a transient ion pair (Nu^+ and L^-), which quickly forms the ligand-nucleophile coupled product (Scheme 1.2, **11**).

The process is energetically favourable because it transforms the hypervalent iodine (III) atom to its standard valence (I). In this description, the nucleophile has its charge reversed, demonstrating the umpolung nature of hypervalent iodine reactivity.



Scheme 1.2: Mechanisms of λ^3 -iodane reactivity

1.3 Iodonium Salts

A special variety of aryl- λ^3 -iodanes used in synthesis are iodonium salts.²² Iodonium salts typically consist of a hypervalent aryl iodide with one carbon R-group ligand (Figure 1.5, R = Aryl **12**, R = vinyl **13**, R = alkynyl **14**), and an opposing ligand which acts as a counterion, (X = BF₄, OTf) designating the name iodonium salt. In accordance with its theoretical structure, X-ray data shows that iodonium salts are a type of λ^3 -iodane, with trigonal bipyramidal geometry (T-shape) and R-I-Ar bond angle close to 90 degrees. X-ray data also shows significant secondary bonding between the counterions.²¹ The most common type of iodonium salt are the diaryliodonium salts; they are used as electrophilic arylating agents in conjunction with heterocycles, silyl enol ethers, and other nucleophiles.²³ They are bench stable reagents and the aryl R-group is sufficiently electron-withdrawing to stabilize the negative charge in the hypervalent bond. A good example of the synthetic utility of a diaryliodonium salt is in the total synthesis of (\pm)-tabersonine (Scheme 1.3),²³ where the silyl enol ether **15** was arylated using the diaryliodonium reagent **16** transferring

the most electron deficient arene to furnish **17** in 94% yield. The high reactivity of these compounds is explained by the hypernucleofugality of the aryl iodide leaving group, which is approximately 10^{12} times greater than iodide (I⁻), and 10^6 greater than that of triflate (TfO⁻).²⁴ Other iodonium salts, such as vinyl (aryl)iodoniums and alkynyl (aryl)iodoniums, contain a carbon ligand and possess a similar reactivity as ligand transfer reagents.

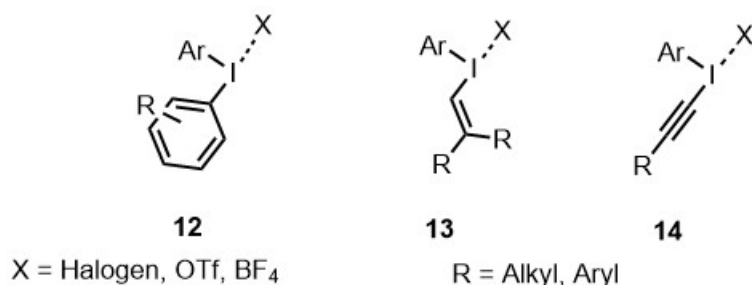
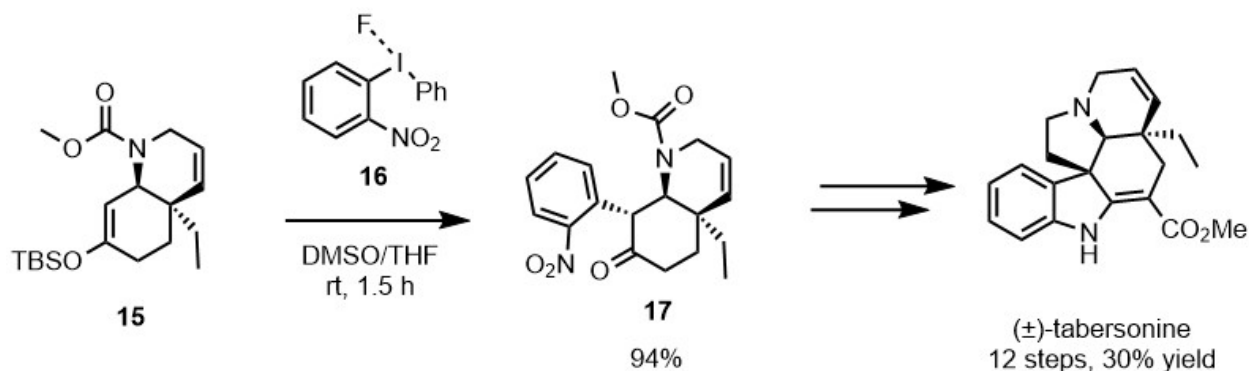
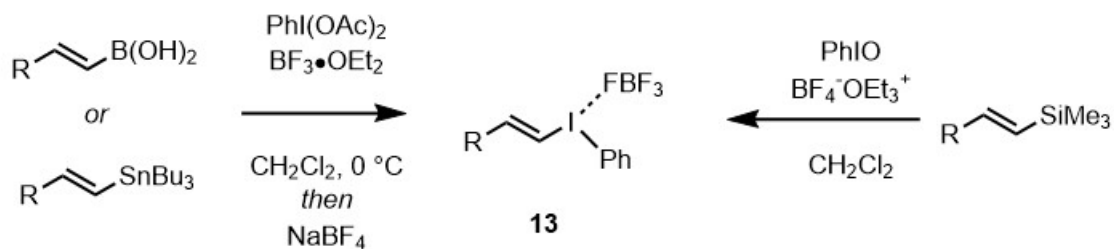


Figure 1.5: Common hypervalent iodine reagents and aryl iodonium salts



Scheme 1.3: Arylation of silyl enol ether in the total synthesis of (±)-tabersonine

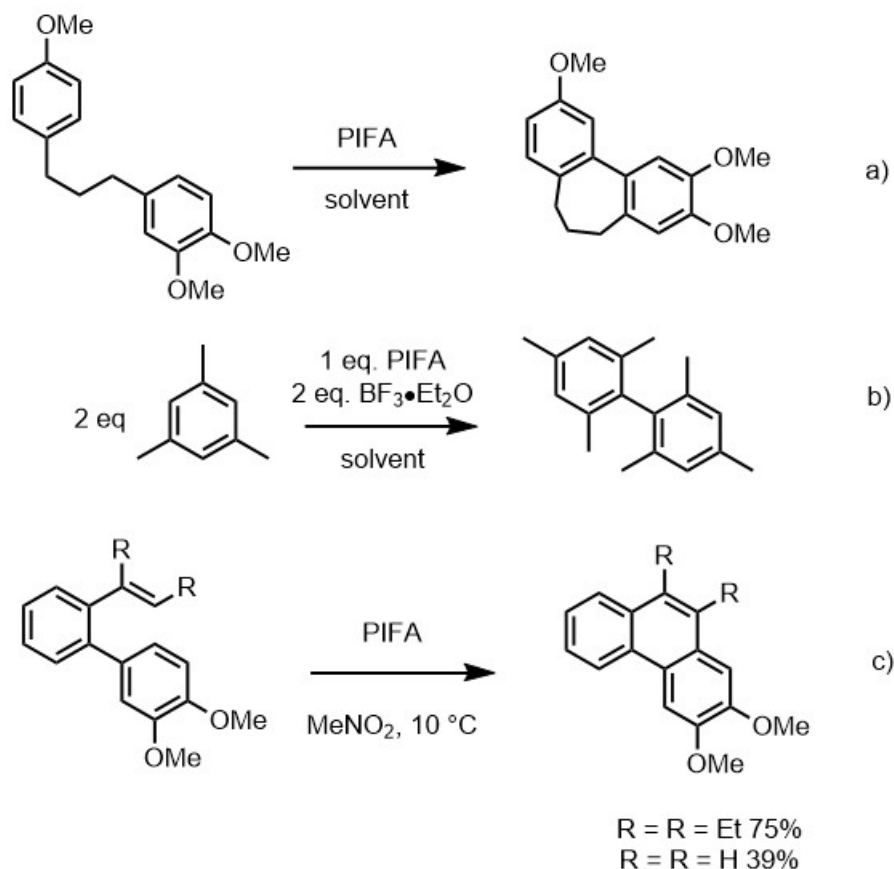
Vinyl (aryl)iodonium salts have typically seen less synthetic use in part due to their lower stability than the diaryliodonium salts, and their difficulty of preparation (Scheme 1.4, **13**). They are often prepared from vinyl silanes,²⁷ vinyl boronic acids²⁸ or vinyl stannanes²⁹ with silanes suffering from low yields and the need of excess reagents, and the latter two, which are already standalone precursors for Suzuki and Stille couplings (Scheme 1.5).¹⁵



R = alkyl, aryl

Scheme 1.4: Preparation of vinyl (aryl)iodonium salts from vinyl boronic acids, stannanes, and silanes

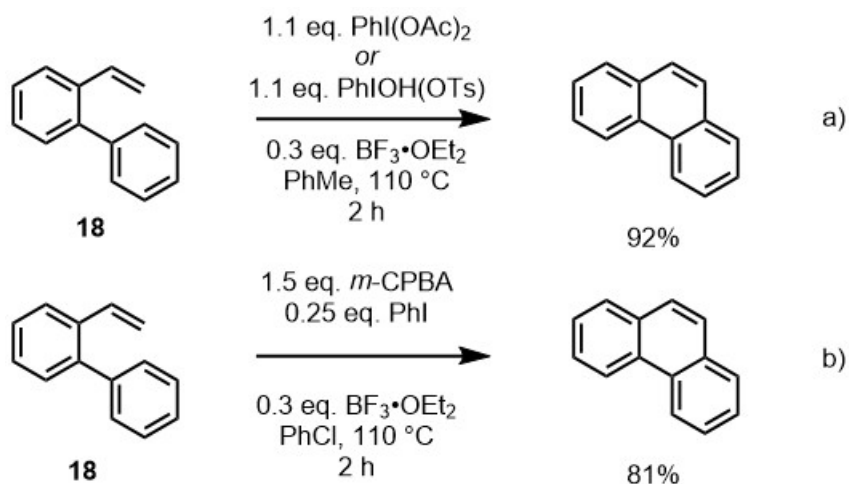
Hypervalent iodine has been observed to mediate oxidative biaryl coupling in electron rich systems both intramolecularly³⁰ (Scheme 1.5, a) and intermolecularly³¹ (Scheme 1.5, b) in sterically congested arenes. Recently, a paper was published describing the PIFA mediated intramolecular oxidative coupling of alkenes with electron rich arenes in the synthesis of phenanthrenes (Scheme 1.5, c).³² Good yields were obtained with substituted styrenes, while yields with the unsubstituted styrene were moderate.



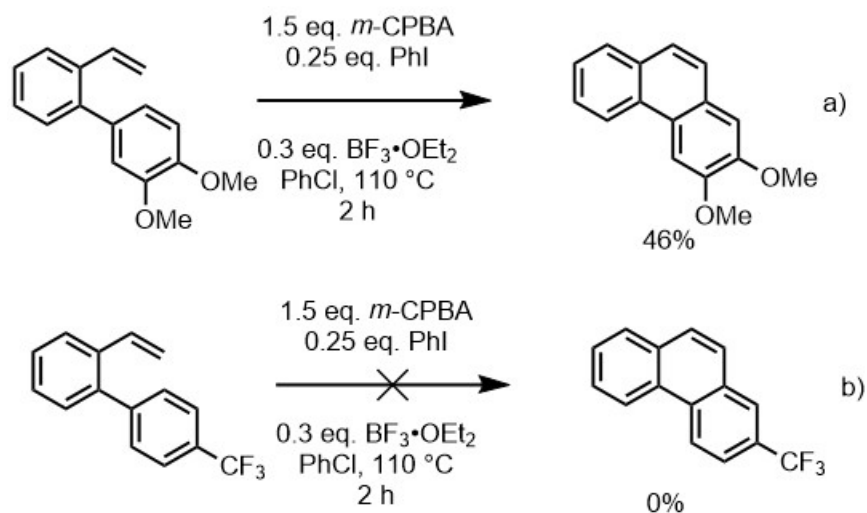
Scheme 1.5: Examples of aromatic C-C bond couplings mediated by PIFA

1.4 Catalytic Synthesis of Phenanthrene using Hypervalent Iodine Reagents

In the Murphy lab, it was found that the reaction with the unsubstituted *ortho*-phenyl styrene (Scheme 1.6, **18**) could proceed in excellent yield with phenyliodonium diacetate $\text{PhI}(\text{OAc})_2$ or Koser's reagent ($\text{PhI}(\text{TsO})\text{OH}$) and boron trifluoride diethyl etherate ($\text{BF}_3 \cdot \text{OEt}_2$) as a Lewis acid (Scheme 1.6, a). It was then found that this reaction could be carried out with a catalytic amount of iodobenzene and an oxidant, in good yields (Scheme 1.6, b). Electron rich substituents often gave good yields (Scheme 1.7, a), but with strong electron-withdrawing substituents on the *ortho*-arene the reaction failed (Scheme 1.7, b).

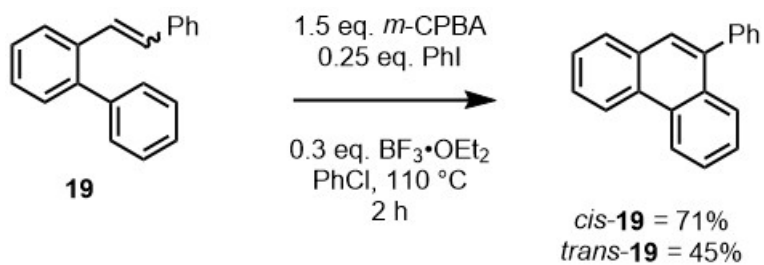


Scheme 1.6: Catalytic oxidative alkene coupling of arenes in the synthesis of phenanthrenes

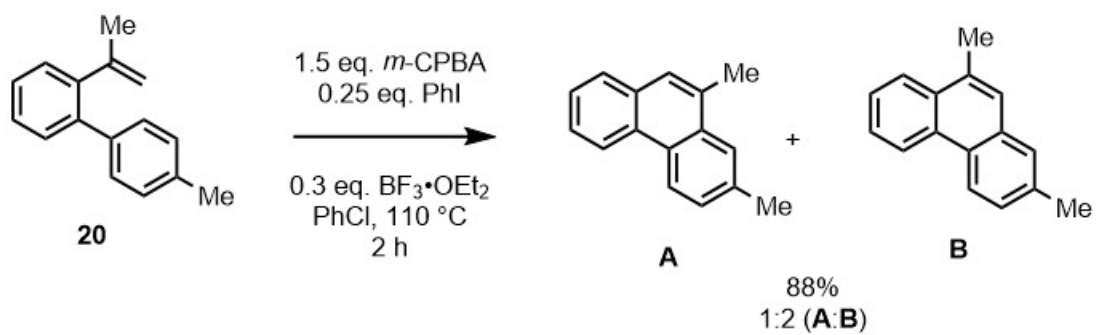


Scheme 1.7: Coupling of arenes with electron donating substituents and electron-withdrawing substituents

Interestingly, it was found that *cis*- and *trans*-alkenes gave different yields (Scheme 1.8, *cis*-**19**, *trans*-**19**), and unsymmetrical substrates provided a mixture of isomers (Scheme 1.9, **20**). While Breder only published the reaction of *trans*-alkenes, and with unsymmetrical examples, Breder reported only a single isomer (Scheme 1.5, c).³² This, along with the harsher reaction conditions (110 °C in PhCl and BF₃·OEt₂ vs 10 °C in MeNO₂) leads us to believe that our reaction must be proceeding through a different mechanism.



Scheme 1.8: Differences in yield of *cis*- and *trans*-isomers

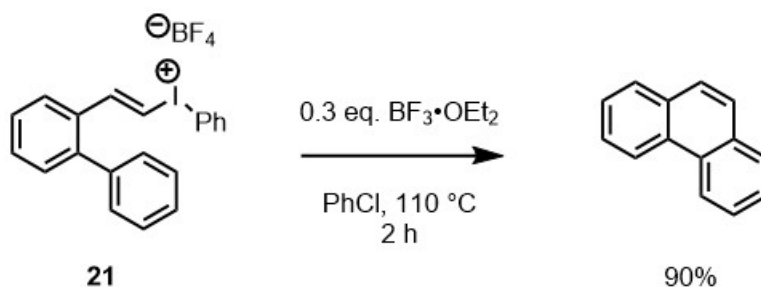


Scheme 1.9: α -methyl styrene substrate producing a mixture of regioisomers

Chapter 2: Mechanistic Studies

2.1 Background: Vinylene Phenonium Cation

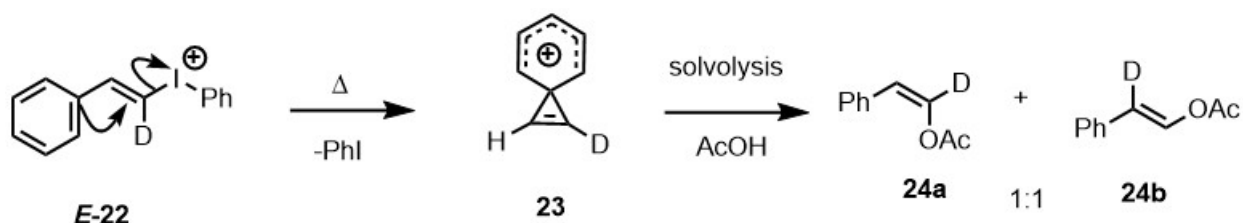
It was thought that the reactivity of *ortho*-phenyl styrenes was related to that of styryl(aryl)iodonium salts.³³⁻⁴⁰ This idea was tested in a control experiment where the iodonium tetrafluoroborate salt **21** was synthesized and subjected to the reaction conditions to give phenanthrene in 90% yield (Scheme 2.1).



Scheme 2.1: Synthesis of phenanthrene by decomposition of vinyl (aryl)iodonium salt **20**

Vinyl (aryl)iodonium salts have been demonstrated to act as vinyl cation precursors.³³⁻⁴⁰ Vinyl cations are highly reactive and unstable due to their relatively poor ability to stabilize a positive charge. They can be generated by the separation of a leaving group from a vinylic sp^2 carbon; as this is an unfavourable process, it typically requires harsh reaction conditions. Hypervalent iodine as a hypernucleofuge is an extremely good leaving group, and thus able to generate these reactive vinyl cation intermediates under relatively mild conditions. Vinyl cations with a phenyl substituent have been shown to re-arrange into a unique and symmetric carbocation called a vinylene phenonium ion (Scheme 2.2, **23**).^{33, 36, 39, 41} Okuyama and Ochiai investigated the solvolysis of styryl(phenyl)iodonium salts^{33, 36-38} and found that different products were produced depending on the stereochemistry of the styryl(phenyl)iodonium salt precursor.^{36, 37} When applied to deuterated styryl(phenyl)iodonium salt *E*-**22** (Scheme 2.2), it produced a 1 : 1

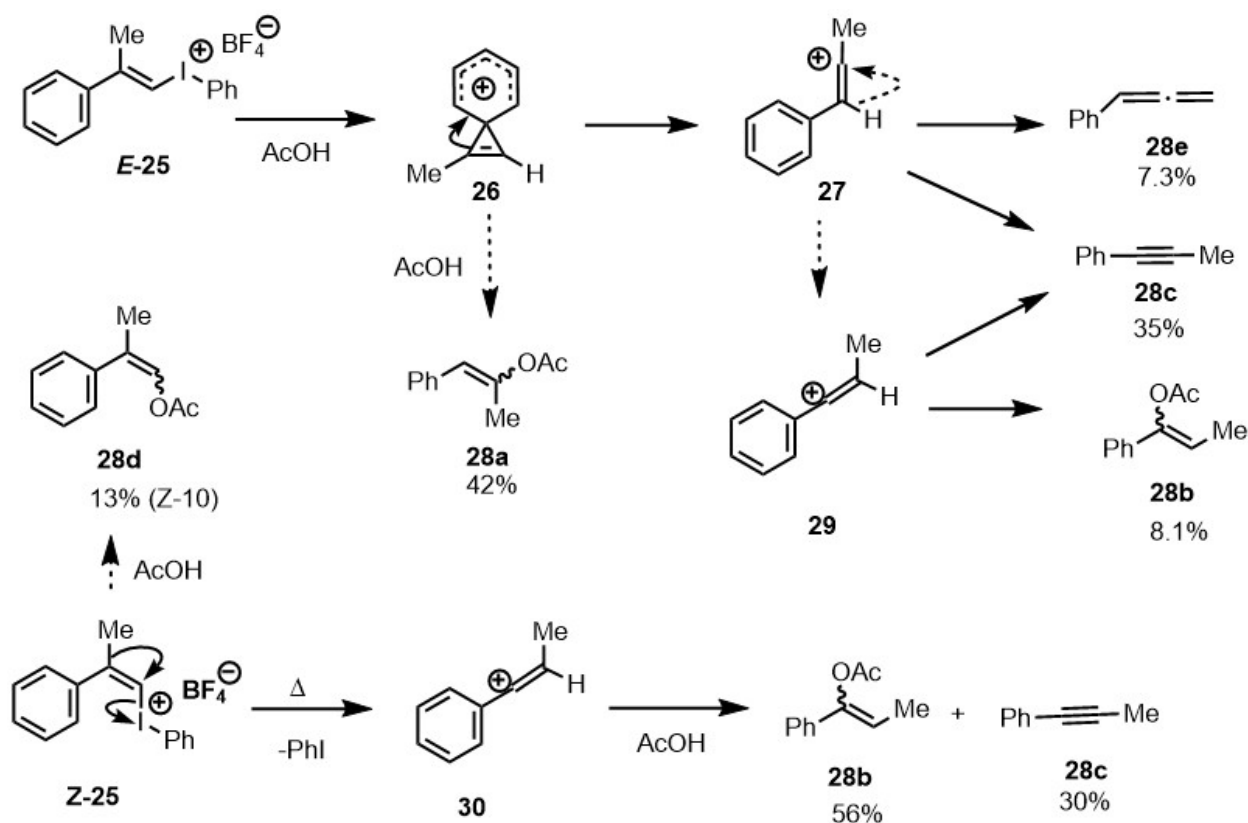
mixture of phenyl migrated products **24a** and **24b**, prompting the authors to suggest the presence of a vinylene phenonium ion (**23**) as the dominant cationic intermediate after decomposition of the iodonium salt. Okuyama and Ochiai studied the product distributions of the α -methyl styryl(phenyl)iodonium salts *E*-**25** and *Z*-**25** thoroughly and used that information to map out some potential cationic intermediates and mechanistic pathways to explain the yielded products (Scheme 2.3).



Scheme 2.2: Solvolysis of *E*-22 produced an equal mixture of regioisomers 24a and 24b

The iodonium salt *Z*-**25** produced no phenyl migrated products and was found to react 4000 times slower than *E*-**25**, which gave primarily 1,2-methyl shifted products **28b** and **28c** and some of the un-rearranged product **28d** (Scheme 2.3). This is consistent with the expected properties of the vinylene phenonium ion, which requires anti-periplanar geometry with the vinyl (phenyl)iodonium species to undergo nucleophilic attack. The extreme difference in reaction rate between *Z*-**25** and *E*-**25** demonstrates that *E*-**25** has a much lower energy activation barrier, which infers the strong stabilizing effect of the vinylene phenonium ion in comparison to the other vinyl cations. The *E*-**25** iodonium salt produced primarily product **28a**, suggesting the most substituted carbon is the most electropositive site of the vinylene phenonium ion for nucleophilic attack by the solvent. *E*-**25** also produced methyl-migrated products **28b** and **28c**, suggesting rearrangement to vinyl cation **27** and then vinyl cation **29** to offer the 1,2-methyl shifted product **28b**. The reverse rearrangement from *Z*-**25** to vinyl cation **29** did not occur.

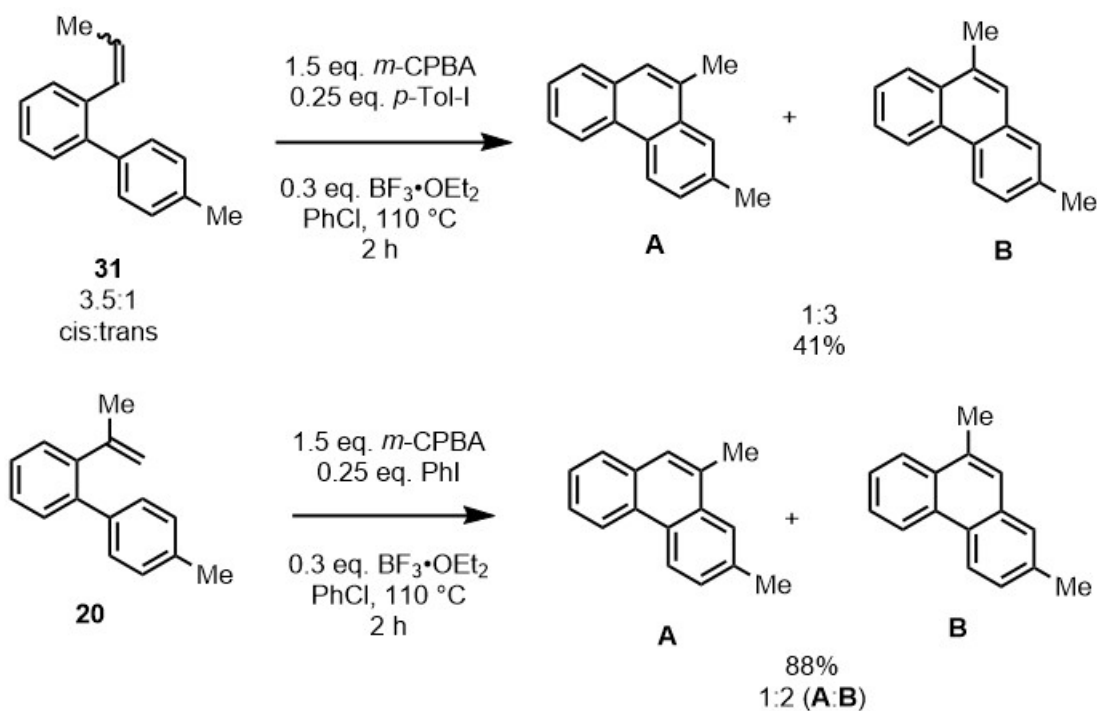
Elimination of the iodobenzene without a 1,2-shift is thought not to occur because it would produce the unstable primary vinyl cation. Should a primary cation exist, it would be expected to immediately rearrange to the vinylene phenonium ion before being captured by the solvent. Since these products were not observed in the decomposition of *Z*-**25**, the un-rearranged product **28d** is understood to be formed by another rare mechanism in a direct fashion by vinylic S_N2.³⁶⁻³⁸ As it is the least favourable pathway, **28d** was not observed in the solvolysis of *E*-**25**, and was only observed in the solvolysis of *Z*-**25** as a minor product. The relative reaction rates for solvolysis are as follows: vinyl phenonium cation > 1,2-methyl shift > vinylic S_N2.³⁶



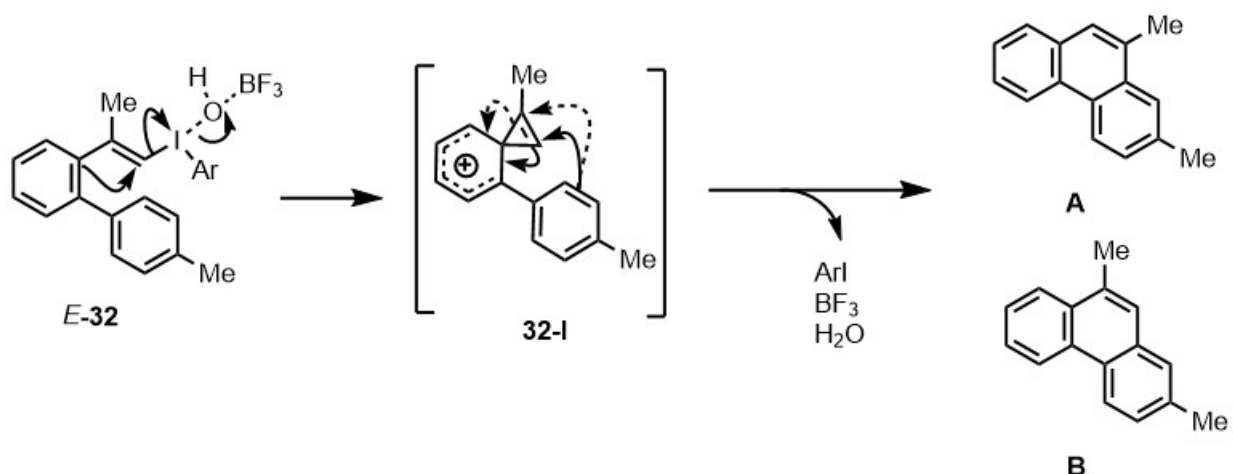
Scheme 2.3: Rearrangement products of *E*-25** and *Z*-**25** iodonium salt**

2.2 Mechanistic Studies of the HVI Catalyzed Reaction

In the HVI catalyzed reaction, we observed the same mixture of products **A** and **B** when reacting the α -methyl styrene (Scheme 1.9, **20**) and the β -methyl styrene (Scheme 2.4, **31**). In both cases we saw a preference for product **B**. If vinyl iodonium salt (Scheme 2.6, **20**) is acting as an intermediate in our HVI catalyzed reaction, the presence of a similar vinylene phenonium intermediate ion (Scheme 2.5, **32-I**) could account for the rearrangement and explain why we observe a mixture of products **A** and **B** after the reaction of the methylated styrenes **20** and **31**.

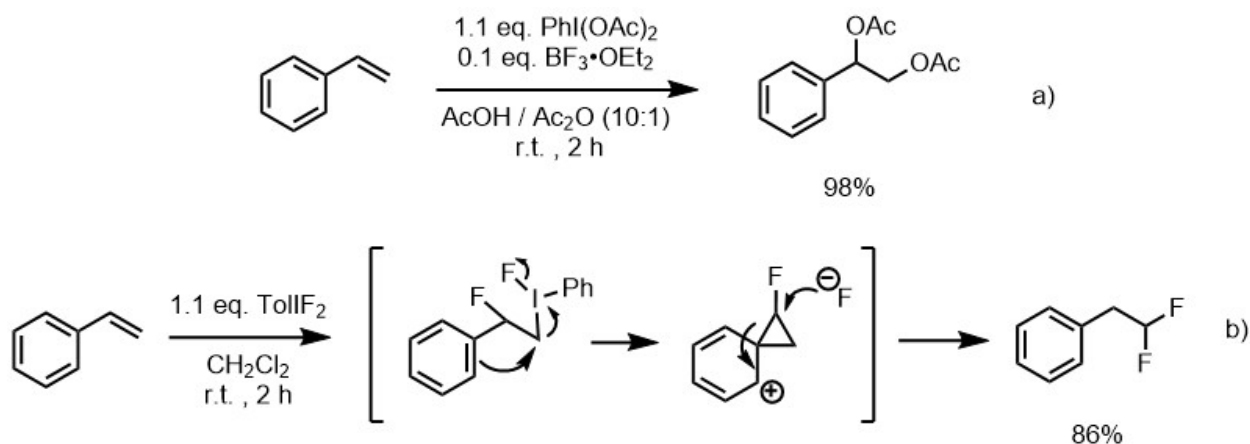


Scheme 2.4: Mixture of isomers **A** and **B** in β -methyl styrene substrate



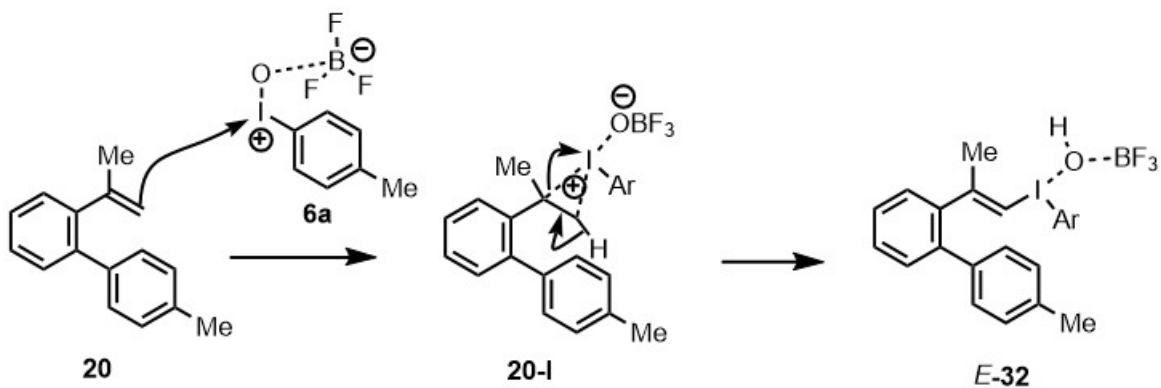
Scheme 2.5: Proposed vinylene phenonium intermediate in phenanthrene synthesis

As mentioned previously, vinyl iodonium salts are not typically synthesized directly from alkenes. Typically, the reaction of hypervalent iodine and styrenes involves an electrophilic addition to the double bond followed by reductive elimination of the iodine(III) intermediate, resulting in the incorporation of two nucleophiles in the disubstituted alkane^{20,42-44} (Scheme 2.6, a) displaying the characteristic umpolung reactivity of hypervalent iodine. Rearrangement by a 1,2-phenyl shift has been observed before in reactions with iodanes and styrene reacting with iodotoluene difluoride (TollF₂) to give 1,1-difluorinated alkanes (Scheme 2.5, b).^{45,46}



Scheme 2.6: Umpolung electrophilic addition reactions of styrenes and iodine(III) reagents to give 1,2-disubstituted alkanes

However, in this case we are observing a reactivity like that of iodonium salts, suggesting that the alkene **20** is reacting with the hypervalent iodine species and instead undergoing an addition-elimination reaction to form a vinyl iodonium salt (Scheme 2.7, *E-32*). This vinyl iodonium salt acting as a transient intermediate in the reaction can be captured by the *ortho*-arene to form the product. This novel reactivity prompted us to question why our styrene was reacting this way. Since the more common pathway in the reaction of HVI and styrenes is a double addition, some of the differences in reactivity might be understood by considering thermodynamic control versus kinetic control of the reaction. Water is a by-product formed as a result of the activated iodosyl complex **6a** reacting with the styrene (Scheme 2.7, **20**). The first elimination step produces an equivalent of H⁺ (Scheme 2.7, **20-I**), which combines with hydroxide after reductive elimination of the hypervalent iodine species (Scheme 2.5, *E-32*). These end products, water and phenanthrene, are both thermodynamically favourable, which could be driving forces for the mechanism.



Scheme 2.7: Elimination to form vinyl iodonium salt

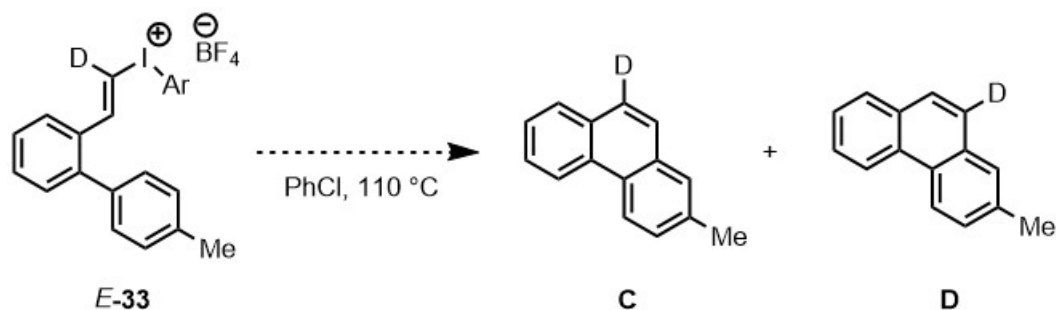
Looking to the solvolysis studies,³³⁻⁴⁰ there are apparent differences between our reaction and the reactions studied by Ochiai *et al.* Assuming that the α -methyl styrene **20** and/or the β -methyl styrene **31** proceeds via a vinylene phenonium ion intermediate (Scheme 2.5, **32-I**), it would suggest that our system differs in important ways: the *ortho*-arene nucleophile is

intramolecular, and the reactive site is sterically congested in comparison to *E*-**25** (Scheme 2.3, **26**). Since the nucleophile is intramolecular, vinylic S_N2 becomes more probable as an alternate mechanism. The mixture of products could also be a result of multiple competing mechanisms. The β-methyl styrene tested was a mixture of *cis*- and *trans*-isomers, and, we do not yet know how these behave individually except for in the symmetrical stilbene substrate where the *trans*-isomer gives a poorer yield (Scheme 1.8, **19**). However, this cannot be translated to the methyl substituted substrate due to differences in sterics and electronics between the molecules. It is also possible that the intermediate is not a vinyl iodonium salt at all, but only a similar behaving intermediate. The purported elimination step may happen at a later stage in the mechanism, akin to an acid catalyzed dehydration of an alcohol or epoxide to form the phenanthrene.

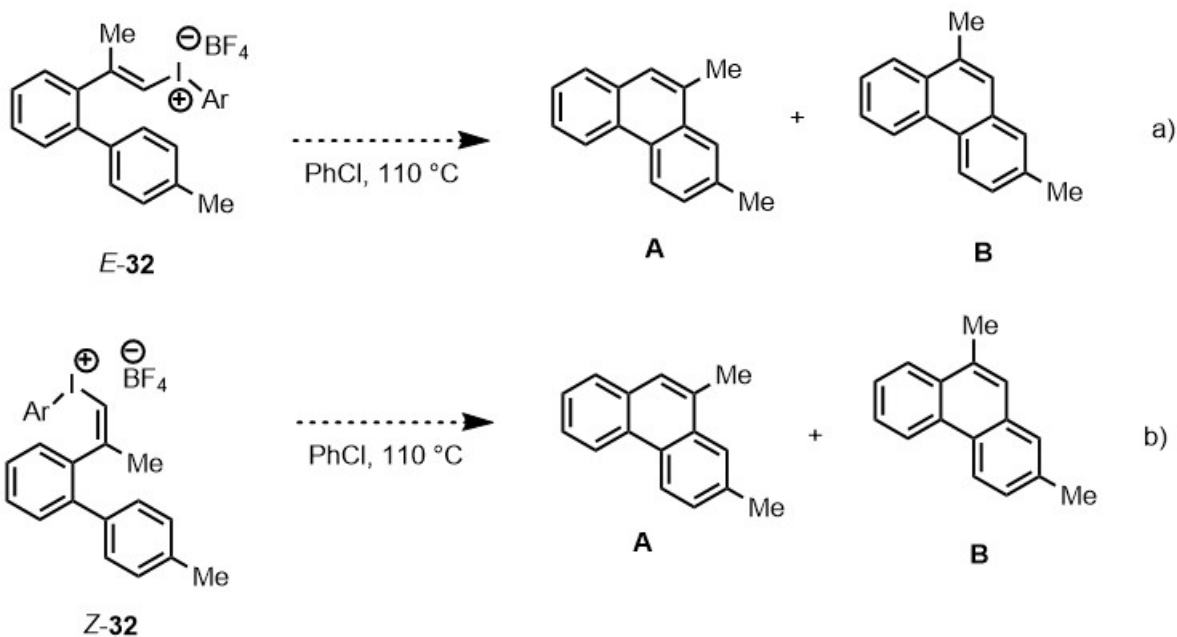
In order to test this hypothesis, we set out to synthesize a series of vinyl (aryl)iodonium salts to explore their reactivity as hypothetical reaction intermediates. If the vinyl (aryl)iodonium salts decompose via vinylene phenonium ions, then we should expect to see a mixture of phenanthrene products. We can compare the distribution of products to that of the catalytic reaction with the corresponding styrene. We will also prepare purified *cis*- and *trans*-isomers of the β-methyl styrene **31** to probe the effects of stereoisomerism of the alkene on the reaction and the product ratio. These results will also serve as a baseline control for comparison with the results of the vinyl (aryl)iodonium salts. We will also test the styrene epoxide to explore the possibility of a side reaction that could lead to the same product.

In order to exclude the variables associated with the methyl substitution of β-methyl styrene **31** and iodonium salts *E*-**32** and *Z*-**32**, we will prepare the corresponding deuterated *E*-vinyl (aryl)iodonium salt *E*-**33** and subject it to the reaction conditions (Scheme 2.8). If the decomposition of *E*-**33** occurs through a vinylene phenonium ion intermediate, we should expect

to see an equal ratio of observed products **C** and **D**. The **Z-33** isomer, however, likely cannot be prepared due to facile β -elimination of *cis*-2-phenylvinyl (aryl)iodonium salts^{36, 47} as previously reported, and thus cannot be isolated as a salt. We will prepare both *E*- and *Z*-2-methylvinyl (aryl)iodonium analogues **E-32** and **Z-32** and subject them to the reaction conditions in order to observe the effect of the stereochemistry on the distribution of products, which we can compare to the ratio of products observed with the α -methyl styrene (Scheme 2.9, a, **20**) and β -methyl styrene (Scheme 2.9, b, **31**) observed in the catalytic reaction.



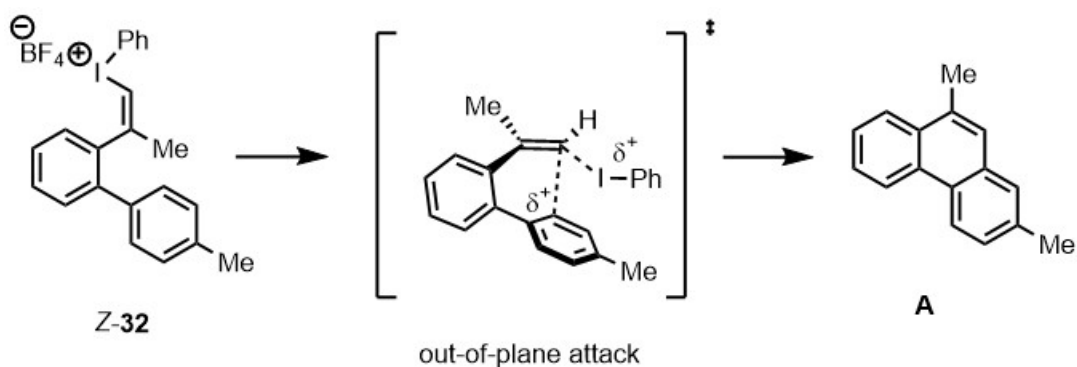
Scheme 2.8: Proposed reaction with deuterated *E*-33



Scheme 2.9: Proposed reactions with methyl isomers *E*-32 and *Z*-32

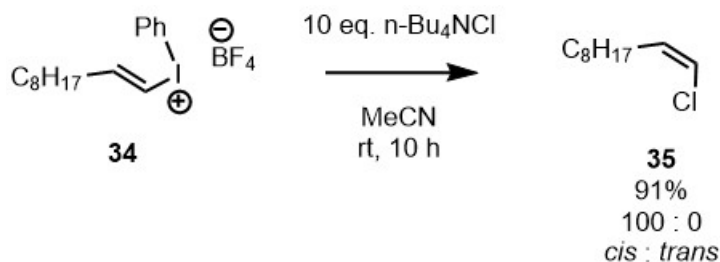
If we observe a similar distribution of phenanthrenes (1 : 2, **A** : **B**) with the vinyl (aryl)iodonium salt (*E*-**32**), it would suggest that *E*-**32** is a close or true intermediate, and the reaction is proceeding through a vinylene phenonium ion intermediate. If this is the case, then we should not expect to see the same ratio of products with *Z*-**32**, since the generation of the vinyl phenonium intermediate requires the aryl ring to be anti-periplanar to the iodonium species.³⁶

A possible competing reaction we might observe is vinylic S_N2. The 3D geometry of the substrate is such that the π-system of the arene nucleophile is situated close in space and slightly below the (aryl)iodonium species. Two types of vinylic S_N2 are possible: 1) in-plane mechanisms and 2) out-of-plane mechanisms. In-plane mechanisms occur by backside attack on the σ* orbital of the C-I bond and give products with inversion. Out-of-plane mechanisms occur by attack on the π* orbital and give products with retention. If either mechanism takes place, we should expect to see a preference for product **A**. The in-plane mechanism should not be possible with *Z*-**32**, as it cannot form the inverted product, and the σ* orbital is inaccessible; if the out-of-plane mechanism takes place, we might expect to see exclusive formation of product **A**, assuming that the competing 1,2-methyl shift (Scheme 2.2, **30**) as demonstrated in solvolysis studies would only lead to other by-products (Scheme 2.10).



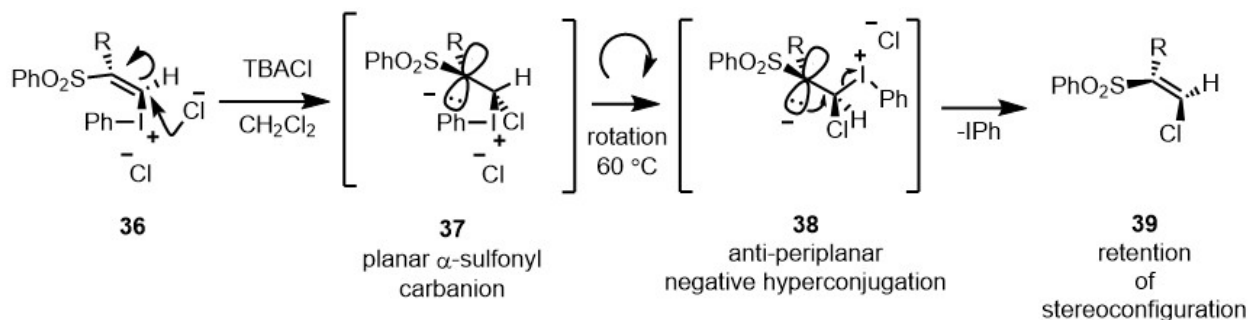
Scheme 2.10: Out-of-plane vinylic S_N2 with retention of configuration

Another mechanism to consider is a nucleophilic addition-elimination ($\text{Ad}_{\text{N}}\text{-E}$).⁴⁸ This could proceed by nucleophilic attack of the arene into the π^* orbital generating a carbanionic lone pair on the benzylic carbon. Reductive elimination of the iodonium species regenerates the double bond. However, when *E*- β -alkylvinyl (phenyl)iodonium salts are reacted with nucleophilic halides, a nucleophilic substitution reaction occurs providing exclusively the *Z*-alkenyl halide product.⁴⁹



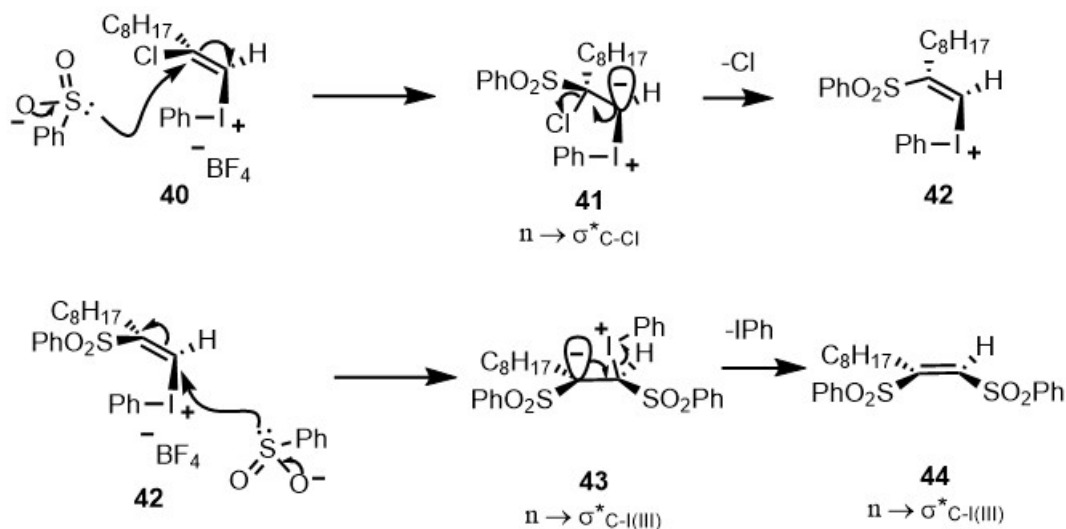
Scheme 2.11: Intermolecular vinylic $\text{S}_{\text{N}}2$ reaction with halides and vinyl (aryl)iodonium salts, inversion of stereoconfiguration

This serves as an excellent example of a vinylic $\text{S}_{\text{N}}2$ reaction. Nucleophilic addition-elimination ($\text{Ad}_{\text{N}}\text{-E}$) pathways are incompatible with exclusive inversion because the addition step provides an intermediate with free rotation (37), and therefore a mixture of isomers would be obtained. Especially in our case, $\text{Ad}_{\text{N}}\text{-E}$ generates crowded tetrahedral intermediates and a benzylic anion that is not energetically favourable.



Scheme 2.12: Nucleophilic addition-elimination mechanism with sulfonyl substituted vinyl (aryl)iodonium salt with retention of stereoconfiguration

An Ad_N-E mechanism has been documented for vinyl (phenyl)iodonium tetrafluoroborates that contain an anion stabilizing sulfonyl group on the benzylic position (Scheme 2.12). A β-phenylsulfonyl group makes possible the perpendicular attack of halide ions to the π* orbital, which produces an α-sulfonyl-stabilized carbanion (**37**). The internal 60° rotation yields **38**, followed by reductive elimination of the iodonium species, giving (Z)-(phenylsulfonyl)vinyl halides (**39**) stereoselectively. Negative hyperconjugation between the carbon-iodine bond and the carbanionic electron pair in **37** accounts for the preference of the 60° rotation over the 120° rotation of **36**. Similarly, the presence of a β-phenyl substituent would facilitate the nucleophilic vinylic substitutions via a multi-step addition-elimination route, as was observed in the reaction of *E*-**32**. However, β,β-disubstitution in *E*-**32** makes the S_N2 type transition state very difficult, because of the severe steric repulsion between the aryl groups. To our knowledge, this is the only example of an Ad_N-E process occurring with alkenyl (aryl)iodonium salts and is specific for those that contain atoms or groups which can either stabilize a negative charge in the intermediate or act as leaving groups.

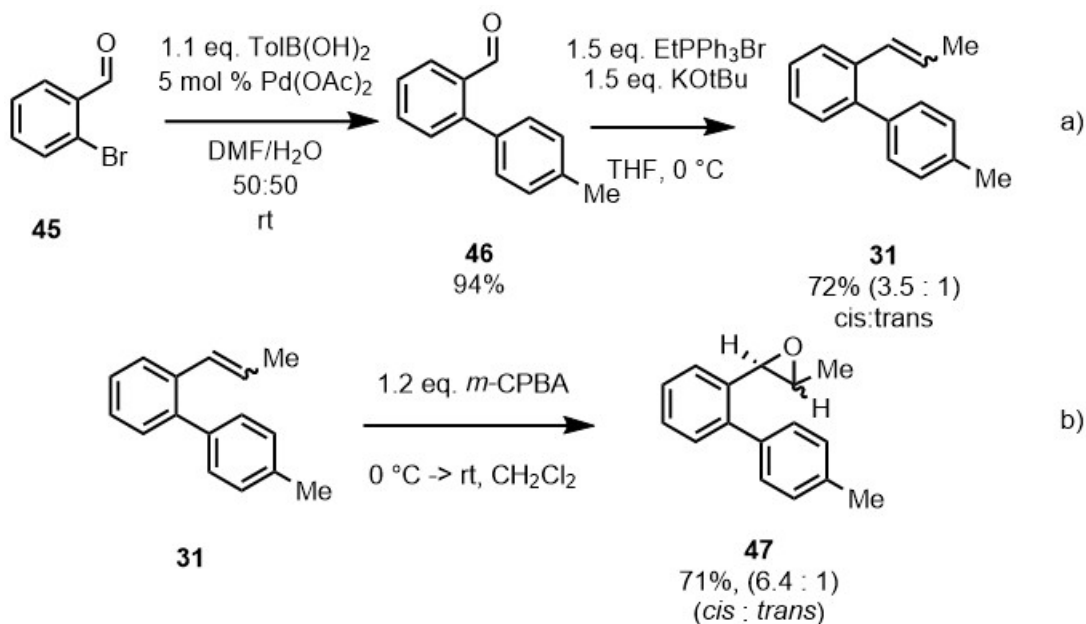


Scheme 2.13: Double substitution of chlorovinyl (aryl)iodonium salt with sulfonate through double Ad_N-E mechanism

By probing the HVI catalyzed reaction and mapping the results we observe onto those of the solvolysis studies,^{33, 36-38} we can support the possible presence of a vinylene phenonium ion, or direct us to an alternate explanation. The goal of this project is to gain deeper understanding of the reactivity, mechanism, and potential intermediates of the hypervalent iodine mediated aryl alkene coupling, and then use this knowledge to expand the scope of the reaction as a potential novel pathway to important polycyclic aromatic compounds.

2.3 Synthesis of Styrenes and Epoxide Control Reactions

We began the mechanistic studies by first conducting control experiments designed to rule out alternate pathways which might lead to phenanthrene formation. For example, in the catalytic reaction, *m*-CPBA is used as an oxidant. The styrene (**31**) could react with *m*-CPBA to form an epoxide able to undergo a dehydrative cyclization⁵⁰ with the Lewis acid BF₃•OEt₂ to form the phenanthrene product **A**. In order to rule out this possibility, the epoxide (**47**) was synthesized and subjected to the reaction conditions (Table 2.1). We chose to first test the epoxide prepared from the β -methyl styrene (**30**). The epoxide (**47**) was prepared in 3 steps starting from 2-bromobenzaldehyde (**45**) and 4-tolylboronic acid using a ligand free Suzuki reaction (Scheme 2.14, a).⁵¹ The styrene was then synthesized from the aldehyde (**46**) by Wittig olefination to yield styrene as a mixture of isomers (Scheme 2.14, a, **31**, *cis* : *trans* = 3.5 : 1).¹



Scheme 2.14: Synthesis of β -methyl styrene (31**) and epoxide (**47**) as a *cis/trans* mixture**

The epoxide (**47**) was then synthesized from the β -methyl styrene by reaction with *m*-CPBA (Scheme 2.14, b, **47**, *cis* : *trans* = 6.4 : 1). The reaction contained unreacted *trans*-styrene (*trans*-**31**), which accounted for the difference in product ratios as the *cis*-styrene (*cis*-**31**) reacted faster in the epoxidation. The epoxide (**47**) was subjected to varied conditions to explore its reactivity. When subjected to the standard conditions of the HVI catalyzed reaction, a low yield of phenanthrene **A** was produced as a single isomer (Table 2.1, entry 1). When the reaction was run using $\text{BF}_3 \cdot \text{OEt}_2$ only, phenanthrene **A** was produced in a better yield. With a full equivalent of $\text{BF}_3 \cdot \text{OEt}_2$, phenanthrene **A** was obtained in good yield as a sole isomer. These results indicated that the epoxide (**47**) was not acting as an intermediate in the HVI catalyzed reaction since the styrene (**31**) produced a mixture of isomers (**A** and **B**). This suggested that our reaction was going through an alternate mechanism.

The use of one equivalent of $\text{BF}_3 \cdot \text{OEt}_2$ alone in reaction with the epoxide increased the yield of **A** significantly. The regioselectivity of phenanthrene **A** is controlled by the $\text{BF}_3 \cdot \text{OEt}_2$

promoted ring opening of the epoxide as **A** is produced after elimination of H₂O. This indicates that the reaction of the *m*-CPBA with the iodoarene is much faster than the reaction of *m*-CPBA with the styrene. To further support this, when the β -methyl styrene (**31**) was reacted with a stoichiometric equivalent of hypervalent iodine reagent PhI(OAc)₂ (Figure 1.2) or Koser's reagent (PhI(TsO)OH) instead of iodotoluene and *m*-CPBA, the same product distribution was obtained as with the catalytic variant. If epoxide formation and cyclization was a competing mechanism, we would expect to see a greater presence of product **A**. In some cases, it was found that if the reaction was placed into a pre-heated 110 °C oil bath without pre-stirring the reaction mixture, the product distribution would significantly favour product **A**. However, if the reaction mixture was pre-stirred for 5 minutes at room temperature or placed in a room temperature bath and then slowly heated to 110 °C, then the 2 : 1 ratio **A** : **B** was reliably obtained. This suggests that in those cases without sufficient mixing of the reactants, the epoxide was being produced instead.

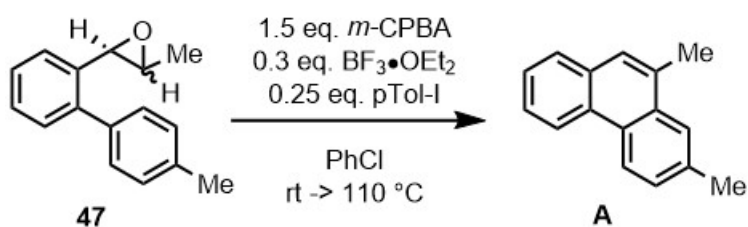
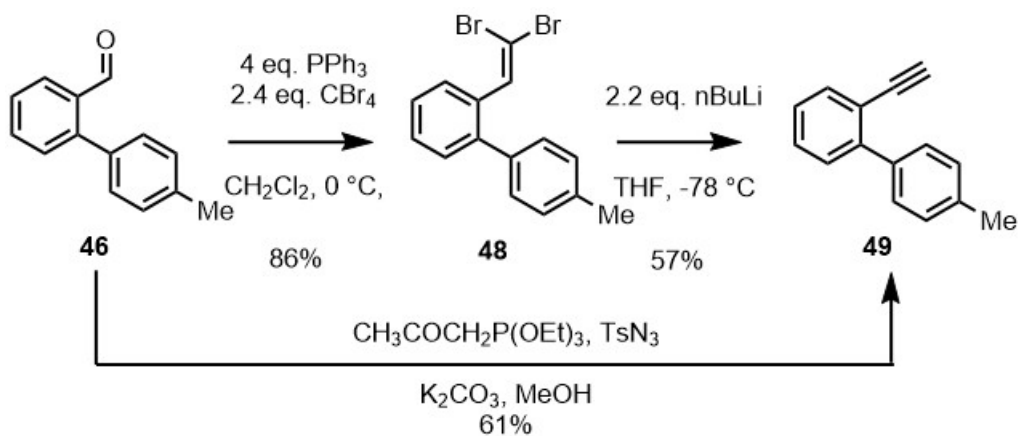


Table 2.1: Probing the reactivity of epoxide (47) in the HVI catalyzed reaction

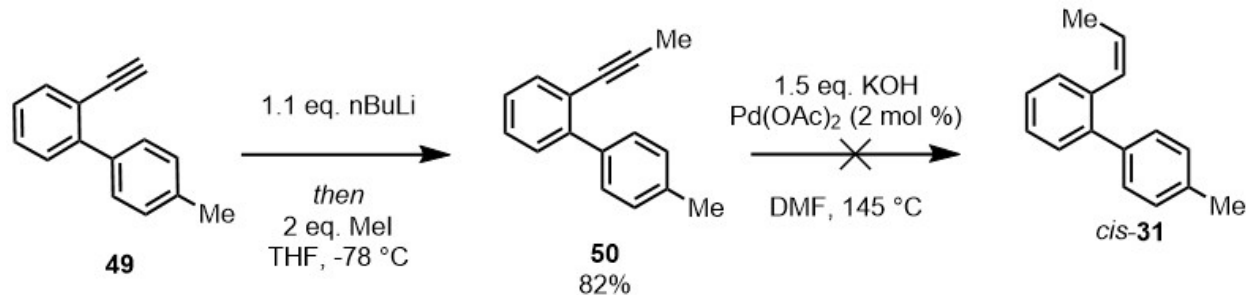
Entry	<i>m</i> -CPBA	BF ₃ ·OEt ₂	<i>p</i> -iodotoluene	solvent	Temp (°C)	yield
1	1.5 eq.	0.3 eq.	0.25 eq	PhCl	Rt -> 100 °C	17%
2	0 eq.	0.3 eq.	0 eq.	PhCl	Rt -> 100 °C	41%
3	0 eq.	1 eq.	0 eq.	PhCl	Rt -> 100 °C	93%

2.4 Synthesis of *cis*- and *trans*- β -methyl Styrene Isomers

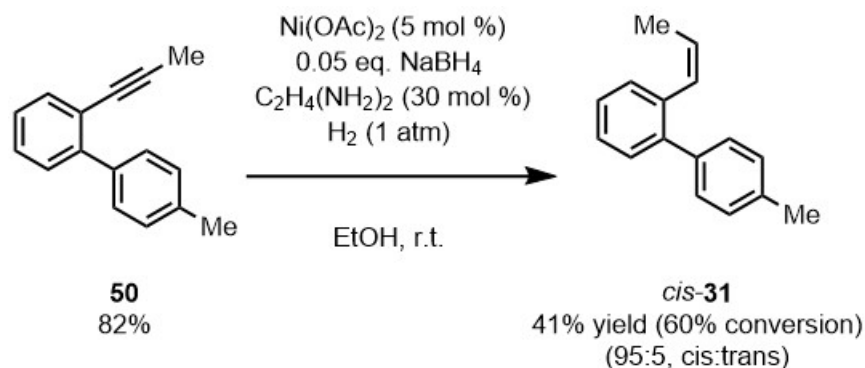
To test if the stereochemistry of the alkene had any effect on the product distribution and/or yield, the pure *cis*- and *trans*-isomers of the β -methyl styrene (**31**) needed to be individually prepared and isolated. The pure stereoisomers were sought-after by synthetic routes, since the chromatographic separation of these isomers from a mixture obtained by Wittig reaction was not trivial. We proposed the *cis*-styrene could be synthesized by a catalytic semi-reduction of the alkyne (**49**), while the *trans*-styrene could be obtained simply by thermodynamic isomerization of the *cis/trans* mixture (**31**) obtained previously by Wittig olefination (Scheme 2.14, a), which should give the *trans*-**31** product. Beginning with the *cis*-styrene, the terminal alkyne (**49**) was prepared from aldehyde (**46**) by the 2-step Corey-Fuchs reaction,⁵² and alternatively via a one-pot Horner–Wadsworth–Emmons (HWE) type reaction using the Ohira-Bestmann reagent.⁵³ The terminal alkyne was deprotonated with n-butyllithium and methylated with methyl iodide to give the alkyne (**50**). Selective semi-reduction of the alkyne (**50**) was challenging, and the reaction times were long, presumably due to the steric bulk of the *ortho*-arene. A ligand free catalytic transfer hydrogenation⁵⁴ using Pd(OAc)₂, dimethylformamide (DMF) and KOH was attempted, but produced low yields and low selectivity. Eventually success was found with the use of P2-nickel⁵⁵ and after 24 hours the *cis*-styrene *cis*-**31** was detected in 60% conversion and further isolated by column chromatography in 41% yield (*cis* : *trans* = 98 : 2).



Scheme 2.15: Preparation of terminal alkyne (49)



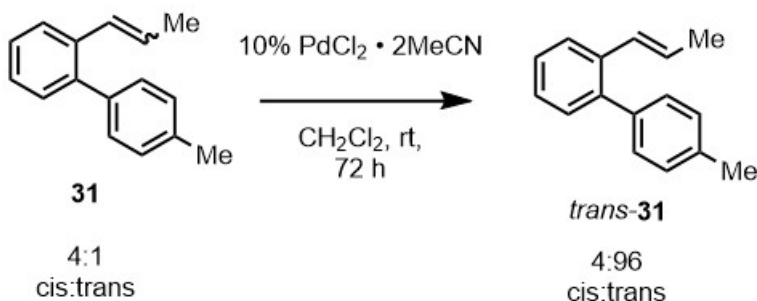
Scheme 2.16: Unsuccessful semi-reduction of alkyne



Scheme 2.17: Synthesis of *cis*-31** by semi-reduction of **50** using P₂-nickel**

The *trans*-alkene *trans*-**31** was obtained by applying a palladium catalyzed alkene isomerization⁵⁶ to the mixture of isomers obtained previously (**31**, Scheme 3.15, a.). The styrene (**31**) was stirred with the palladium catalyst in CH₂Cl₂ and aliquots were periodically monitored

by ^1H NMR. After 24 hours, the ratio was measured, and the reaction was incomplete (*cis* : *trans* = 1 : 3). After 48 hours, the ratio was 1 : 9, and after 72 hours, the ratio was a satisfying 4 : 96 (*cis* : *trans*) (Scheme 2.18).



Scheme 2.18: Palladium(II) catalyzed isomerization of styrenes to obtain *trans*-31

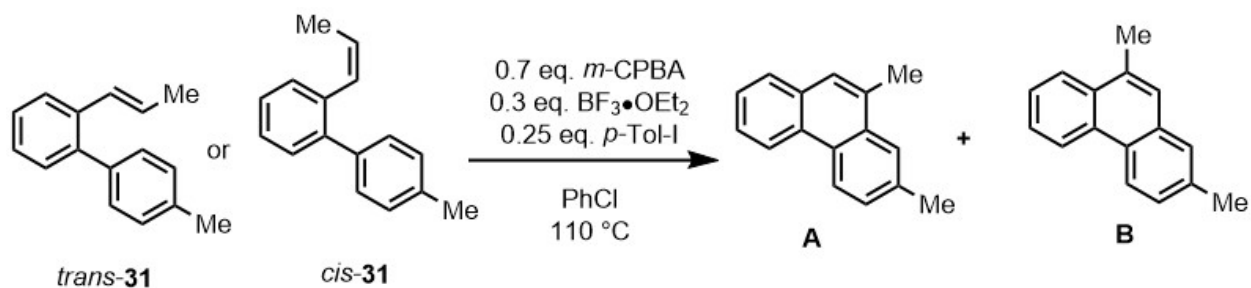


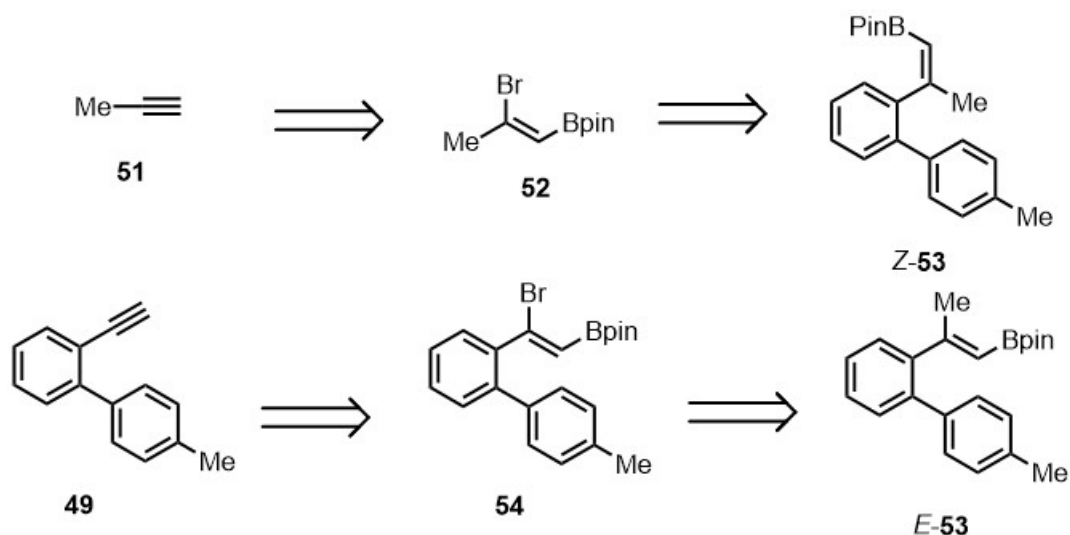
Table 2.2: Screening of *cis/trans* isomers under the reaction conditions

Entry	<i>cis</i> : <i>trans</i>	<i>m</i> -CPBA	Ratio A : B	Yield (A : B)	Recovered 31 (<i>cis</i> : <i>trans</i>)
1	98 : 2	1.5 eq.	Rt -> 110 °C	29% (1 : 2.3)	0
2	98 : 2	1.5 eq.	110 °C	38% (1 : 1.6)	0
3	4 : 96	1.5 eq.	Rt -> 110 °C	36% (1 : 1.2)	0
4	4 : 96	1.5 eq.	110 °C	28% (1 : 1.6)	0
5	1 : 1	0.7 eq.	Rt -> 110 °C	39% (1 : 2.0)	13% (1 : 3)
6	1 : 1	0.7 eq.	110 °C	52% (1 : 1.9)	14% (1 : 1.8)

The obtained *cis*- and *trans*-styrenes were tested in the reaction conditions with the varying temperature baths, but no significant difference in the yield or isomer ratio was observed (Table 2.2, entries 1-4). This suggests that the improved yield of *cis*-stilbenes observed in prior work¹ was more likely due to steric crowding of the internal alkene. In order to test the differing rates of reactivity between the *cis*- and *trans*-alkenes, a 1 : 1 mixture of *cis* : *trans* styrene was subjected to the reaction conditions with half the requisite amount of *m*-CPBA oxidant (Table 2.2, entries 5&6). In both temperature conditions, an excess of the *trans*-alkene was recovered. This is indicative that the *cis*-alkene was faster to react. The first step of the reaction occurs with nucleophilic attack by the alkene onto the activated iodosyl arene. The *cis*-alkene is able to react faster due to its increased polarizability and lesser steric hindrance.

2.5 Vinyl (aryl)iodonium salts

We proposed the *E*- and *Z*- vinyl (aryl)iodonium salts (*E*-**32** and *Z*-**32**) could be synthesized from their respective vinyl boronates (*E*-**53** and *Z*-**53**) by employing the iodine(III) exchange method described by Ochiai.^{36,46} The bromovinyl boronate (Scheme 2.19, a, **52**) is a known precursor accessible by the bromoborylation of propyne⁵⁷ (**51**), and has been used previously for the stereoselective synthesis of *Z*-trisubstituted alkenes as reported by Negishi.⁴⁸ Following this strategy, we proposed that the *Z*-boronate ester (*Z*-**53**) could be prepared from **52** by Negishi coupling with the 2-bromobiaryl compound (Scheme 2.21, **55**). With this strategy we expected challenges due to steric crowding of the *ortho* biaryl group substituted *cis*- relative to the pinacol boronate. Analogously, the *E*-boronate (*E*-**53**) could be obtained by bromoborylation of the previously prepared alkyne (**49**), followed by a Negishi coupling with a methyl zinc reagent (Scheme 2.19).⁴⁷



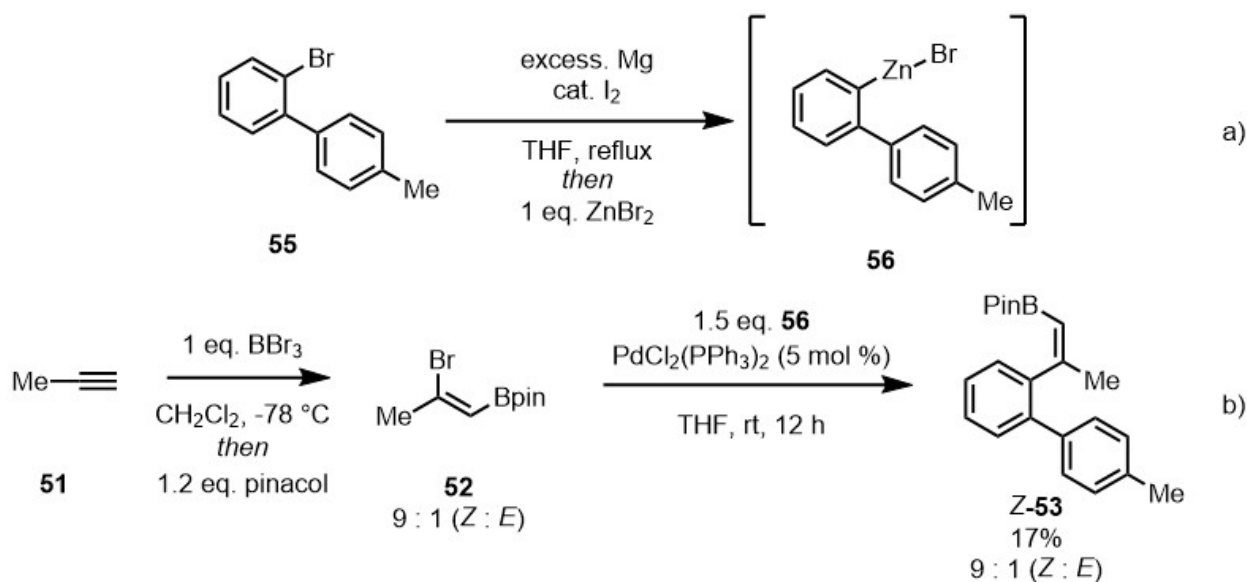
Scheme 2.19: Retrosynthesis of iodonium salts *E*-53 and *Z*-53

Vinyl boronate (**52**) was prepared by bromoborylation of propyne,⁵⁸ which gave the product (**52**) as a 1 : 9 (*E* : *Z*) mixture of stereoisomers (Scheme 2.20, b).

The bromoborylation of propyne is a highly stereoselective reaction, but the product (**52**) is known to isomerize.^{58, 59} However, the 1 : 9 mixture was sufficient to be used for the purposes of answering our mechanistic question, therefore the synthesis was continued. We proposed two possible strategies for the preparation of the biaryl **55**. Typically, a bromobiaryl is prepared in two steps from 2-bromoaniline via Suzuki coupling with a boronic acid, followed by a Sandmeyer reaction diazotization, and a halogen exchange. We proposed that a more direct route could be devised by employing the Suzuki coupling of 4-tolylboronic acid with 2-bromoiodobenzene. The 2-bromoiodobenzene (Scheme 2.21, **57**) possesses two strong electron-withdrawing groups (EWG) and therefore the C-I bond is highly activated toward oxidative addition. The product (**55**) possesses the less reactive C-Br bond adjacent to the newly installed *o*-arene which, due to steric

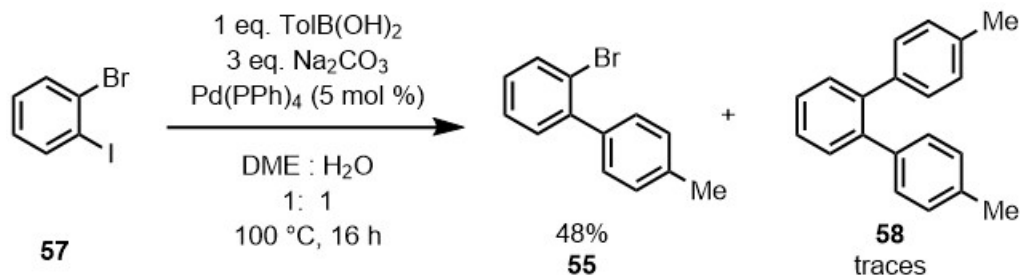
hindrance, will further impede its reactivity in the Suzuki reaction. Consequently, the desired product (**57**) can be synthesized without overaddition to the C-Br bond.

With this in mind, we attempted the Suzuki coupling⁶⁰ of 2-bromoiodobenzene (**57**) and 4-tolylboronic acid (Scheme 2.21). The reaction was successful with most of the desired product **55** having been produced. Traces of the overaddition product terphenyl (**58**) were also produced as a minor product and could be removed by column chromatography or vacuum fractional distillation. (48% yield after distillation) The organozinc compound **56** is prepared *in situ* via Grignard reaction and ion exchange with anhydrous ZnBr in tetrahydrofuran (THF) (Scheme 2.20, a).



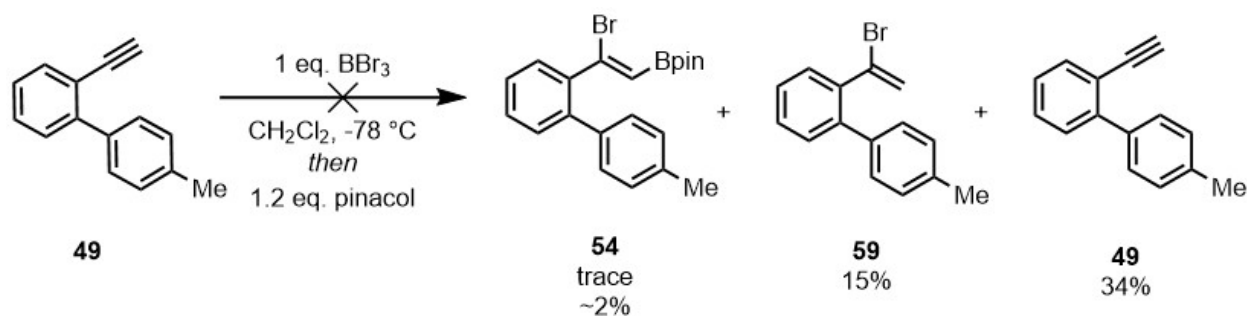
Scheme 2.20: Preparation of Z-53 and associated precursors

The THF solution containing the organozinc reagent **56** was transferred by cannula to a reaction flask containing the vinyl boronate **52** in the presence of PdCl₂(PPh₃)₂, providing Z-**53** in 17% yield as a 1 : 9 (E : Z) mixture of stereoisomers (Scheme 2.20, b). The yield of this reaction was low, presumably due to steric crowding of both precursors.

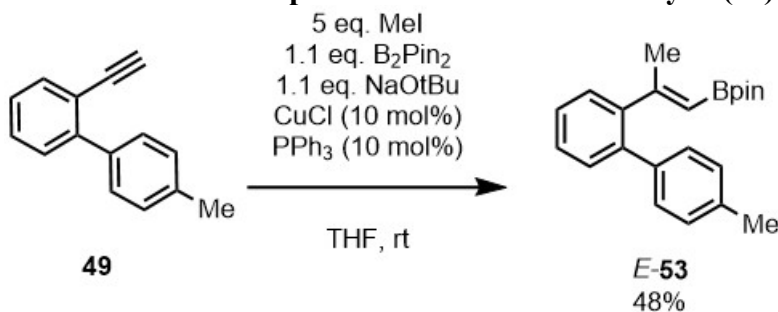


Scheme 2.21: Preparation of 2-bromobiaryl (50)

Attempts to produce the *E*-vinyl (aryl)iodonium isomer *E*-53 by the same strategy was unsuccessful. When the first attempt failed, the bromoborylation reaction was attempted again with freshly distilled BBr₃, and a third time by reverse addition. However, in each attempt only trace amounts of the bromoalkene **54** were detected. Instead, protodeborylation product **59** was isolated, and the largest fraction represented the recovered starting material **49**. A more direct method was realized employing a copper catalyzed carboborylation,⁶¹ which gratifyingly produced methylated product (*E*-53) directly in 48% yield as a single stereoisomer (Scheme 2.23).



Scheme 2.22: Attempts at bromoboration of alkyne (49)



Scheme 2.23 : Copper(I) catalyzed carboborylation⁶¹ in production of *E*-53

The boronates *E*-**53** and *Z*-**53** were converted to the respective vinyl (aryl)iodonium tetrafluoroborate salts *E*-**32** and *Z*-**32** by reaction with PIDA (PhI(OAc)₂) and boron trifluoride diethyl etherate (BF₃•OEt₂). The iodonium salts were converted to their tetrafluoroborate derivatives with the addition of aqueous (5% w/w) sodium tetrafluoroborate solution, (aq. NaBF₄) and then extracted with dichloromethane, isolated by rotary evaporation, and placed in a freezer for crystallization (-20 °C) (Table 2.3). The iodonium salts were not stable at room temperature and slowly decomposed to give product phenanthrenes **A** and **B** (Table 2.3). When the crude iodonium salts were heated in chlorobenzene, they converted completely to give the product phenanthrenes (Table 2.3). This instability prevented isolation and the full characterization of the vinyl iodonium salts *E*-**32** and *Z*-**32**; however, it did provide additional data toward the question of the supposed mechanism of the decomposition. Analysis of both crude *E*-**32** and *Z*-**32** iodonium salts obtained by crystallization of the reaction mixture indicated the presence of phenanthrene products **A** and/or **B** in approximately 5-10% conversion of vinyl iodonium salt (Table 2.3, (**A** : **B**) in **32**). The phenanthrenes formed by the *E*-**32** iodonium salt gave an approximately 1 : 2 ratio of products **A** : **B** (Table 2.3, entries 1 & 2). Conversely, analysis of the crude *Z*-**32** iodonium salt depicted solely the unrearranged phenanthrene **B** as a single isomer. When *Z*-**32** was heated in the oil bath, it gave almost exclusively product **B** (Table 2.3, entries 3 & 4). This suggests that the *Z*-isomer itself is less stable and does not decompose via the same pathway as the *E*-isomer.

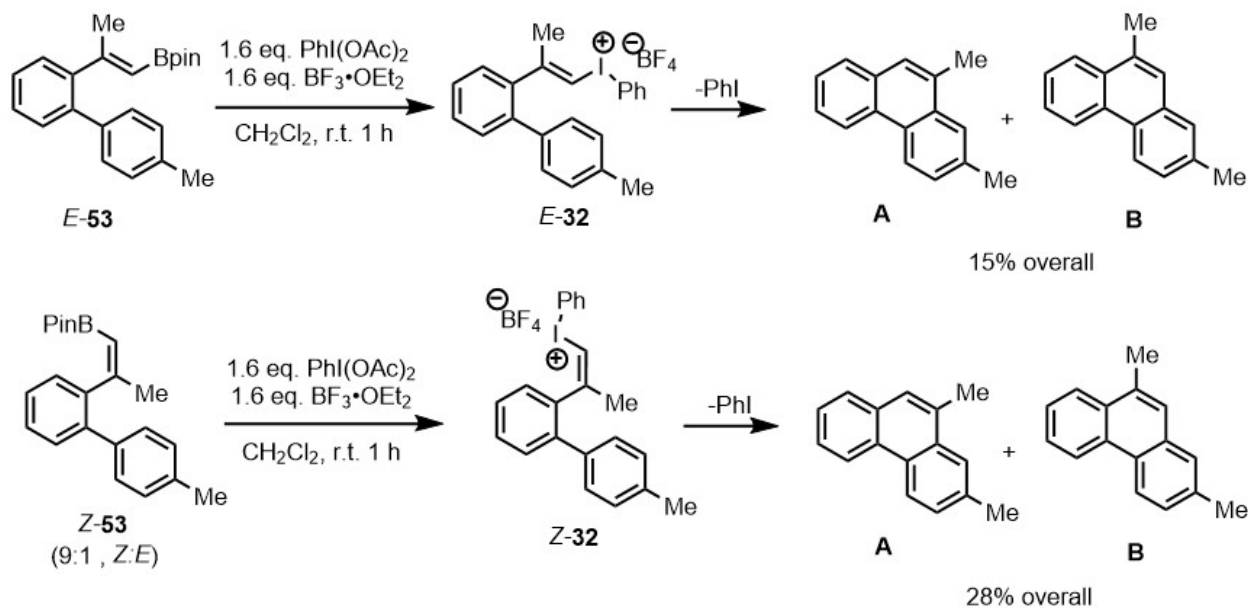


Table 2.3: Screening of *E*- and *Z*-iodonium salts in reaction conditions

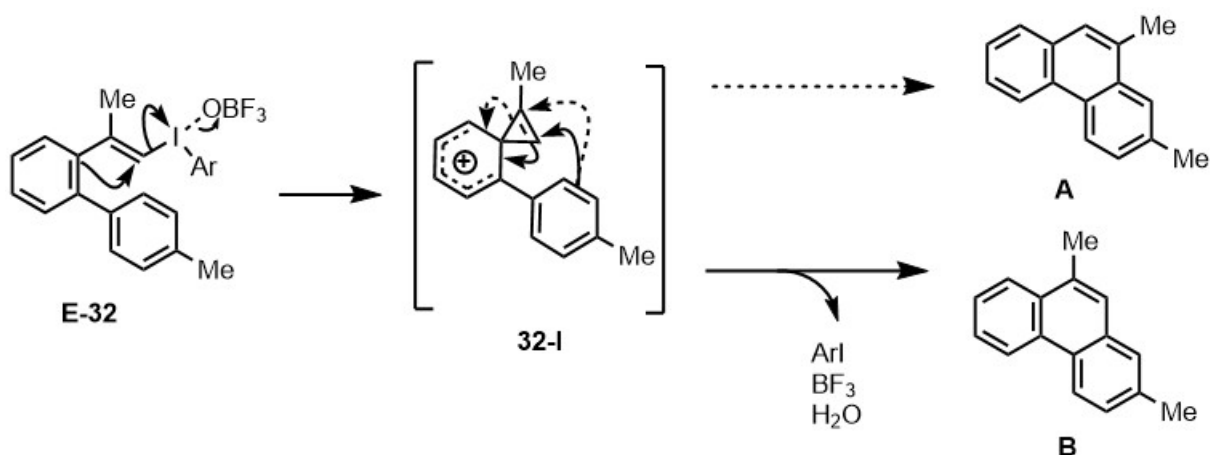
Entry	Isomer (<i>E</i> : <i>Z</i>)	Temperature (°C)	(A : B) in 32	Yield (A : B)
1	<i>E</i>	Rt -> 110 °C	1 : 3 (50%)	15%* (1.0 : 1.0)
2	<i>E</i>	110 °C	1 : 3 (50%)	15% (1.0 : 1.7)
3	<i>Z</i> (1 : 9)	Rt -> 110 °C	0 : 1 (63%)	28%* (1.0 : 4.0)
4	<i>Z</i> (1 : 9)	110 °C	0 : 1 (63%)	28% (1.0 : 10)

*Combined yield

2.6 Discussion

These results were consistent with our initial expectations outlined in the proposal, and with the previous work on solvolysis of the α -methyl styryl(phenyl)iodonium salts *E*-25 and *Z*-25 (Scheme 2.3) put forward by Ochiai. These results support the possibility of a vinyl iodonium species *E*-47 as an intermediate in the reaction, and that the stereochemistry is essential to provide the rearrangement and resulting mixture of products.

Referring back to the solvolysis studies of styryl(phenyl)iodonium salts (Chapter 1.5), Ochiai found that the *E*-**25** displayed 1,2-phenyl shift rearrangement via a vinylene phenonium ion, which requires anti-periplanar geometry with the vinyl (phenyl)iodonium species to undergo nucleophilic attack. The *Z*-**25** isomer on the other hand displayed 1,2-methyl shift rearrangements, due to the methyl group anti-periplanar alignment with the (aryl)iodonium substituent. However, these rearrangements occurred much more slowly due to a higher energy transition state in comparison to that seen in the *E*-isomer via the phenonium ion. The authors reported the vinylene phenonium ion was captured preferentially at the most substituted carbon, and the alternate product is produced via a rearrangement to another vinyl cation (Scheme 2.3). We observed a different distribution in our studies, with phenanthrene **B** as the major dominant isomer in a 1 : 2 ratio (Scheme 2.24).

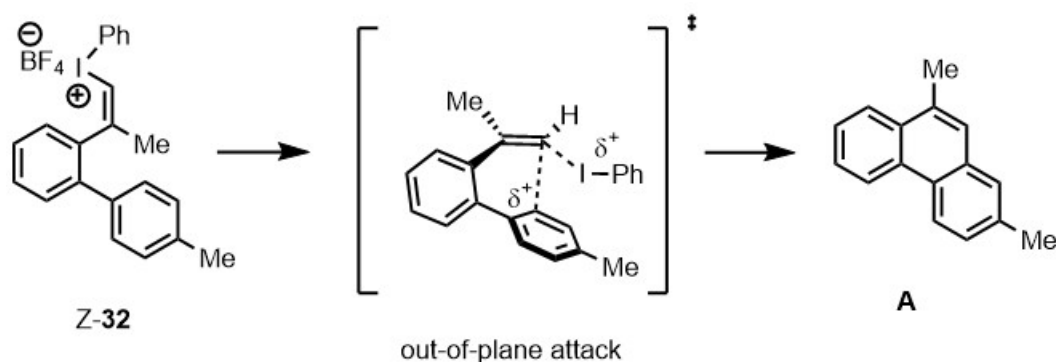


Scheme 2.24: Proposed vinylene phenonium intermediate (32-I) produced from *E*-32

This suggests that the proposed common intermediate vinylene phenonium ion (**32-I**) is captured at the less substituted carbon, or that an alternate pathway occurs. In the reaction of *Z*-**32**, we did not observe 1,2-methyl shifted products but instead, the production of phenanthrene **A** as the sole or dominant isomer. In the solvolysis studies, Ochiai reported vinylic $\text{S}_{\text{N}}2$ was the least

prevalent pathway in both *E*-**25** and *Z*-**25** isomers (Scheme 2.3), this is likely because it is an intermolecular mechanism, relying on the collision with a solvent nucleophile.

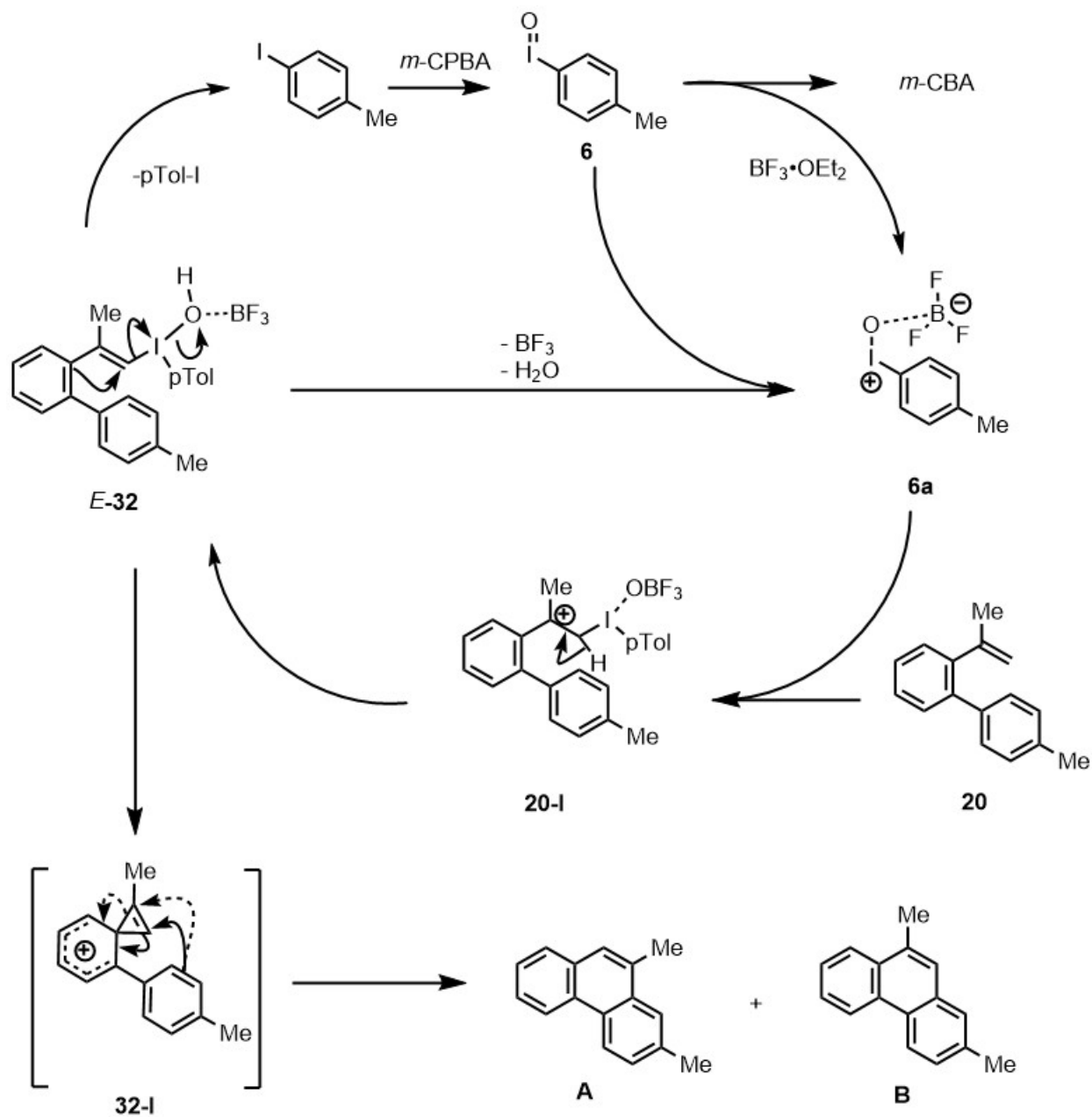
In the reaction of *Z*-**32**, direct intramolecular vinylic S_N2 by *ortho*-arene could likely be the dominant pathway in the production of **A**. Since the σ* orbital is inaccessible to the *ortho*-arene in the *Z*-**32** isomer, this leaves the out-of-plane mechanism as the most likely scenario by nucleophilic attack on the π* orbital (Scheme 2.25). This makes sense since the π-system of the alkene and the *ortho*-arene are very close in space, which is favourable for the intramolecular S_N2 to occur.



Scheme 2.25: Out-of-plane vinylic S_N2 with retention of configuration

The mechanism of phenanthrene formation is likely occurring through a vinyl (aryl)iodonium intermediate, followed by either vinylic S_N2 or vinylene phenonium ion, depending on the substitution of the styrene, to give the phenanthrene product **A**. This result suggests that the mechanism of the reaction is occurring with an intermediate of the *E*-stereoconfiguration (*E*-**32**). A mechanism was proposed that could account for the rearrangement proceeding through the vinyl (aryl)iodonium salt *E*-**32** as an intermediate (Scheme 2.26). The activated iodosyl arene (**6a**) is attacked by the alkene (**20**) and is followed by the elimination of H⁺ to produce the iodonium salt, (*E*-**32**) which is captured by the arene in a vinylic S_N2 manner to produce a vinyl phenonium

species, (**32-I**), which is then captured by the *ortho*-substituted phenyl group in an intramolecular electrophilic aromatic substitution to produce products **A** and **B**.

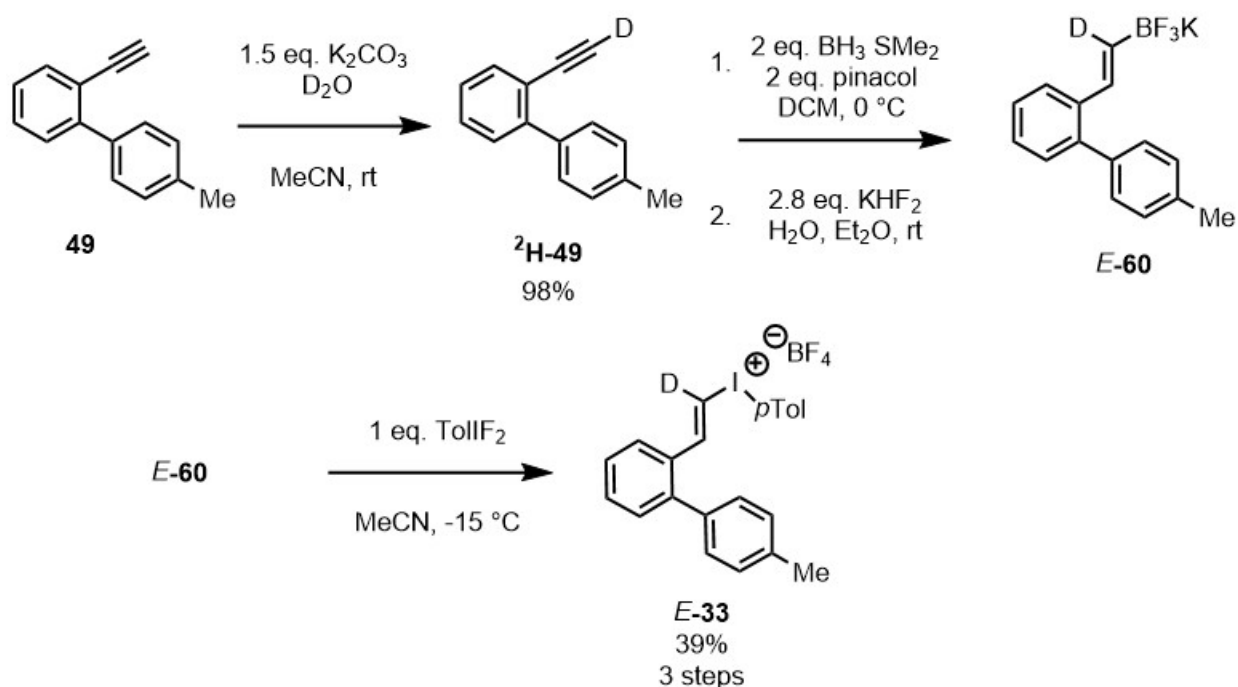


Scheme 2.26: Complete reaction with catalytic cycle and suggested mechanism for alkene-arene coupling reaction

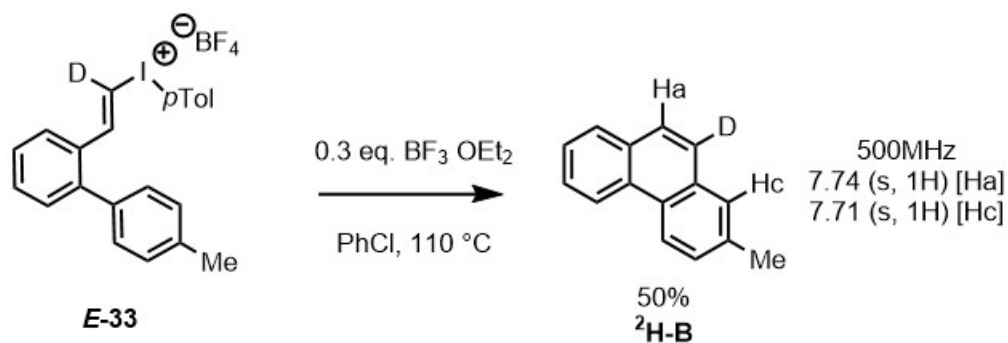
To test the role of the steric and electronic effects of the β -substituted methyl group of *E*-**32** and *Z*-**32** on the rearrangement, we proposed the synthesis of deuterated iodonium salt *E*-**33** to

further investigate this mechanism. If the mechanism with the methylated styrene *E-32* is producing a vinylene phenonium ion and cyclizing to favour the rearranged product, then a deuterated styrene should cyclize to give a 1 : 1 mixture of isomers.

Instability issues with *E-32* and *Z-32* prompted us to try alternatives in the synthesis of *E-33*. Boron-iodine(III) exchange with vinyl BF_3K salts and TollF_2 ⁶² is known to be a mild and high yielding method in the synthesis of alkenyl and alkynyl iodonium tetrafluoroborate salts. The deuterated vinyl (aryl)iodonium salt *E-33* was prepared from the alkyne precursor (**49**). Starting with deuterium-proton exchange⁴⁴ of the terminal alkyne (**49**) to give the deuterated alkyne ²**H-49**, hydroboration⁶³ and treatment with KHF_2 provided vinyl trifluoroborate *E-60*. Boron-iodine(III) exchange with TollF_2 ⁶² and aqueous workup (sat. NaBF_4) gave the iodonium salt *E-33* in a 39% NMR yield.

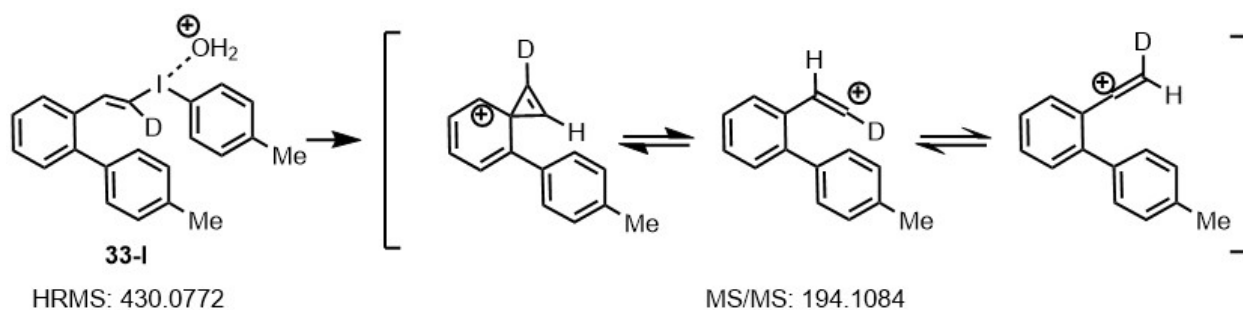


Scheme 2.27: Synthesis of deuterated vinyl (aryl)iodonium salt *E-33*



Scheme 2.28: Decomposition of *E*-33 to yield ²H-B as a single isomer

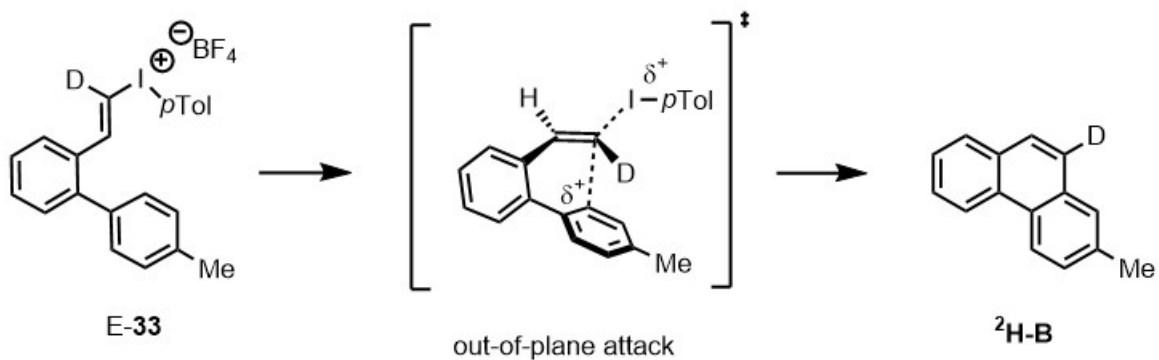
When iodonium salt *E*-33 was subjected to the reaction conditions, unexpectedly, deuterated phenanthrene ²H-B was isolated as the sole product. Dissolving *E*-33 in acetonitrile and analyzing by ESI-HRMS allowed us to observe and trap its water adduct (**33-I**, X=H₂O, HRMS: 430.0772), whose fragmentation gave a peak corresponding to vinyl cation-type structures, (HRMS: 194.1084) or isomers thereof.



Scheme 2.29: HRMS of the iodonium salt water-adduct (33-I**) and fragment vinyl cation in MS/MS mode**

This result indicates that the iodonium salt may be decomposing to the phenanthrene via a similar mechanism to that of iodonium salt *Z*-32 (Scheme 2.25). This is unexpected since our assumption was that the vinylene phenonium ion intermediate was the lowest energy pathway. The MS peaks suggest that the vinyl cation is still capable of forming, but we are not observing

rearrangement in the products. This suggests that direct vinyl S_N2 by the *ortho*-arene is the most probable mechanism, and that it is the preferred pathway of the unsubstituted styrene (Scheme 2.30). A possible explanation for this result is that the vinylene phenonium ion lacking a methyl group is less stable and therefore the direct vinylic S_N2 pathway is lower in energy (Scheme 2.25). Consequently, vinylic S_N2 becomes the preferred pathway even though the vinylene phenonium ion is permitted by stereoconfiguration. The methyl substituted vinyl (aryl)iodonium salts may prefer vinylene phenonium ion formation due to the methyl group's stabilizing effect on the vinyl cation through hyperconjugation. It cannot be said for sure if this result translates to the catalytic reaction, but it is likely. This could be verified by submitting a 1,1-*gem*-deuterated *ortho*-phenyl styrene to the reaction conditions to determine if there is any rearrangement.



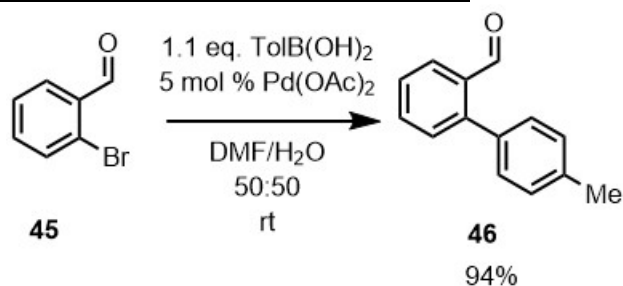
Scheme 2.30: Out-of-plane vinylic S_N2 with retention of stereochemistry

2.7 Experimental Procedures for Chapter 2

General Experimental and Characterization Details: Reactions were carried out in oven-dried glassware under a nitrogen atmosphere. Solvents were dried and purified using a JC Meyer solvent purification system, and were used without further purification. Transfer of anhydrous solvents and reagents was accomplished with oven-dried glass syringes. Thin layer

chromatography was performed on glass plates pre-coated with 0.25 mm Kieselgel 60 F254 (Silicycle). Flash chromatography columns were packed with 230-400 mesh silica gel (Silicycle). Radial chromatography was carried out on a Chromatotron 7924T (Harrison Research) equipped with 4 mm silica gel 60 F254 with gypsum binder (EM) thick-layer plates on glass rotors. Infrared spectra were recorded on a Perkin Elmer FT-IR Spectrum Two with SI-1ATR Two. Proton NMR spectra (^1H NMR) were recorded at 300 or 500 MHz, and are reported (ppm) relative to the residual chloroform peak (7.26 ppm), and coupling constants (J) are reported in hertz (Hz). Carbon NMR spectra (^{13}C NMR) were recorded at 125 or 75 MHz and are reported (ppm) relative to the center line of the triplet from CDCl_3 (77.16 ppm). Fluorine NMR spectra (^{19}F NMR) were recorded at 282 or 470 MHz, and are reported (ppm) relative to the peak of trifluoroacetic acid (-76.53 ppm). High resolution mass spectrometry was performed on a Thermo Fisher Scientific Q-Exactive hybrid mass spectrometer equipped with an Agilent HPLC pump interfaced with the Q-Exactive's ESI source.

2.7.1 Synthesis of 2-(4-methylphenyl)benzaldehyde (46)

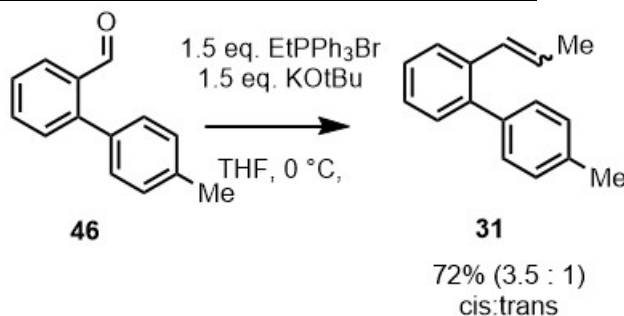


A 100 mL round bottom flask was charged with 2-bromobenzaldehyde (**45**) (33.6 mmol, 1 eq.), 4-tolylboronic acid (37.0 mmol, 1.1 eq.), K_2CO_3 (67.2 mmol, 2 eq.), 10 mL of DMF and 10 mL of distilled water. The reaction mixture was stirred as a suspension and then evacuated and refilled with nitrogen. The flask was reopened and $\text{Pd}(\text{OAc})_2$ (1.0 mmol, 3 mol%) was added. The flask was quickly resealed, then evacuated and refilled with nitrogen. The reaction was allowed to

stir for 1 hour at room temperature. The reaction was then diluted with ethyl acetate (50 mL) and filtered through a plug of celite. The reaction was then poured into a separatory funnel, diluted with water (150 mL) and extracted with ethyl acetate (3 x 50 mL). The collected organic extracts were dried over anhydrous MgSO₄ and concentrated by rotary evaporation. The residue was purified by silica gel column chromatography (10% Et₂O/hexanes) to yield **46** (94%) as a colourless oil.

¹H NMR (300 MHz, CDCl₃) δ 10.00 (s, 1H), 8.02 (d, *J* = 7.7 Hz, 1H), 7.57 (t, *J* = 7.5 Hz, 1H), 7.48 – 7.37 (m, 2H), 7.30 – 7.21 (m, 4H), 2.40 (s, 3H). Spectral data was consistent with those reported in the literature.¹

2.7.2 Synthesis of 4'-methyl-2-(prop-1-en-1-yl)-1,1'-biphenyl

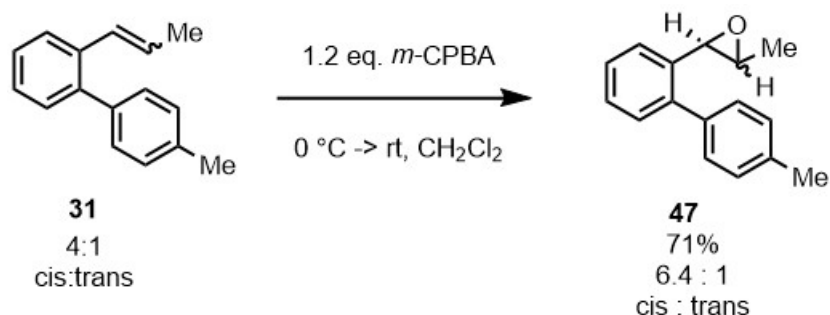


In an oven dried flask was added phosphonium salt (1.5 equiv) followed by THF (2.5 mL/mmol). Then t-BuOK (1.5 equiv) was added and the resulting yellow suspension was stirred at room temperature for 60 minutes. To this suspension, a solution of aldehyde (**46**) (1.0 equiv) was added in one portion and the resulting mixture was further stirred at room temperature overnight. Water and dichloromethane were added to the reaction mixture, and the aqueous phase was extracted with dichloromethane (3 × 50 mL). The combined organic phases were washed with saturated brine solution, dried over Na₂SO₄, and the solvent removed under reduced pressure. The

reaction mixture was purified by column chromatography over silica gel (5% Et₂O / hexanes) to yield **31** (72%, *cis* : *trans* = 3.5 : 1) as a colourless oil.

¹H-NMR (300 MHz; CDCl₃): δ 7.58 (d, *J* = 6.8 Hz, 1H), 7.42-7.20 (m, 40H), 6.45-6.40 (m, 1H), 6.31 (dd, *J* = 11.5, 1.4 Hz, 4H), 6.19 (dd, *J* = 15.7, 6.6 Hz, 1H), 5.73 (dq, *J* = 11.5, 7.0 Hz, 4H), 2.44 (s, 15H), 1.86-1.81 (m, 15H). Spectral data was consistent with those reported in the literature.¹

2.7.3 Synthesis of epoxide: 2-methyl-3-(4'-methyl-[1,1'-biphenyl]-2-yl)oxirane

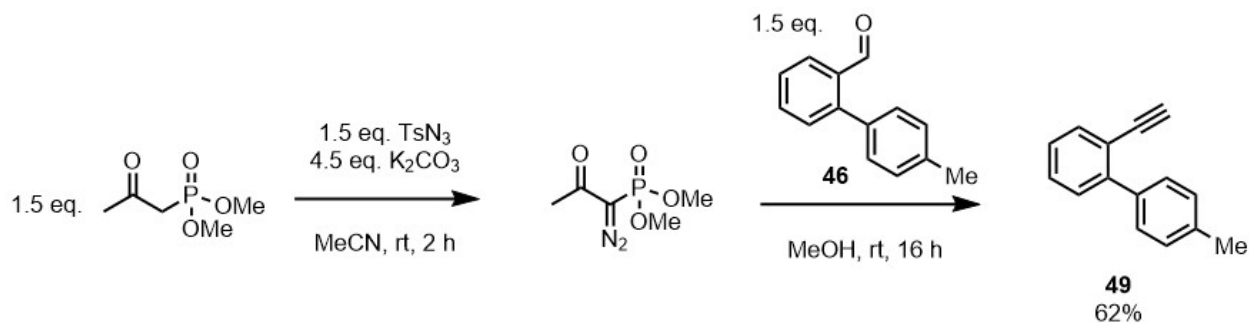


Step 1: To an oven dried 50 ml round bottom flask with a magnetic stir bar was charged with (E)-1-[o-(p-Tolyl)phenyl]-1-propene (**31**) (1.17 mmol, 2 eq.) and anhydrous dichloromethane (10 mL) and cooled in an ice bath (0 °C). *m*-CPBA was added one portion, and the reaction was allowed to warm to room temperature and stirred for 16 hours. The reaction was monitored by TLC, and the starting material was completely consumed. The solvent was removed by rotary evaporation and the residue extracted with diethyl ether, washed 2 x with water and 1 x with brine. The organic solvent was dried over anhydrous MgSO₄ and evaporated by rotary evaporation. The residue was purified by column chromatography (10% Et₂O/hexanes) to yield **47** (86%, *cis* : *trans* = 6.4 : 1) as a colourless oil.

¹H NMR (300 MHz, CDCl₃) δ, 7.52 – 7.45 (m, 1H), 7.44 – 7.24 (m, 8H), 3.97 (*cis*, d, *J* = 4.2 Hz, 1H), 3.60 (*trans*, d, *J* = 2.1 Hz, 1H) 3.32 (*cis*, dq, *J* = 5.4, 4.2 Hz, 1H), 3.06 (*trans*, dq, *J* = 5.1, 2.1 Hz, 1H) 2.46 (s, 3H), 1.43 (*trans*, d, *J* = 5.1 Hz, 3H), 1.21 (*cis*, d, *J* = 5.4 Hz, 3H).

¹³C NMR (75 MHz, CDCl₃) δ 141.4, 137.5, 137.1, 132.9*, 129.6*, 129.1, 129.0, 127.6(2C)*, 127.5, 127.0, 126.9, 124.3*, 59.3*, 58.1*, 57.3, 56.0, 21.3, 17.6*, 12.8.). Spectral data was consistent with those reported in the literature.⁶⁴ * = *trans*

2.7.4 Synthesis of 2-ethynyl-4'-methyl-1,1'-biphenyl (49)



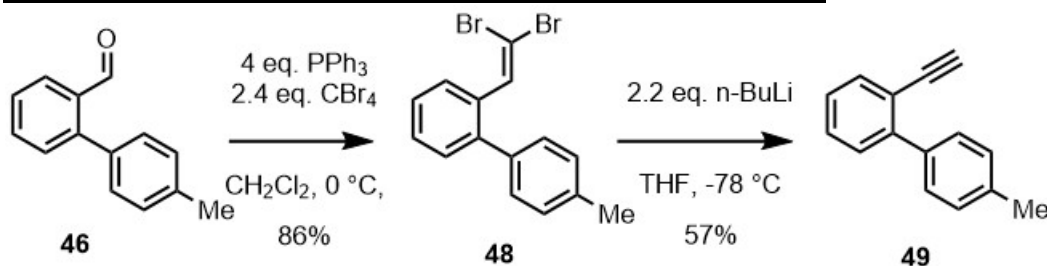
Step 1: In a 250 mL round bottom flask was charged with dimethyl (2-oxopropyl)phosphonate (16.4 mmol, 1.5 eq.), tosyl azide (16.4 mmol, 1.5 eq.) and 50 mL of anhydrous acetonitrile. K₂CO₃ (49.2 mmol, 4.5 eq.) is added, and the reaction is evacuated and refilled with a nitrogen atmosphere and allowed to stir at room temperature for 2 hours. The crude product produced *in situ* is used directly in the next step of the reaction.

Step 2: 2-(*p*-tolyl)benzaldehyde (**46**) (11 mmol, 1 eq.) is dissolved in 20 mL of methanol, and added to the flask in one portion. The reaction was allowed to stir at room temperature overnight. The reaction was filtered, and the organic solvent was removed by rotary evaporation.

The residue was dissolved in diethyl ether and transferred to a separatory funnel and washed with distilled water (50 mL), saturated sodium bicarbonate (20 mL), and brine (20 mL). The organic layer was dried over anhydrous MgSO_4 , and concentrated by rotary evaporation to yield a yellow oil. The residue was purified by silica gel column chromatography (5% Et_2O /hexanes) to yield **49** (62%) as a colourless oil.

$^1\text{H NMR}$ (300 MHz, CDCl_3) δ 7.62 ($J = 8.0$ Hz, 1H), 7.50 (d, $J = 8.1$ Hz, 2H), 7.41 – 7.36 (m, 2H), 7.32 – 7.22 (m, 3H), 2.98 (s, 1H), 2.40 (s, 3H). Spectral data was consistent with those reported in the literature.¹

2.7.5 Alternate synthesis of 2-ethynyl-4'-methyl-1,1'-biphenyl (49)



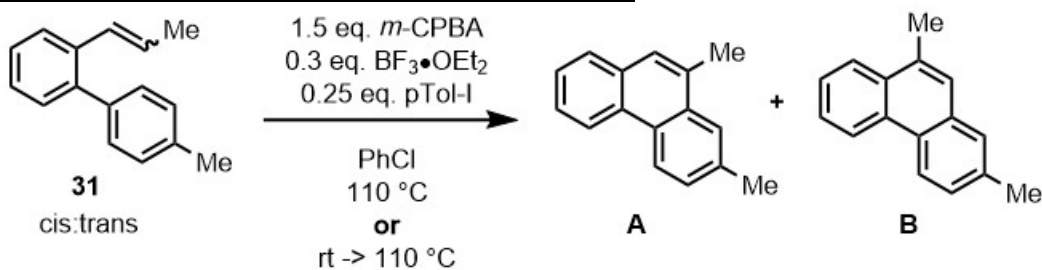
Step 1: Under an atmosphere of nitrogen, a solution of triphenylphosphine (4 eq.) and tetrabromomethane (2 eq.) in anhydrous dichloromethane (0.15 M) was stirred at $0\text{ }^\circ\text{C}$ for 30 minutes. Then the aldehyde (**46**) was added over a period of 5 minutes, and the mixture as stirred at $0\text{ }^\circ\text{C}$ for 1 hour. After addition of water, the layers were separated, and the aqueous layer was extracted with dichloromethane (3 x). The combined organic layers were dried over MgSO_4 and the solvent was removed under reduced pressure. The crude product was dry loaded on silica and purified by flash chromatography (5% Et_2O /Hexanes) to yield **48** (86%) as a colourless oil.

Step 2: Under an atmosphere of nitrogen, $n\text{-BuLi}$ (2.1 eq., 1.6 M in n -hexane) was added over a period of 30 minutes via syringe pump to a solution of **48** (1 eq.) in abs THF (0.4 M) at $-78\text{ }^\circ\text{C}$, and the mixture was stirred at this temperature for 1 hour and allowed to warm to room

temperature and stirred for an additional 1 hour. The reaction was again cooled to $-78\text{ }^{\circ}\text{C}$, and quenched with the slow addition of wet THF. The reaction was allowed to warm to room temperature and stirred for 10 minutes. The organic solvent was removed by rotary evaporation, the residue redissolved in diethyl ether and transferred to a separatory funnel and washed with distilled water (50 mL), saturated sodium bicarbonate (20 mL), and brine (20 mL). The organic layer was dried over anhydrous MgSO_4 , and concentrated by rotary evaporation to yield a yellow oil. The residue was purified by silica gel column chromatography (5% Et_2O /hexanes) to yield **49** (62%) as a colourless oil.

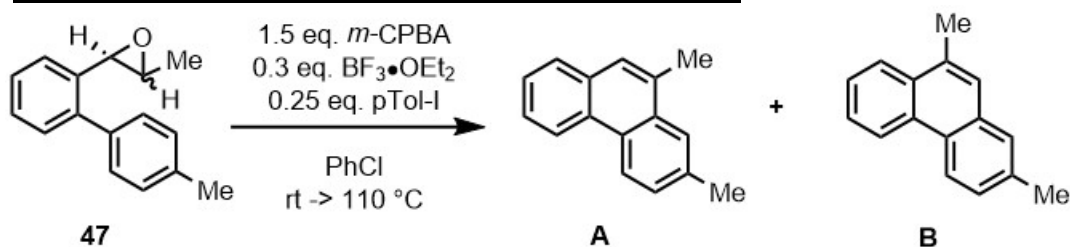
$^1\text{H NMR}$ (300 MHz, CDCl_3) δ 7.62 ($J = 8.0$ Hz, 1H), 7.50 (d, $J = 8.1$ Hz, 2H), 7.41 – 7.36 (m, 2H), 7.32 – 7.22 (m, 3H), 2.98 (s, 1H), 2.40 (s, 3H). Spectral data was consistent with those reported in the literature.¹

2.7.6 General procedure for phenanthrene synthesis



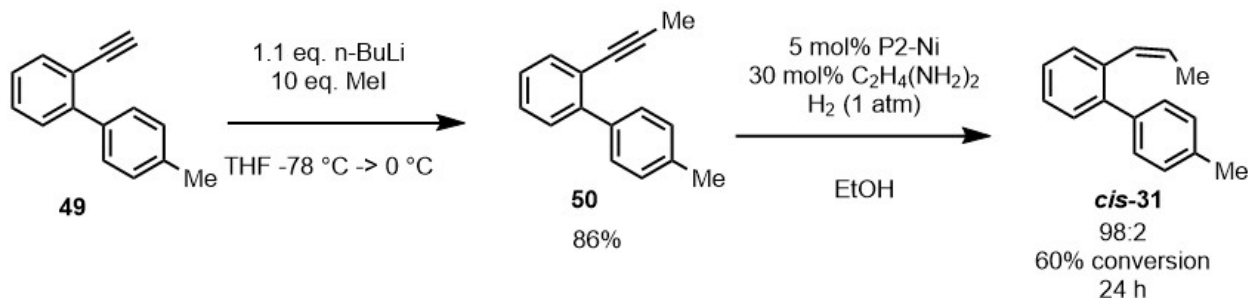
To an oven dried microwave vial with a magnetic stir bar was charged with **31** (0.1 mmol, 1 eq.), iodotoluene (0.025 mmol, 0.25 eq.), *m*-CPBA (0.15 mmol, 1.5 eq.) and anhydrous chlorobenzene (1 mL) and was stirred for 1 minute. Boron trifluoride diethyl etherate (0.03 mmol, 0.3 eq.) was added by syringe, and the vial immersed in a preheated $110\text{ }^{\circ}\text{C}$ oil bath, or a room temperature oil bath and then heated to $110\text{ }^{\circ}\text{C}$. After 2 hours, the reaction was allowed to cool to room temperature, the solvent was removed by rotary evaporation and the product yield and isomeric ratio was measured by NMR spectroscopy of the crude product.

2.7.7 General procedure for control reactions with epoxide



To an oven dried microwave vial with a magnetic stir bar was charged with **47** (0.1 mmol, 1 eq.), iodotoluene (0.025 mmol, 0.25 eq.), *m*-CPBA (0.15 mmol, 1.5 eq.) and anhydrous chlorobenzene (1 mL) and was stirred for 1 minute. Boron trifluoride diethyl etherate (0.03 mmol, 0.3 eq.) was added by syringe, and the vial was immersed in a preheated 110 °C oil bath, or a room temperature oil bath and then heated to 110 °C. After 2 hours, the reaction was cooled to room temperature, the solvent was removed by rotary evaporation and the product yield and isomeric ratio was measured by NMR spectroscopy of the crude product. Spectral data was consistent with those reported in the literature.¹

2.7.8 Synthesis of *cis*-4'-methyl-2-(prop-1-en-1-yl)-1,1'-biphenyl



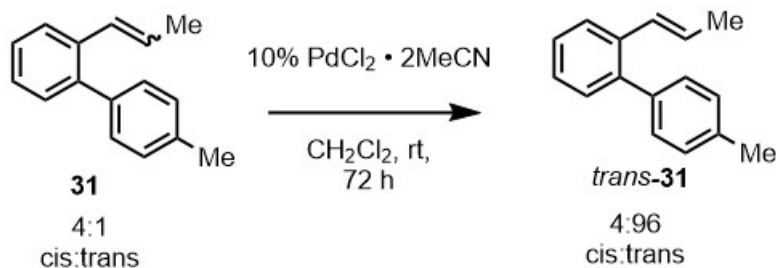
Step 1: To a 25 mL round bottom flask was added a solution of 1-[*o*-(*p*-Tolyl)phenyl]-1-ethyne (**49**) (2.23 mmol, 1 eq.) in anhydrous THF (10 mL) and cooled to -78 °C with stirring. A

solution of *n*-BuLi (0.22 mL, 1.1eq.) was added dropwise. After complete addition, the reaction was stirred at -78 °C for 1 hour and then allowed to warm to room temperature. The reaction was stirred for 1 additional hour, then was cooled to -78 °C and methyl iodide (0.416 mL, 3 eq.) was added dropwise. The reaction was allowed to warm to room temperature and stirred overnight. The reaction was quenched with wet THF, and the solvent was removed by rotary evaporation. The residue was extracted with diethyl ether, washed 2 x with water and 1 x with brine. The organic solvent was dried over anhydrous MgSO₄ and evaporated by rotary evaporation. The residue was purified by column chromatography (10% Et₂O/hexanes) to give **50** (86%) as a colourless oil. Spectral data was consistent with those reported in the literature.¹

¹H NMR (300 MHz, CDCl₃) δ 7.60 – 7.52 (m, 3H), 7.42 – 7.23 (m, 5H), 2.45 (s, 3H), 1.98 (s, 3H).

Step 2: To a suspension of nickel(II) acetate tetrahydrate (18mg, 5 mol%) and absolute ethanol in a 50 mL round bottom flask was added NaBH₄ (6mg, 5 mol%), and then stirred for 15 minutes. Ethylenediamine was added (30 μL, 30 mol%) and was followed by 1-[*o*-(*p*-Tolyl)phenyl]-1-propyne (**50**) (1.45 mmol, 1 eq) and the reaction was placed under an atmosphere of hydrogen using a hydrogen balloon. The reaction was allowed to stir for 24 hours, crude HNMR indicated a 60% conversion of starting material to product. The solvent was removed by rotary evaporation, and the residue was purified by column chromatography (10% Et₂O/hexanes) to give *cis*-**31** (46%, *cis* : *trans* = 98 : 2) as a colourless oil. ¹H-NMR (300 MHz; CDCl₃): δ 7.58 (d, *J* = 6.8 Hz, 1H), 7.42-7.20 (m, 7H), 6.31 (dd, *J* = 11.5, 1.4 Hz, 1H), 5.73 (dq, *J* = 11.5, 7.0 Hz, 1H), 2.44 (s, 3H), 1.86-1.81 (d, *J* = 7.0 Hz 3H). Spectral data was consistent with those reported in the literature.¹

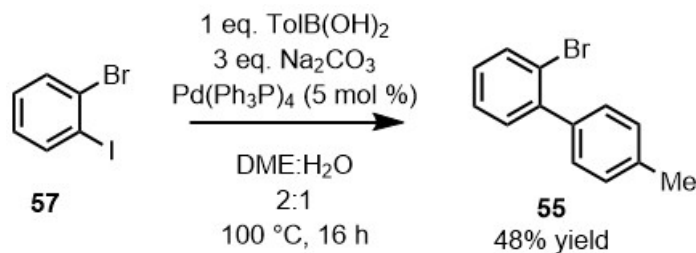
2.7.9 Synthesis of *trans*-4'-methyl-2-(prop-1-en-1-yl)-1,1'-biphenyl



To an oven dried 25 mL round bottom flask with a magnetic stir bar was charged with 1-*o*-(*p*-Tolyl)phenyl]-1-propene (**31**) (1.17 mmol, 2 eq.) as a mixture of *trans* and *cis* isomers. The flask was evacuated and filled with nitrogen, 10 mL of anhydrous CH₂Cl₂ was added followed by 25 mg of PdCl₂·MeCN. The reaction was allowed to stir for 72 hours, the reaction mixture was filtered through a silica plug and eluted with a 10% solution of diethyl ether in hexanes. The solvent was removed by rotary evaporation to yield *trans*-**31** (98%, *cis* : *trans* = 4 : 96) as a colourless oil. Spectral data was consistent with those reported in the literature.¹

¹H-NMR (300 MHz; CDCl₃): δ 7.58 (d, *J* = 6.8 Hz, 1H), 7.42-7.20 (m, 7H), 6.45-6.40 (d, *J* = 15.7, 1H), 6.19 (dq, *J* = 15.7, 6.6 Hz, 1H), 2.44 (s, 3H), 1.86-1.81 (d, 3H).

2.7.10 Synthesis of 2-bromo-4'-methyl-1,1'-biphenyl

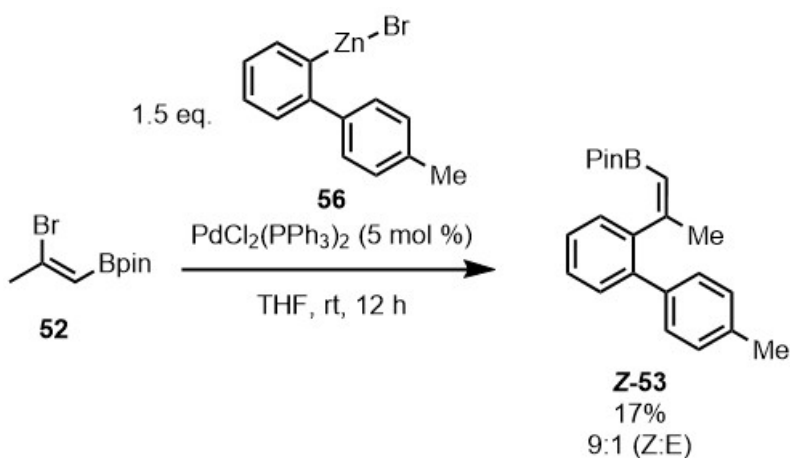


To a dry 50 mL round bottom flask was added *p*-tolueneboronic acid (33 mmol, 1 eq.), 1-bromo-2-iodobenzene (**57**) (33 mmol, 1 eq.), sodium carbonate, (99 mmol, 3 eq.) dimethoxyethane (140 mL) and water (70 mL). The vial was evacuated and filled with argon (3 x),

tetrakis(triphenylphosphine)palladium (1.65 mmol, 5 mol%) was added and the flask was resealed and purged with nitrogen. The reaction flask was immersed in a 100 °C oil bath and allowed to stir for 16 hours. The solvent was removed by rotary evaporation, and the residue extracted with diethyl ether, washed 2 x with water and 1 x with brine. The organic solvent was dried over anhydrous MgSO₄ and concentrated by rotary evaporation. The residue was purified by vacuum distillation to give **55** (48%) as a colourless oil. Spectral data was consistent with those reported in the literature.¹

¹H NMR (300 MHz, CDCl₃) δ 7.62 (*J* = 8.0 Hz, 1H), 7.50 (d, *J* = 8.1 Hz, 2H), 7.41 – 7.36 (m, 2H), 7.32 – 7.22 (m, 3H), 2.40 (s, 3H).

2.7.11 Synthesis of (Z)-4,4,5,5-tetramethyl-2-(2-(4'-methyl-[1,1'-biphenyl]-2-yl)prop-1-en-1-yl)-1,3,2-dioxaborolane (Z-53)

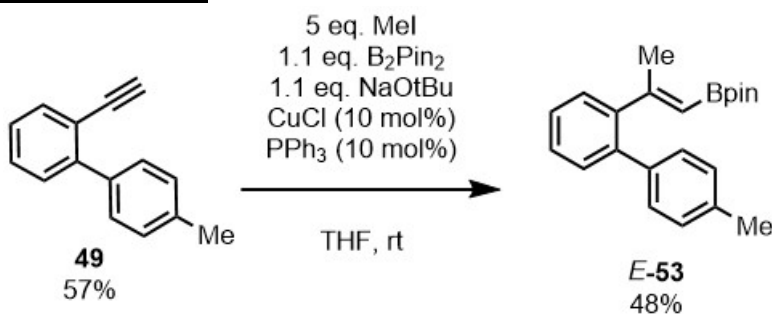


Step 1: To a dry 25 mL round bottom flask was added 2-bromo-4'-methyl-1,1'-biphenyl **55** (1.75 mmol, 1.2 eq.), and 3 mL of THF. The reaction flask was cooled to -78 °C, and a solution of *n*-butyllithium (2.2 mmol, 1.2 eq.) was added dropwise. After complete addition, the reaction was stirred for 1 hour and allowed to warm to room temperature and was then transferred by cannula to a flask containing zinc bromide (2.92 mmol, 2 eq.) and allowed to stir for 30 minutes.

Step 2: A microwave vial was charged with (Z)-2-(2-bromoprop-1-en-1-yl)-4,4,5,5-tetramethyl-1,3,2-dioxaborolane (**52**) (1.47mmol, 1 eq.), Pd₂(dba)₃ (0.04mmol, 3 mol%) and SPhos (0.04mmol, 3 mol%) as a suspension in 1 mL THF. The vial was flushed with nitrogen, and the reaction mixture was transferred by cannula into the microwave vial and allowed to stir overnight.

The solvent was removed by rotary evaporation and the residue extracted with diethyl ether, washed 2 x with water and 1 x with brine. The organic solvent was dried over anhydrous MgSO₄ and evaporated by rotary evaporation. The residue was purified by column chromatography over silica gel (200-300 mesh) (5% Et₂O/hexanes) to give Z-**53** (17%) as a colourless oil. (Z : E = 9 : 1) ¹H NMR (300 MHz, CDCl₃) δ 7.37 (J = 7.9 Hz, 2H), 7.34 – 7.10 (m, 8H), 5.46 (s, 1H), 2.37 (s, 3H), 1.70 (s, 3H), 1.08 (s, 12H). ¹³C NMR (75 MHz, CDCl₃) δ 160.5, 143.1, 139.1, 139.0, 136.4, 129.5 (2C), 128.9, 128.6, 127.0, 126.3, 82.6, 28.0, 24.6, 21.2.

2.7.12 Synthesis of (E)-4,4,5,5-tetramethyl-2-(2-(4'-methyl-[1,1'-biphenyl]-2-yl)prop-1-en-1-yl)-1,3,2-dioxaborolane

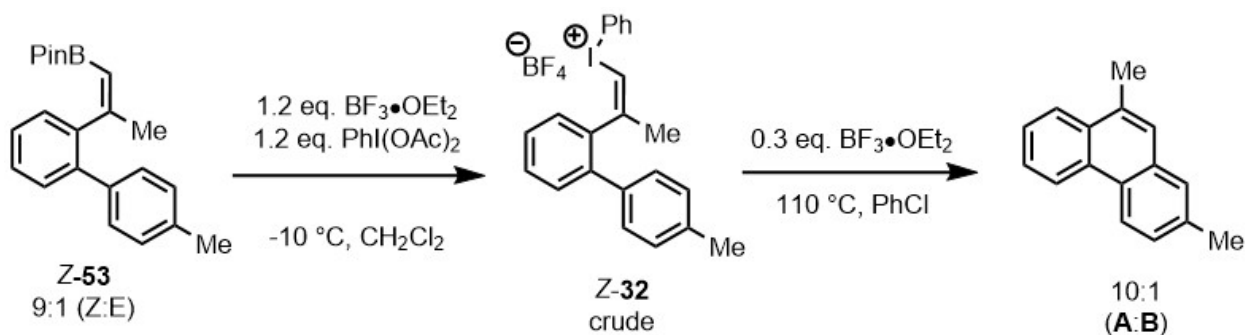


To a dry microwave vial was added bis(pinacolato)diborane (3.77 mmol, 1.1 eq.), triphenylphosphine (0.03mmol, 0.1 eq.) and copper(I) chloride (0.03 mmol, 0.1 eq.) and then the vial was evacuated and filled with nitrogen (3 x). 1 mL of THF was added and stirred to form a suspension. A solution of sodium *tert*-butoxide (3.77 mmol, 1.1 eq.) was added dropwise in THF. After addition, the solution was stirred for 5 minutes. A solution of 2-ethynyl-4'-methyl 1,1'-biphenyl (**49**) (0.343 mmol, 1 eq.) in anhydrous THF (0.3 mL) was added by syringe to the reaction

vial to give a final reaction concentration of 0.1 M. The reaction was stirred for 16 hours at room temperature. The solvent was removed by rotary evaporation and the residue extracted with diethyl ether, washed 2 x with water and 1 x with brine. The organic solvent was dried over anhydrous MgSO₄ and evaporated by rotary evaporation. The residue was purified by column chromatography over silica gel (200-300 mesh) (5% Et₂O/hexanes) to give **E-53** (48%) as a colourless oil.

¹H NMR (300 MHz, CDCl₃) δ 7.36 – 7.24 (m, *J* = 8.0 Hz, 6H), 7.16 (d, *J* = 8.0 Hz, 2H), 5.50 (s, 1H), 2.38 (s, 3H), 1.87 (s, 3H), 1.28 (s, 12H). ¹³C NMR (75 MHz, CDCl₃) δ 162.5, 145.8, 139.0, 138.1, 136.5, 130.0, 128.9, 128.8, 128.7, 127.3, 127.0, 82.8, 31.6, 24.9, 22.2, 21.2.

2.7.13 General procedure for preparation and reaction of *E*- and *Z*- iodonium salts



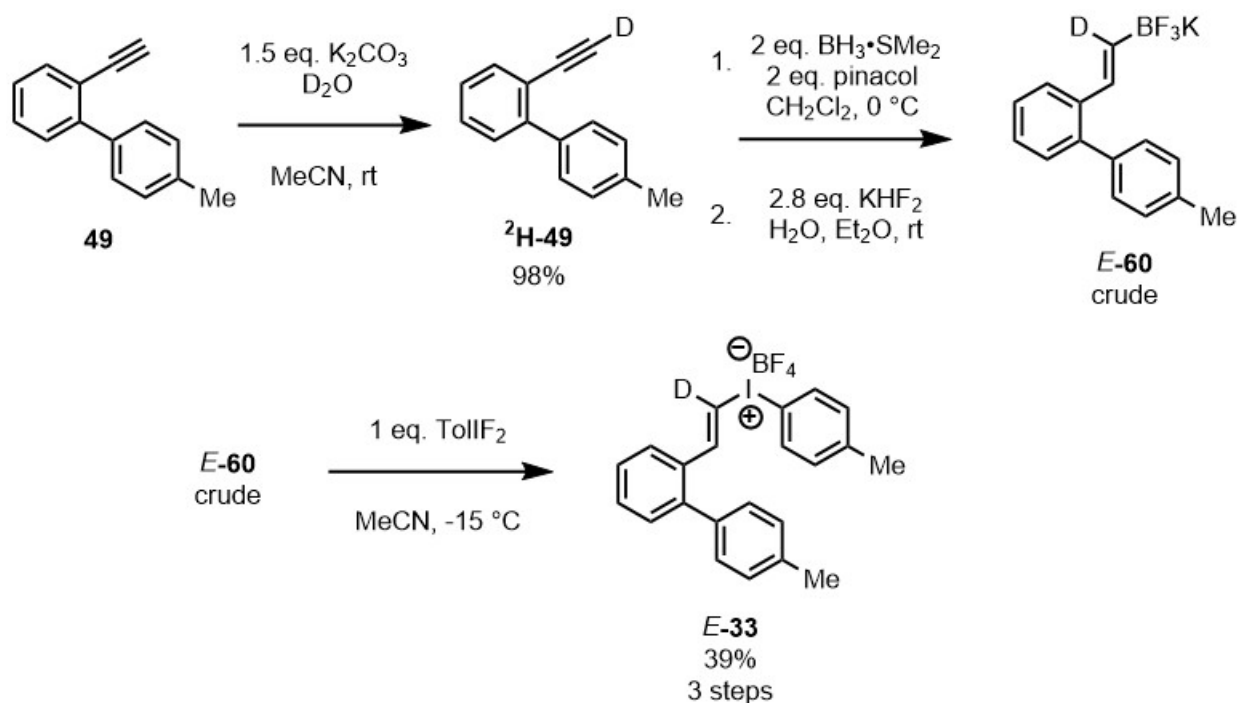
Step 1: To an oven dried 10 mL round bottom flask with a magnetic stir bar was charged with boronate ester (0.1 mmol, 1 eq.) and anhydrous dichloromethane and placed in a brine bath with stirring. Boron trifluoride diethyl etherate (0.12 mmol, 1.2 eq.) was slowly added dropwise as a 10% solution in dichloromethane over a period of 5 minutes. After complete addition, the reaction was stirred at -10 °C for 10 minutes. Iodobenzene diacetate (0.12 mmol, 1.2 eq.) dissolved in 1 mL of dichloromethane was added dropwise over a period of 5 minutes. After complete addition, the reaction was allowed to stir and slowly warm to room temperature over 30 minutes. A saturated aqueous solution (2 mL) of NaBF₄ was added and the mixture was stirred for another

5 minutes. The reaction flask was added to a separatory funnel and the organic layer is collected. The organic solvent was removed by rotary evaporation to give a dark coloured oil. The crude product was analyzed by NMR spectroscopy before proceeding with the next step.

^{19}F NMR (282 MHz, CDCl_3) δ -147.7.

Step 2: The crude product from the previous reaction was diluted with anhydrous chlorobenzene (2 mL) and divided into two microwave vials with 1 mL each and stirred for 1 minute. $\text{BF}_3 \cdot \text{OEt}_2$ (0.03 mmol, 0.3 eq.) was added by syringe, and one vial immersed in a preheated 110 °C oil bath, and the other placed in a room temperature oil bath and then heated to 110 °C. After 2 hours, the reaction was allowed to cool to room temperature, the solvent was removed by rotary evaporation and the product yield and isomeric ratio was measured by NMR spectroscopy of the crude product.

2.7.14 Synthesis of (*E*)-(2-(4'-methyl-[1,1'-biphenyl]-2-yl)vinyl-1-D)(*p*-tolyl)iodonium tetrafluoroborate (*E*-33)



Step 1: To a 25 mL round bottom flask, a solution of 2-ethynyl-4'-methyl-1,1'-biphenyl (1.56 mmol, 1 eq.) in anhydrous acetonitrile (5 mL), K_2CO_3 (3.12 mmol, 2 eq.) and 1.5 mL of D_2O was added and stirred at room temperature under nitrogen for 2 hours. The solvent was evaporated with a rotary evaporator and the residue extracted with diethyl ether, washed 2 x with water and 1 x with brine. The organic solvent was dried over anhydrous $MgSO_4$ and evaporated to give **²H-49** (98%) as a colourless oil.

¹H NMR (300 MHz, $CDCl_3$) δ 7.62 ($J = 8.0$ Hz, 1H), 7.50 (d, $J = 8.1$ Hz, 2H), 7.41 – 7.36 (m, 2H), 7.32 – 7.22 (m, 3H), 2.40 (s, 3H). Spectral data was consistent with those reported in the literature.¹

Step 2: To an oven dried 50 mL round bottom flask with a magnetic stir bar was charged with pinacol (6.5 mmol, 2 eq.) and anhydrous dichloromethane (10 mL) and cooled in an ice bath with stirring. $BH_3 \cdot SMe_2$ (6.5 mmol, 2 eq.) was added dropwise. After complete addition, the reaction was allowed to stir for 2 hours slowly warming to room temperature. **²H-49** was added dropwise as a dichloromethane solution, and allowed to stir for 24 hours. The solvent was evaporated using a rotary evaporator to yield a yellow oil. The yellow oil was diluted with diethyl ether and stirred with KHF_2 (9.1 mmol, 2.8 eq.) and 1 mL of H_2O for 16 hours. The organic solvent was removed by rotary evaporation, and the residue was extracted with acetone and filtered to remove inorganic salts. The organic salt precipitated with addition of diethyl ether and was collected by filtration and dried under vacuum to give a pale-yellow solid ***E*-60** (42%) which was used crude for the next step.

Step 3: To a solution of ***E*-60** (0.2 mmol, 60 mg, 1.0 eq.) in anhydrous acetonitrile (10 mL) in a PFA vial was added iodotoluene difluoride (0.2 mmol, 51 mg, 1.0 eq.) in a -15 °C bath under nitrogen, and the mixture was stirred for 15 minutes. The solvent was evaporated with a rotary

evaporator and the residue was extracted with dichloromethane (5 mL). A saturated aqueous solution (1 mL) of NaBF₄ was added, and the mixture was stirred for another 15 minutes. The reaction was diluted with dichloromethane, and the aqueous layer was removed in a separatory funnel. The organic solvent was washed with brine, dried over MgSO₄ and then filtered with a glass funnel. Rotary evaporation yielded an oil, which was washed several times with hexanes by decantation. Further purification by decantation using hexanes and diethyl ether yielded *E*-**33** (92%) as a pale-yellow oil which darkened upon storage.

¹H NMR (500 MHz, CDCl₃) δ 7.87 (d, *J* = 7.9 Hz, 2H), 7.64 (d, *J* = 7.6 Hz, 2H), 7.50 – 7.29 (m, 10H), 7.13 (d, *J* = 6.4 Hz, 2H) 2.43 (s, 3H), 2.32 (s, 3H). **¹⁹F NMR** (282 MHz, CDCl₃) δ -147.7.

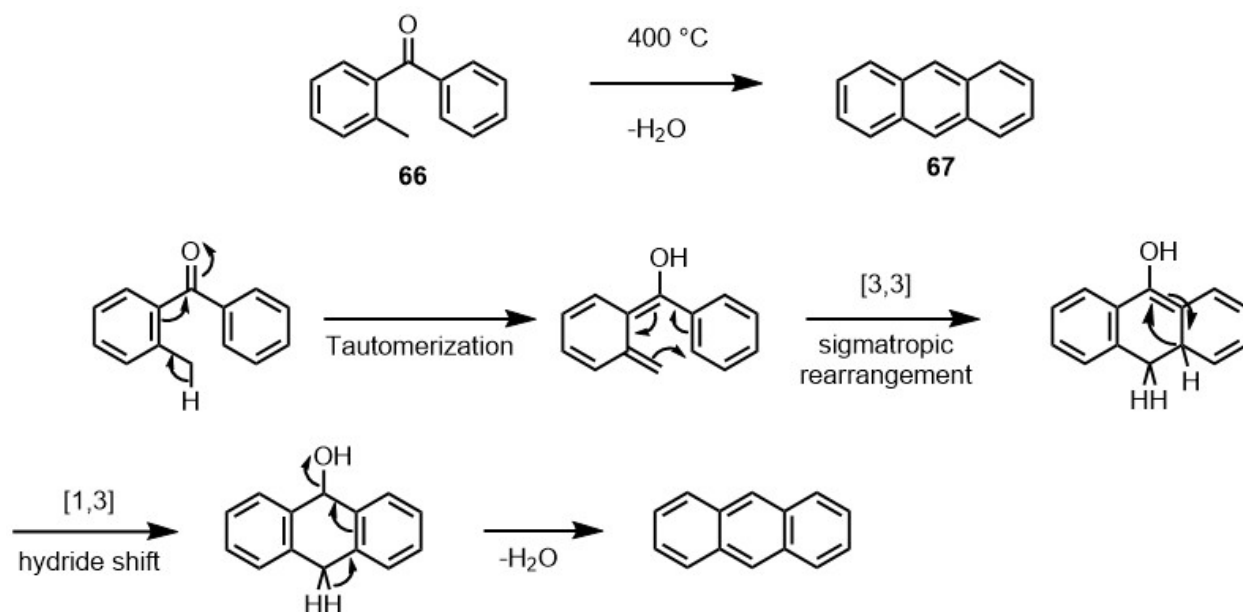
HRMS: 430.0772, MS/MS: 194.1084

Spectral data was consistent with those reported in the literature.¹

Chapter 3: Umpolung Electrophilic Cyclizations

3.1 Background: Phenacenes

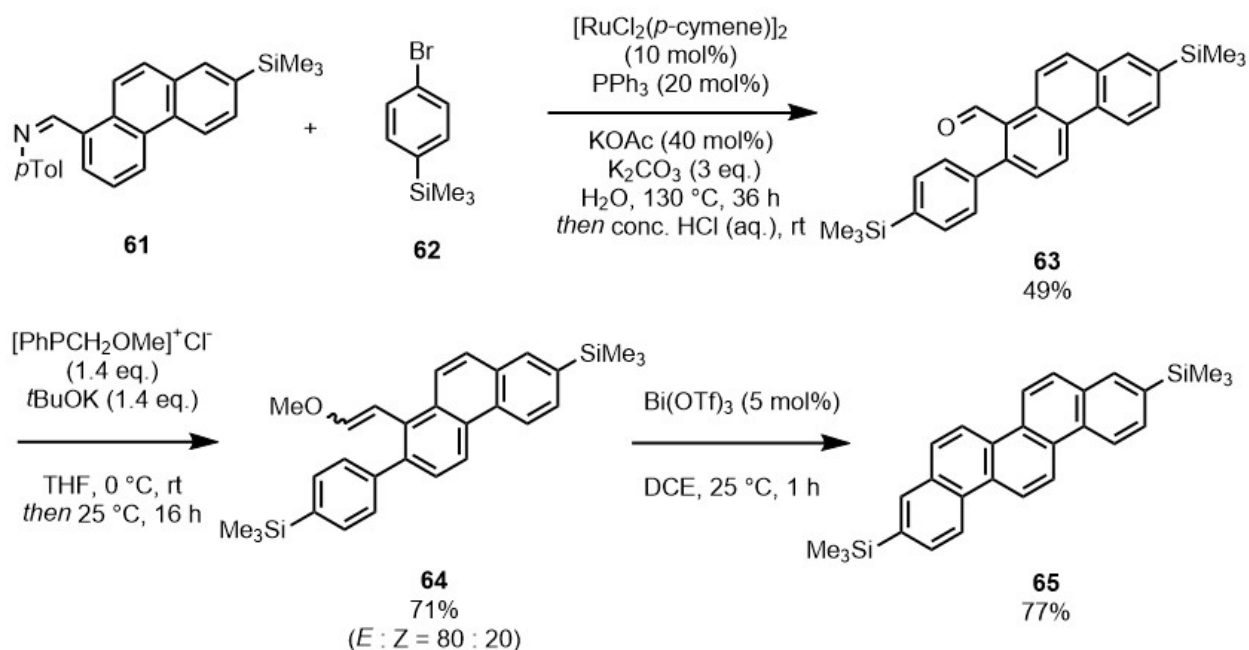
Phenacenes, especially picene, have been shown to be ideal molecules for organic electronics.⁴ Linear acenes, such as pentacene, are well established organic semiconductors, however are prone to oxidation by air and light.⁶⁵ Phenacenes are stable toward oxidation,⁴ however the main drawback with phenacenes is that there is limited synthetic access compared to that of acenes.⁶⁶ One of the oldest methods of acene synthesis is demonstrated in the Elbs reaction, first published in 1884.⁶⁷ It describes the synthesis of [3]acene (**67**) from *ortho*-methyl benzophenone (**66**) which occurs spontaneously after heating to 400 °C. A suggested mechanism occurs through enol tautomerization, a [3,3]-pericyclic reaction, followed by a [1,3]-hydride shift and elimination of water (Scheme 3.1).



Scheme 3.1: Synthesis of acene (67) by Elb's reaction.

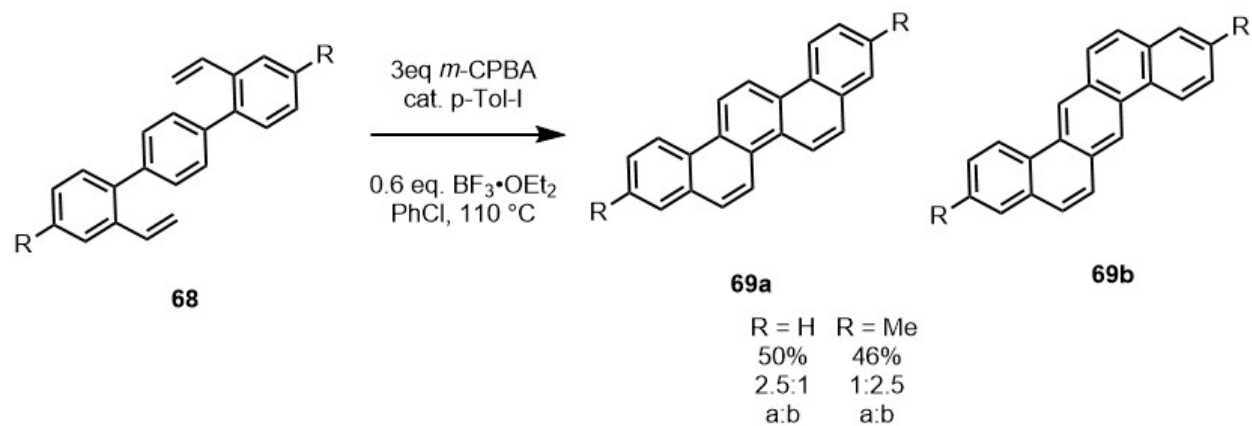
Phenacenes on the other hand, are not as trivial. For example, 3,10-disilyl[5]phenacene **65** can be synthesized in 3 steps from imine precursor **61**.⁶⁸ The imine serves as a transient directing

group. Bromoarene **62** is coupled with imine **61** via a ruthenium catalyzed *ortho*-directed C-H arylation, hydrolysis of the crude product provides aldehyde **63** in 49% yield. Methyl enol ether **64** is prepared from **63** with the methoxymethylenetriphenylphosphine Wittig reagent. Lewis acid catalyzed cyclization of the enol ether with bismuth triflate provides the 3,10-disilyl[5]phenacene **65** in 77% yield (Scheme 3.2, 27% over 3 steps).



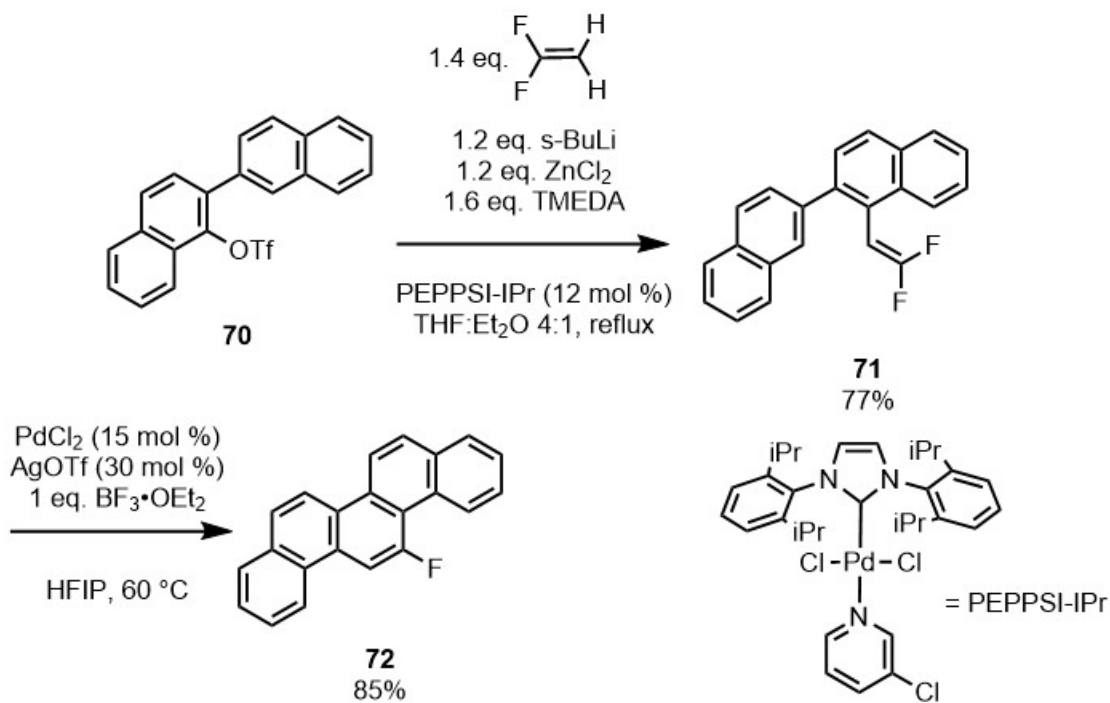
Scheme 3.2: Synthesis of phenacene (65**) via ruthenium catalyzed *ortho*-directed C-H coupling**

It was found that our reaction was suitable to the synthesis of phenacenes¹ on simple substrate **68** it produced picene **69a** and dibenzo[*a,h*]anthracene **69b**. A mixture of regioisomers was obtained, and selectivity appeared to be controlled electronically (Scheme 3.3).



Scheme 3.3: Synthesis of picene and dibenzo[a,h]anthracene by alkene arene coupling

A problem with phenacenes and polycyclic aromatic hydrocarbons (PAHs) in general is their low-solubility in organic solvents as the number of rings increases.⁶⁹ As a result of this, synthesis becomes more difficult and it limits their application in microelectronics. The Ichikawa group found that mono-fluorination of phenacenes can drastically increase the solubility of PAHs without altering their electronic properties as semi-conductors. Fluorine acts as an electron-withdrawing group to increase solubility in organic solvents by inducing a dipole moment in the molecule and enhancing resistance to oxidation by decreasing electron density in the molecule's π -orbitals.⁷⁰ The group synthesized monofluorinated phenacene **72** using a palladium catalyzed Friedel-Crafts type cyclization of a vinylic CF_2 carbon (Scheme 3.4).

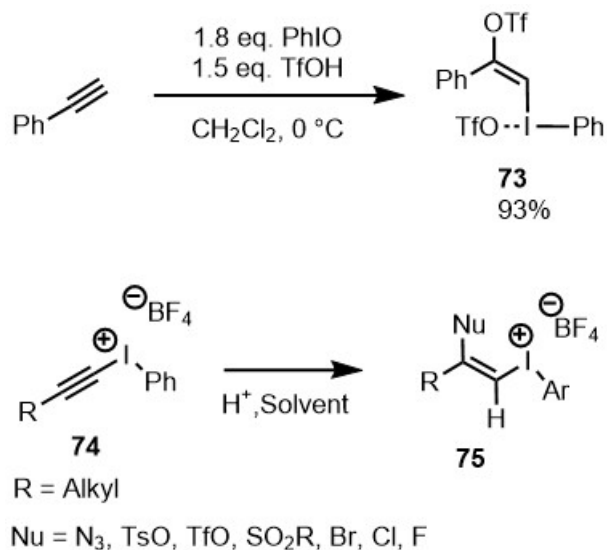


Scheme 3.4: Synthesis of fluorinated phenacene (72) via a palladium catalyzed cyclization

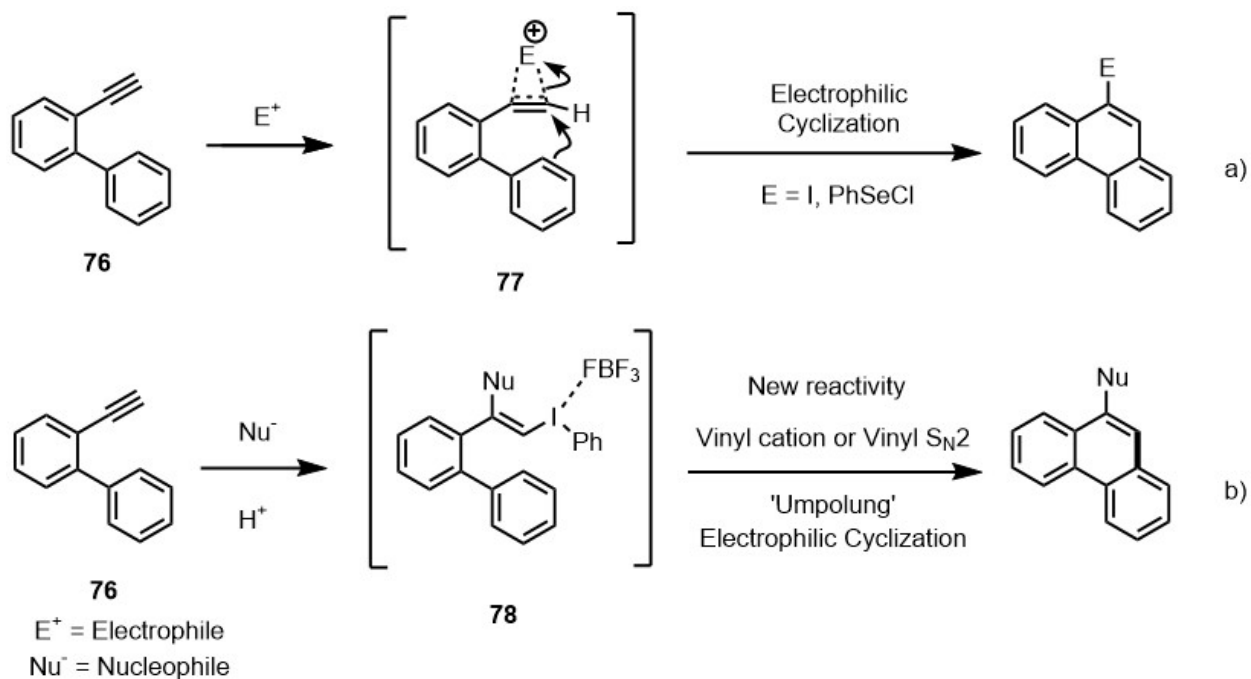
3.2 Fluorovinyl (aryl)iodonium salts

Having identified vinyl (aryl)iodonium salts as possible reaction intermediates, and given that there are many methods to substituted synthesize β -substituted vinyl (aryl)iodoniums via nucleophilic additions to aliphatic alkynes and phenylacetylene (Scheme 3.5),^{71, 72} a hypervalent iodine mediated synthesis of heteroatom-substituted PAHs may be possible. The formal conversion of alkyne **76** to phenanthrene can be achieved through a traditional electrophilic cyclization, in which the α -carbon is rendered nucleophilic (Scheme 3.6, a, **77**). Examples include electrophiles such as ICl and PhSeCl, providing 2-iodophenanthrene and 2-(phenyl)selenylphenanthrene respectively. Here, we propose to reverse the polarity of the alkyne such that a nucleophile is instead added to the α -carbon (Scheme 3.6, b, **78**) resulting in an ‘umpolung’ alkyne electrophilic cyclization (Scheme 3.6, b). The scope of viable nucleophiles includes halogens,⁷³ azides,⁷⁴ triflates,⁷⁵⁻⁷⁸ sulfones,^{79, 80} (Scheme 3.5) and other typically soft

nucleophiles as the starting alkyne **76** will dictate the relative positions of the nucleophile and the bond being formed, there is significant potential for realizing broad product diversity (Scheme 3.6, b).

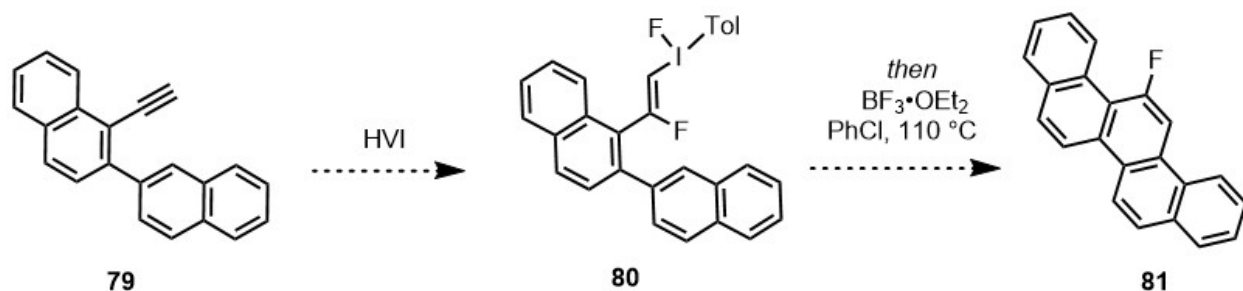


Scheme 3.5: Preparation of triflyl vinyl iodonium triflates and fluorovinyl iodonium tetrafluoroborates from alkynes



Scheme 3.6: Umpolung electrophilic cyclization of alkynes in the synthesis of phenanthrenes

Based on this knowledge, we propose a strategy towards monofluorinated phenacene (Scheme 3.7, **81**) that uses cheap precursors and avoids the use of both transition metals and CF_2 containing precursors. We will attempt to develop the method to synthesize fluorinated phenanthrenes so that it can be applied to the synthesis of fluorinated phenacenes.

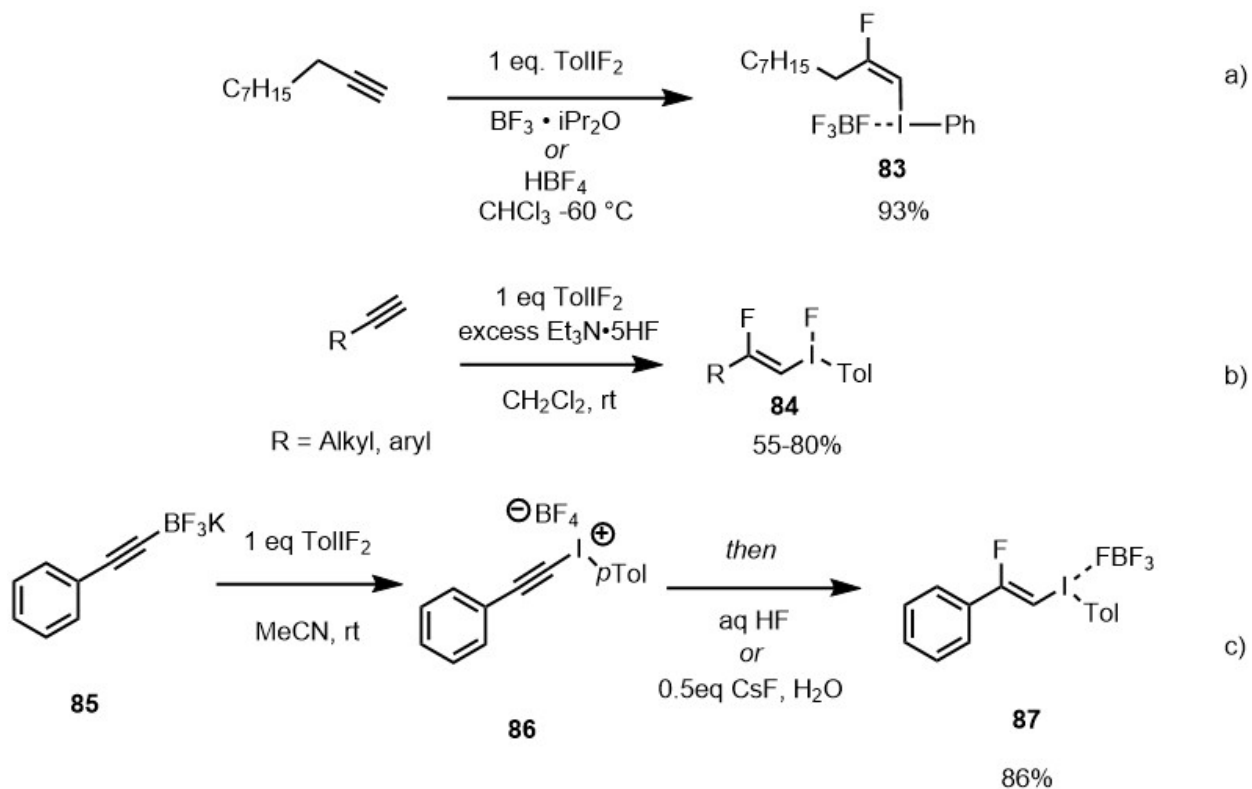


Scheme 3.7: A potential one-pot synthesis of monofluorinated picene (62**) by iodonium salt mediated alkene arene ring closure**

To start, we will examine the various published methods for the synthesis of the *E*- and *Z*-2-fluorovinyl (aryl)iodonium salts, compare and contrast their strengths, weaknesses, and scope of reactivity in order to determine the best strategy to pursue. Most methods to synthesize the 2-fluorovinyl (aryl)iodonium salts are applicable only to alkyl substituted terminal alkynes (Scheme 3.8, a), while the methods for aromatic alkynes are limited. Both stereoisomers of 2-fluorovinyl (aryl)iodonium salts are accessible, either of which could act as an intermediate in the proposed reaction.

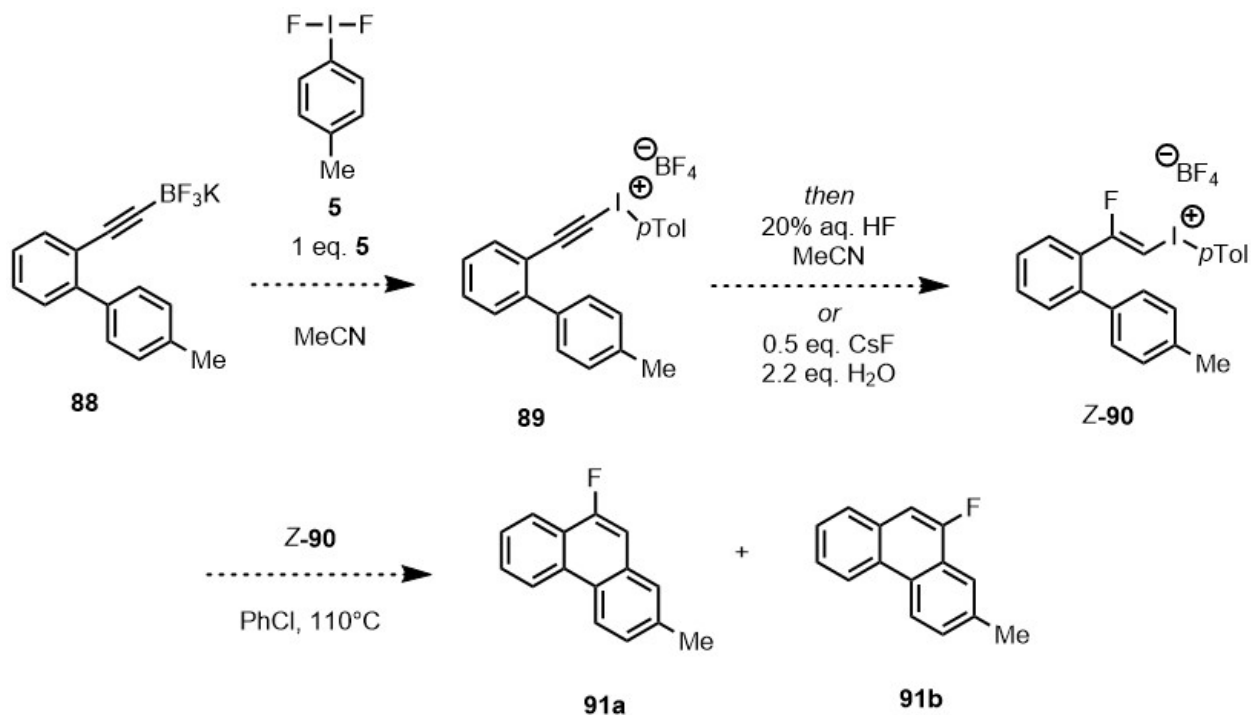
The *E*-2-fluorovinyl (aryl)iodonium salt **83** can be prepared directly from the alkyne in one step in an atom economical fashion from ToIIF_2 and $\text{BF}_3 \cdot \text{OEt}_2$ ⁸¹ or HBF_4 ⁸² (Scheme 3.8, a, **83**), while *Z*-2-fluorovinyl iodonium salts have been prepared in a similar manner with ToIIF_2 and $\text{Et}_3\text{N} \cdot 5\text{HF}$ (Scheme 3.8, b).⁸³ These strategies are attractive because if they work on our substrate alkyne **49**, they could provide a simple, atom economical one-pot procedure for the synthesis of mono-fluorinated phenanthrene from the alkyne (Scheme 3.10, **49**). However, out of all of these

methods, only the *Z*-2-fluorovinyl (aryl)iodonium salts prepared with ToIF_2 and $\text{Et}_3\text{N}\cdot 5\text{HF}$ have been demonstrated to work on phenylacetylene vs aliphatic substituted alkynes.

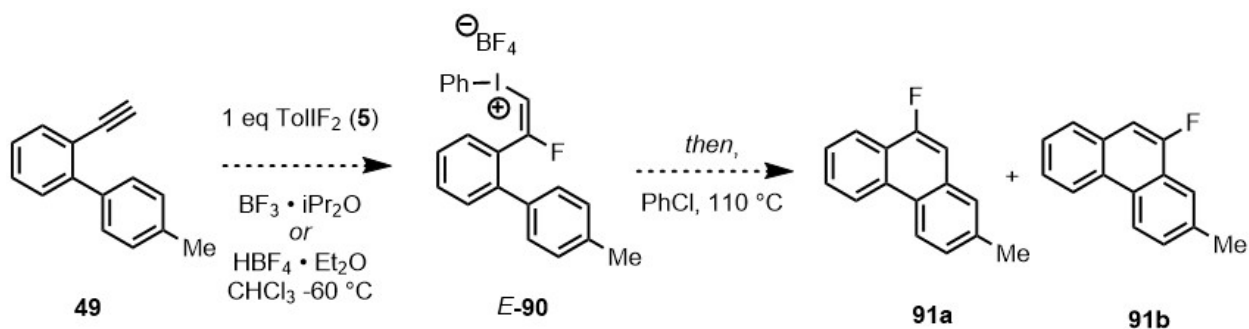


Scheme 3.8: Known synthetic methods to *Z*- and *E*-2-fluoro vinyl(phenyl)iodonium salts

We will prepare the *Z*-2-fluorovinyl iodonium salt **Z-90** from either one of these methods, and then subject it to our reaction conditions. Ideally, we can design a similar one-pot procedure. Alternatively, the alkynyl (phenyl)iodonium salt can be prepared by other means from phenylacetylene^{58,59} and then fluorinated with the stated methods; however, yields are expected to be lower. The alkynyl (aryl)iodonium salt is not very stable towards isolation and known to decompose rapidly after isolation.⁵⁵



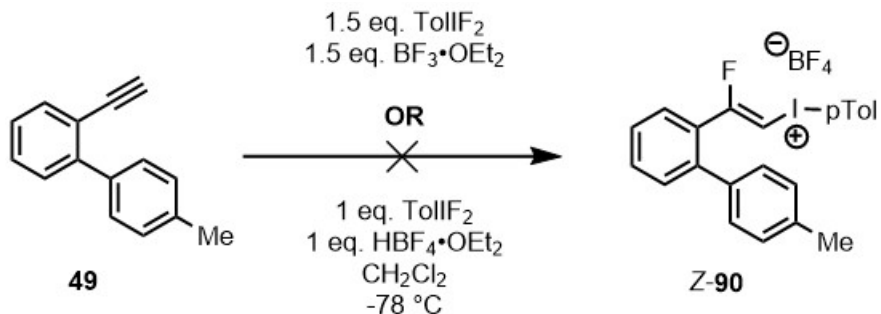
Scheme 3.9: Proposed synthesis of fluorophenanthrenes from tetrafluoroborate salt (88)



Scheme 3.10: Proposed synthesis of fluorophenanthrenes from alkyne (49) and TollIF₂

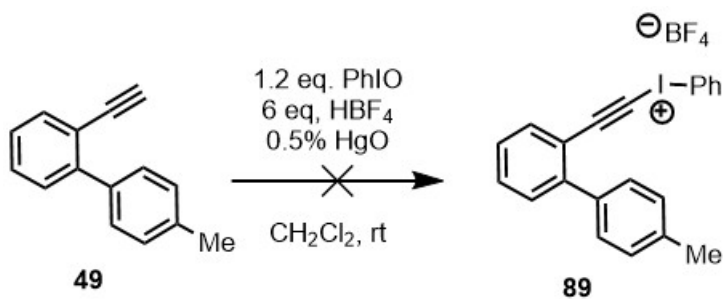
3.3 Results

First, the most direct methods applicable to alkyl substituted alkynes were tested on our alkyne substrate **49**, on the chance that they might offer direct conversion into the fluorinated phenanthrene. In each method tested only tar was produced.



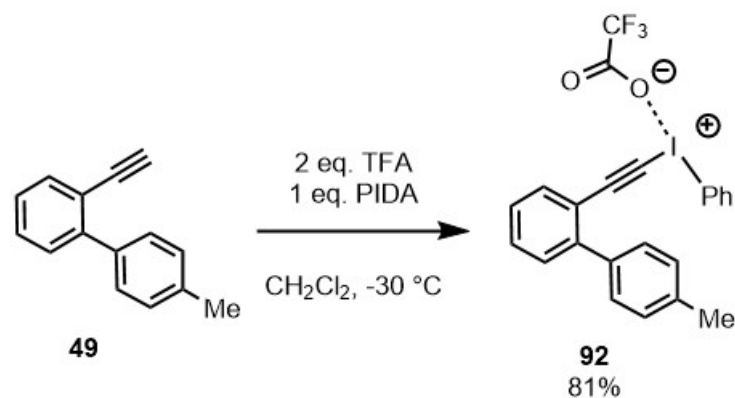
Scheme 3.11: Attempted syntheses of Z-90 from terminal alkyne (49) with TollF₂

In response, it was decided to approach the desired 2-fluorovinyl iodonium Z-90 in a stepwise manner via hydrofluorination of the alkynyl iodonium salt 89, which had precedent for reaction with phenylacetylene in the literature.^{84,85} First, the method by Hara was attempted directly from the alkyne 49. However, the reaction only produced traces of 89 detectable by NMR, and could not be isolated. This method is known to be difficult to reproduce.⁸⁶



Scheme 3.12: Attempted synthesis of alkynyl (phenyl)iodonium salt (89) from 49

In a publication by Dixon and co-workers,⁸⁶ it was found that a combination of PhI(OAc)₂ and trifluoroacetic acid could provide alkynyl iodonium trifluoroacetates in good yield. When our substrate was subjected to these conditions, gratifyingly the alkynyl iodonium trifluoroacetate 92 was obtained in 81% yield and isolated as white crystalline needles. An X-ray diffraction crystal structure was obtained, which displayed the iodonium salt as a dimeric structure, which may account for its stability and crystallinity.



Scheme 3.13: Synthesis of alkynyl (phenyl)iodonium trifluoroacetate (92**)**

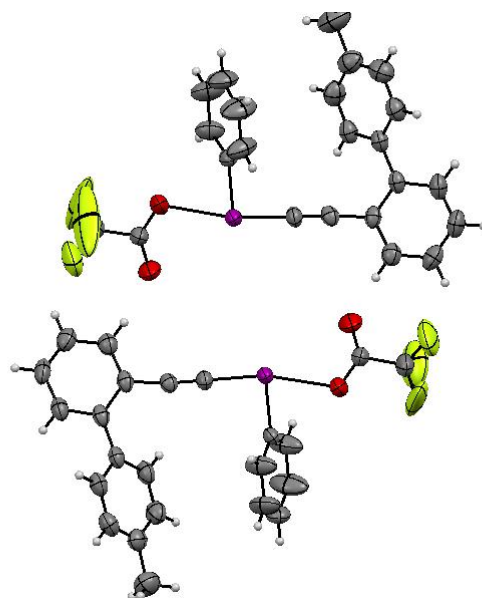


Figure 3.1: X-ray diffraction crystal structure model of **92 as a dimer**

Hydrofluorination was attempted following methods published in the literature by reacting aqueous aq. HF,⁸⁴ Et₃N•3HF,⁸⁴ or CsF/H₂O⁸⁵ with the alkynyl iodonium salt **92**. However, in each case, the alkynyl iodonium was found to be unreactive, or decomposed to give trace yields of complex mixtures and only traces desired fluorinated phenanthrene (Table 3.1, **91a**). Other trace fluorinated products were detected, and these were suspected to be the trifluoroacetyloxyphenanthrene, which might result as a decomposition of **92** with the trifluoroacetate anion acting as a nucleophile. Since the literature examples only contained the

fluorination of alkynyl iodonium tetrafluoroborate salts, it was thought that the trifluoroacetate anion must be too stabilizing and too nucleophilic for the weakly nucleophilic fluoride to compete in the reaction. Anion exchange with a saturated solution of sodium tetrafluoroborate was attempted to produce the alkynyl iodonium tetrafluoroborate salt; however, the trifluoroacetate salt **92** was recovered unchanged. The use of a more strongly polar solvent might facilitate the anion exchange, by coordinating to the iodine center and weakening the bond with the trifluoroacetate. However, instead of pursuing the conditions to exchange the anion, the direct synthesis of the alkynyl iodonium tetrafluoroborate salt **89** was reinvestigated in an effort to develop a more atom efficient and simple process.

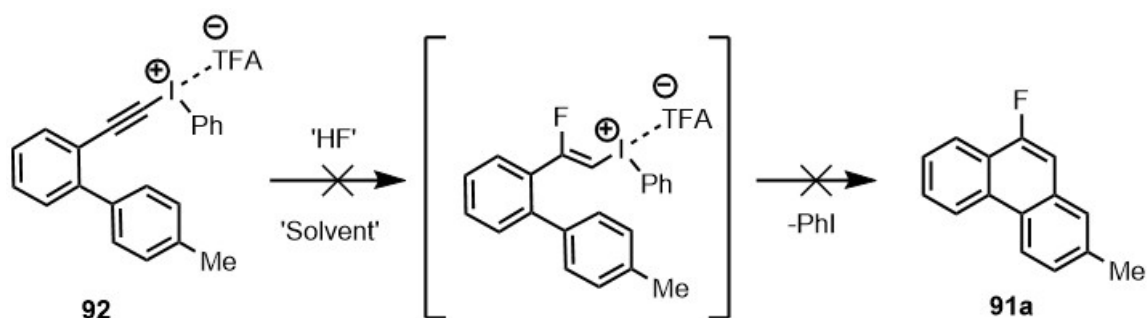
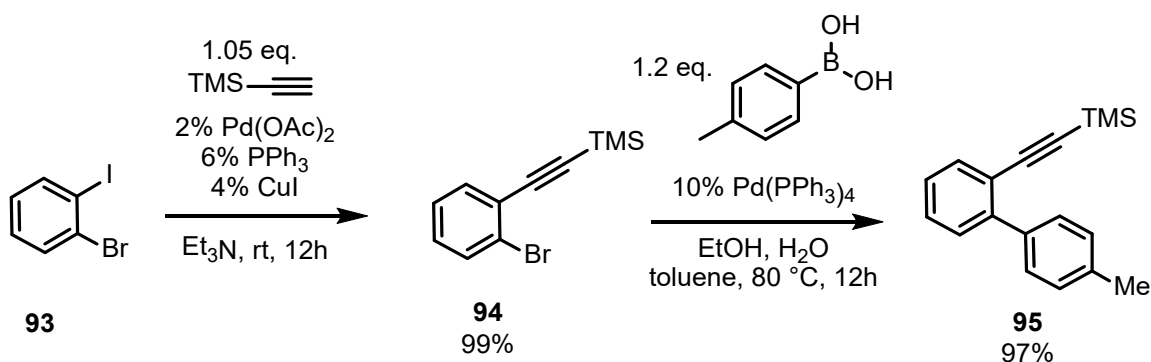


Table 3.1: Attempted fluorination of 92

Entry	HF Source	Solvent	Temperature	% conversion	% yield 91a
1	48% aq. HF	CHCl ₃	rt (22) °C	0%	0%
2	48% aq. HF	MeCN	60 °C	>98%	Trace
3	Et ₃ N • 3HF	CHCl ₃	rt	0%	0%
4	Et ₃ N • 3HF	MeCN	60 °C	>98%	Trace

While we did not have success in preparing the alkynyl iodonium tetrafluoroborate from the terminal alkyne **49**, successful methods have employed substituted alkynes using boron –

iodine(III) exchange,⁶² or the trimethylsilane – iodine(III) exchange.⁸⁷ We decided to investigate the alkynyl trimethylsilane **95** as a precursor, since trimethylsilyl phenylacetylenes can be prepared easily and in excellent yield by Sonogashira reaction of trimethylsilylacetylene and an aryl iodide.⁸⁸ We proposed a 2-step synthesis of the trimethylsilyl substituted alkyne **95** from 2-bromoiodobenzene by sequential Sonogashira and Suzuki reactions,⁶⁰ which proceeded to give **95** cleanly in 97% yield over two steps (Scheme 3.14).



Scheme 3.14: Preparation of alkynyl silane (**95**) in fast 2-step process

With trimethylsilyl alkyne **95** in hand, we attempted the silicon-iodine(III) exchange using the conditions described by Ochiai.⁸⁷ The alkynyl silane was reacted with an iodosoarene which was then activated by $\text{BF}_3 \cdot \text{OEt}_2$. After addition of aq. NaBF_4 solution, the crude alkynyl (aryl)iodonium tetrafluoroborate salt **89** could be isolated by extraction with dichloromethane and crystallization in the freezer as a waxy red solid or oil. The crude product (**89**, 60% NMR yield) was not of good purity, the product quickly darkened and decomposed at room temperature, and could not be crystallized. When the reaction was performed with freshly distilled $\text{BF}_3 \cdot \text{OEt}_2$, it gave a product of higher purity and in greater yield. Cooling the reaction in a dry ice bath before adding the $\text{BF}_3 \cdot \text{OEt}_2$ offered some improvement as well. Since our objective is to produce the 2-fluorovinyl iodonium salt **Z-90**, the crude alkynyl iodonium salt (**89**) without further purification was subjected to the hydrofluorination conditions. We applied the optimized hydrofluorination

conditions reported by Edmond⁸⁵ (CsF/H₂O) and Hara⁸⁴ (aq. HF); however in both cases only traces of the desired vinyl iodonium product **Z-90**, or the fluorinated phenanthrene **91a** were detected. The best result was obtained when Et₃N•3HF was used in combination with acetonitrile (Table 3.2, entry 6), the 2-fluorovinyl iodonium salt was detected by crude NMR (~10%).

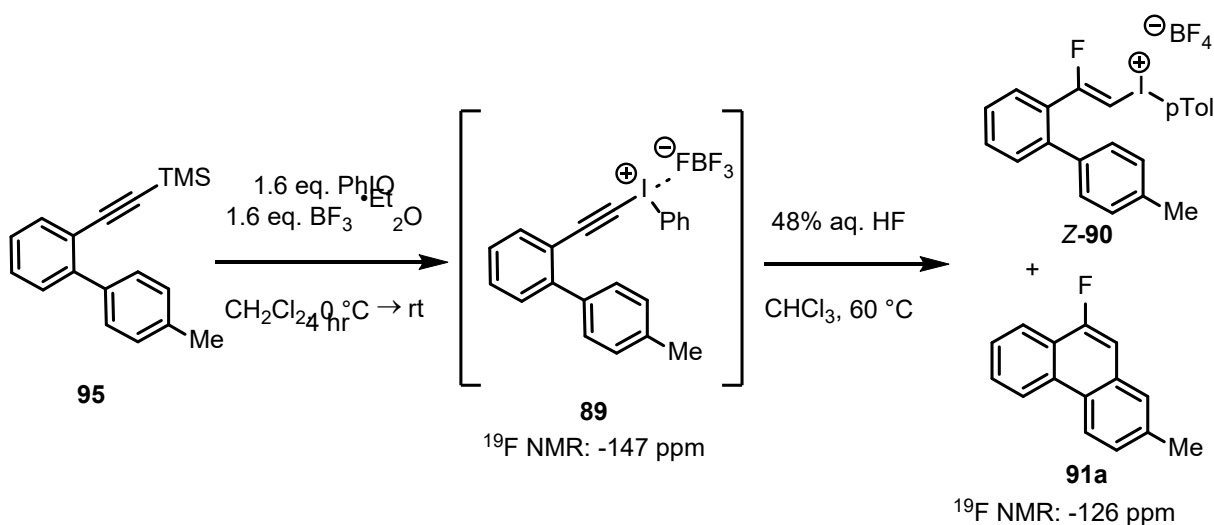
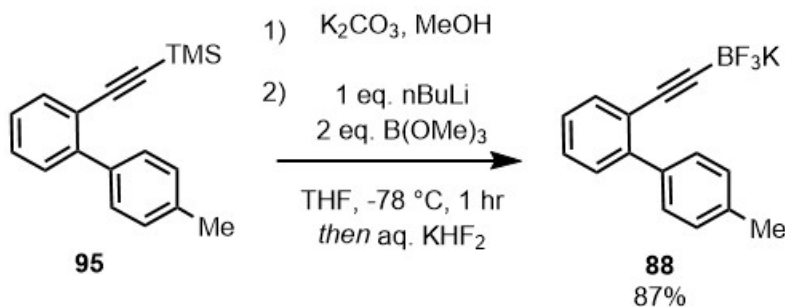


Table 3.2: Fluorination of alkynyl iodonium BF₄ derived from alkynyl-TMS

Entry	HF Source	Solvent	Temperature	% yield Z-89
1	CsF	MeCN	60 °C	0%
2	CsF	MeOH	60 °C	0%
3	20% aq. HF	MeCN	60 °C	Trace
4	20% aq. HF	CHCl ₃	60 °C	Trace
5	48% aq. HF	CHCl ₃	60 °C	~5%
6	Et₃N•3HF	MeCN	60 °C	~10%

Not being satisfied with the quality of the alkynyl iodonium salt intermediate produced from the alkynyl silane **95**, we sought to improve the synthesis. The boron – iodine(III) exchange of alkynyl potassium trifluoroborates with ToIIF_2 ⁶² was selected because it has been demonstrated to provide alkynyl iodonium salts in high yield. The reaction conditions are mild and do not require the addition of an acid for activation. The process is also highly atom efficient, producing only the iodonium tetrafluoroborate salt and potassium fluoride as the sole products, making it ideal for application to a one-pot hydrofluorination reaction for the synthesis of **91**. The best reaction conditions for hydrofluorination of *Z*-**90** is with $\text{Et}_3\text{N}\cdot 3\text{HF}$ (0.2 mL, 30 eq.) and acetonitrile (2 mL) as a solvent. The trifluoroborate **68** can be prepared from the terminal alkyne **49** by preparation of the lithium acetylide and reaction with a triethyl borate, followed by the addition of aqueous potassium bifluoride. Following this strategy, the alkynyl trimethylsilane **95** was transformed into the terminal alkyne **49** by protodesilylation with K_2CO_3 in methanol, and the crude alkyne **49** was used directly to prepare the alkynyl trifluoroborate **88** in 87% yield.



Scheme 3.15: Synthesis of alkynyl trifluoroborate **88 from alkyne **95****

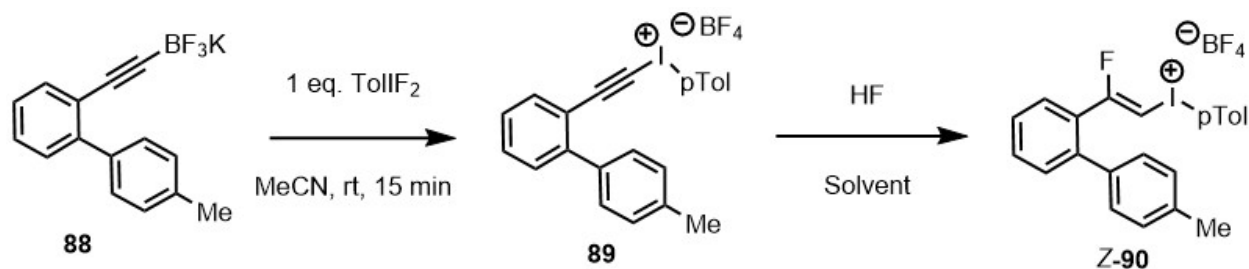


Table 3.3: Optimization of Z-90 synthesis from alkyne trifluoroborate (88**) starting material**

Entry	HF Source	Solvent	Temperature	Time	Yield Z-90
1	20% aq. HF	MeCN	rt	24 h	0%
2	Et ₃ N•3HF	MeOH	rt	24 h	0%
3	Et ₃ N•3HF	MeCN	60 °C	4 h	10%
4	20% aq. HF	CHCl ₃	60 °C	4 h	10%
5	20% aq. HF	MeCN	60 °C	4 h	3%
6	Et ₃ N•3HF	MeCN	rt	72 h	~10%
7	Et ₃ N•3HF	MeCN	40 °C	24 h	35%
8	Et ₃ N•3HF	MeCN	reflux(82 °C)	6 h	8% ^a
9	Et₃N•3HF	MeCN	70 °C	6 h	45%
10	Py•9HF	MeCN	Rt	24 h	trace
11	Py•9HF	MeCN	60 °C	6 h	trace

a) A side product was produced, appearing as a high molecular weight compound derived from acetonitrile and triethylamine

The alkyne trifluoroborate **88** was reacted with TollF₂ in acetonitrile for 15 minutes, and then an aliquot of Et₃N•3HF was added. When allowed to stir at room temperature, the 2-fluorovinyl iodonium salt was detected with the alkyne iodonium unreacted. When increasing the temperature, the conversion and yield was increased. However, refluxing the reaction resulted in

a decreased yield and the production of a polar, unknown side product. Spectroscopic investigations suggested it was derived from the solvent acetonitrile and triethylamine. The reaction was further optimized, it was found that increasing TolIF_2 had no effect on the reaction, suggesting the second step being the limiting step. Increasing the concentration of $\text{Et}_3\text{N}\cdot 3\text{HF}$ (1 : 10, $\text{Et}_3\text{N}\cdot 3\text{HF}$: MeCN, 30 eq HF) had a significant effect on the yield, when the $\text{Et}_3\text{N}\cdot 3\text{HF}$ concentration was increased to 1 : 3 volume ratio of $\text{Et}_3\text{N}\cdot 3\text{HF}$ to MeCN giving an appreciable 64% isolated yield (66% NMR yield) of the 2-fluorovinyl iodonium salt **Z-90** which was isolated as colourless needles. Further optimization has not yet been carried out, but improvements in the yield were obtained by running the reaction in neat $\text{Et}_3\text{N}\cdot 3\text{HF}$, using freshly prepared TolIF_2 , or TolIF_2 prepared *in situ* from an aryl iodide and an oxidant.

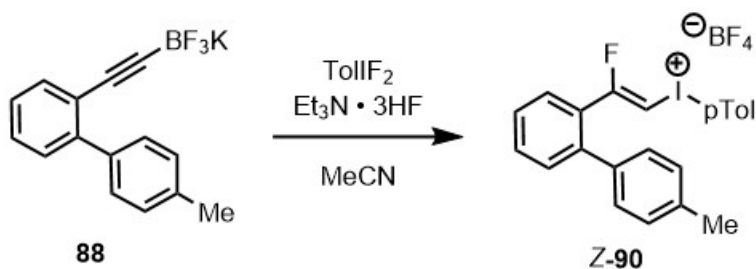
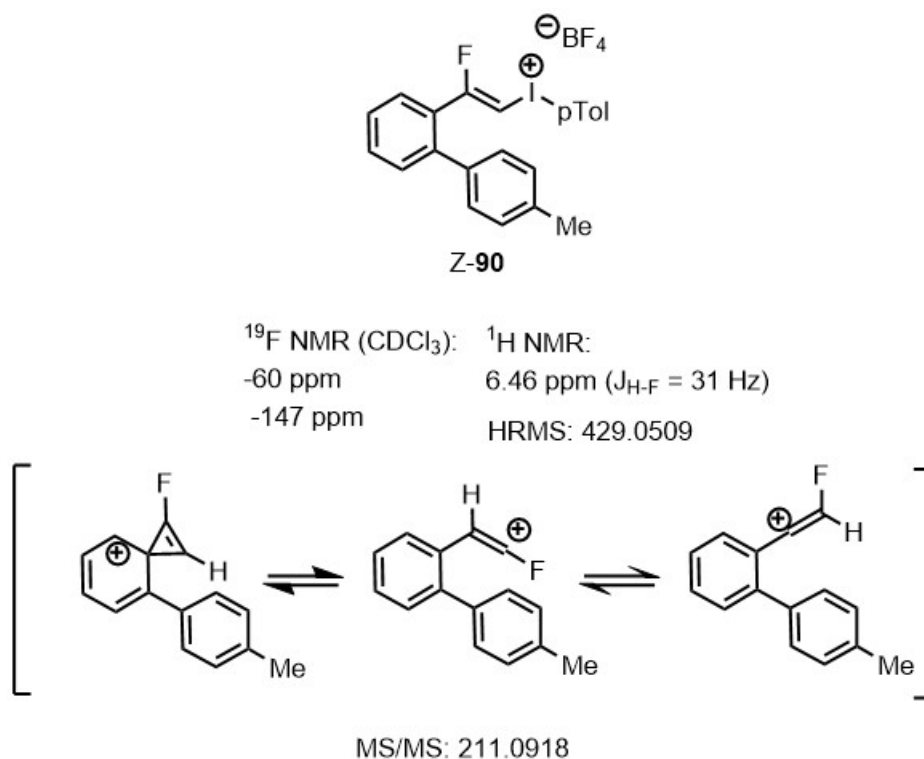


Table 3.4: Further optimization of Z-90 synthesis

Entry	$\text{Et}_3\text{N}\cdot 3\text{HF}$	TolIF_2	Temperature	Time	Yield
1	0.2 mL	1.2 eq.	40 °C	16 h	35%
2	0.2 mL	1.2 eq.	70 °C	16 h	45%
3	0.2 mL	2 eq.	70 °C	6 h	42%
4	1.0 mL	1.2 eq.	70 °C	6 h	66%

^1H NMR displayed a doublet with a chemical shift of 6.46 ppm and coupling value of 31 Hz, characteristic of vinylic trans H-F coupling. ^{19}F NMR displayed the -147 ppm BF_4 peak in

addition to a new -60 ppm peak, which is in the expected region of a vinyl fluoride. An X-ray diffraction crystal structure of the product **Z-90** was obtained, further verifying the product. A high resolution mass spectrum was obtained by electrospray and the iodonium salt with a mass of 429.0509 was detected. When this ion was trapped and fragmented using MS/MS mode, the base peak of 211.0918 was obtained, which indicates a loss of iodotoluene and corresponds to the proposed vinyl cation (Scheme 3.16).



Scheme 3.16: HRMS of Z-90 and fragment ions detected in MS-MS mode

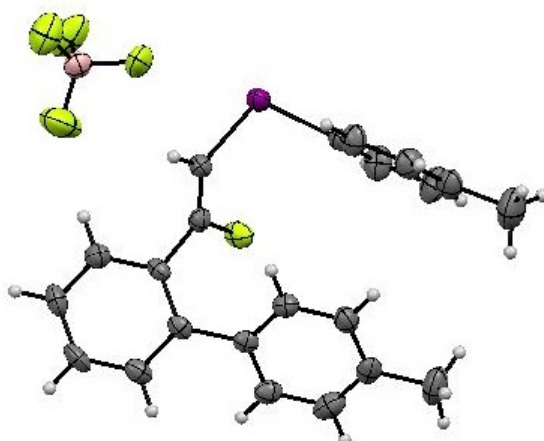


Figure 3.2: X-ray diffraction crystal structure of Z-90

Finally, the 2-fluorovinyl (aryl)iodonium salt **Z-90** was subjected to thermal conditions to test our hypothesis. The iodonium salt was refluxed with a range of solvents. With acetonitrile, no reaction was observed. When DCE was used as a solvent a byproduct was observed, which upon investigation of the coupling constants and chemical shifts observed in the ^1H and ^{19}F NMR spectra appeared to represent the chlorofluoroalkene **96**. Vinyl (aryl)iodonium salts and vinyl cations have been observed to abstract chlorine atoms from chlorinated solvents previously.⁷² Conversion to the expected fluorinated phenanthrene was finally observed when heating with chlorobenzene. Surprisingly, 57% of the 2-fluorovinyl iodonium salt **Z-90** remained unconverted even when heated to 110 °C for 2 hours. To our satisfaction, reflux with chlorobenzene (132 °C) provided the fluorinated phenanthrene **91a** as a single isomer in 100% conversion and quantitative yield (Table 3.5, entry 4).

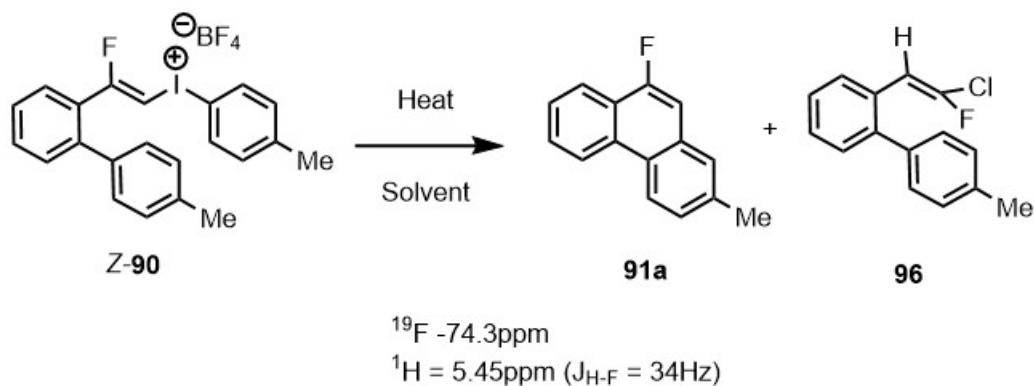


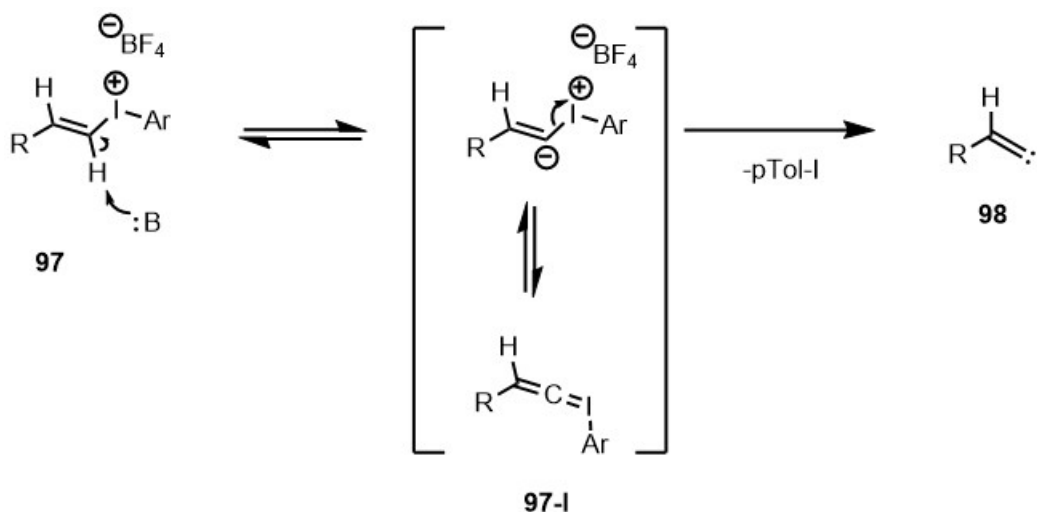
Table 3.5: Solvent and temperature screening in thermal decomposition of Z-90

Entry	Solvent	Temp.	Time	Yield	Products
1	MeCN	reflux (82 °C)	48 h	No rxn	N/A
2 ^a	DCE	reflux (84 °C)	2 h	45%	1.4 : 1 (96 : 91a)
3	PhCl	110 °C	2 h	43%	1.3 : 1 (Z-90 : 91a)
4	PhCl	reflux (132 °C)	2 h	>99%	91a

a) After 2 hours of reflux in DCE, the reaction was refluxed in PhCl for 1 h, to convert unreacted **Z-90** into product **91a**.

3.4 Discussion

Interestingly, the 2-fluorovinyl iodonium salt exhibited remarkable stability, persisting in the reaction mixture for hours at temperatures above 100 °C. In addition, the yield of phenanthrene (**91a**) was quantitative and no other byproducts were detected. This result is a very striking difference between the other vinyl (aryl)iodonium salts investigated in this thesis, including the vinyl (aryl)iodonium salts which decomposed to give a single product in a high yield (Scheme 3.19).

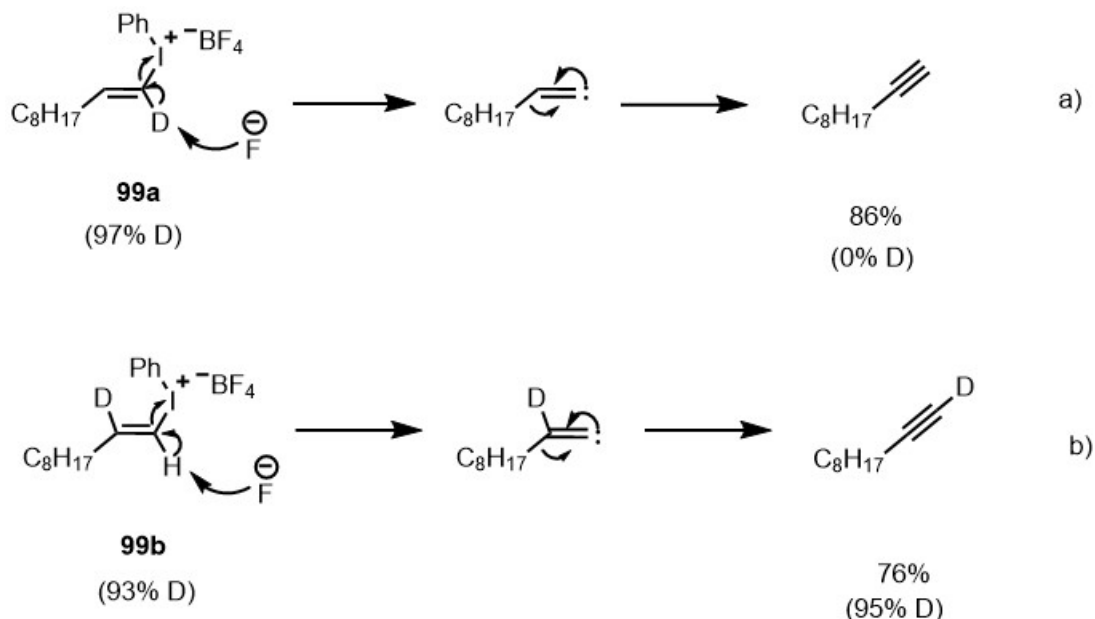


Scheme 3.17: Deprotonation of vinyl (aryl)iodonium salt (75) and α -elimination for generation of vinylidene carbene (76)

We should first discuss a little bit about the reactivity of vinyl (aryl)iodonium salts, in order to answer the question, why is *Z*-**90** stable to thermal decomposition compared to more typical vinyl (aryl)iodonium salts?

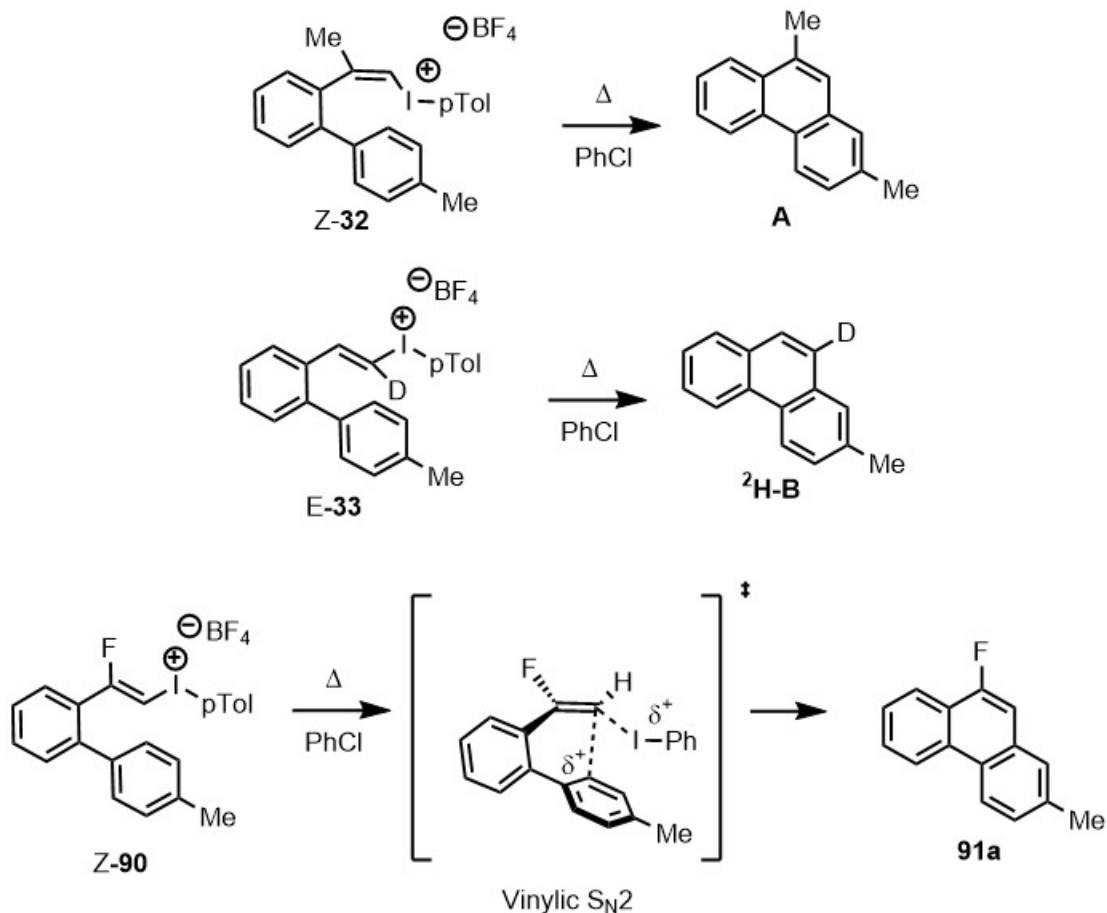
The α -proton in a vinyl (aryl)iodonium salt is relatively acidic, deprotonation leads to the zwitterionic vinylene ylide (**97-I**), this unstable species quickly decomposes by α -elimination to generate a vinylidene carbene (Scheme 3.17, **98**). This pathway that generates the vinylidene carbene **98**, which is generally understood to be the primary means of reaction and is commonly used in preparation of alkynes or for other known reactivities of **97** such as alkyl 1-5 C-H insertion.⁸⁹ Both triethylamine and fluoride have been used to deprotonate vinyl (aryl)iodonium salts to generate vinylidene carbenes.⁸⁹ In one example, decenyl (phenyl)iodonium salt was treated with $n\text{Bu}_4\text{NF}$ (TBAF) at room temperature, the elimination product 1-decyne was obtained with complete conversion as the sole product, while other halides $n\text{Bu}_4\text{NCl}$, $n\text{Bu}_4\text{NBr}$, gave predominantly vinyl substitution products with inversion of configuration (Vinyllic $\text{S}_{\text{N}}2$).⁴⁹ The reaction was then repeated with deuterium labelled iodonium salts, (**99a**, **99b**) providing the

product 1-decyne with 0% D incorporation (Scheme 3.18 a), and 93% D incorporation (Scheme 3.18 b) respectively, confirming the action of fluoride as a base on the α -proton and the α -elimination forming the vinylidene carbene (Scheme 3.17, **98**).



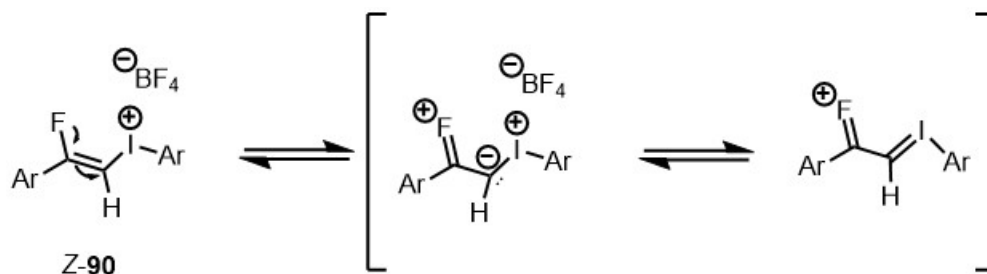
Scheme 3.18: α -elimination in reaction with vinyl iodonium and TBAF to produce alkyne

No rearrangement was observed with the decomposition of the 2-fluorovinyl iodonium *Z*-**90**. This is comparable to the results seen with *Z*-**32** and *E*-**33**, for which we proposed a direct vinylic S_N2 mechanism (Scheme 3.19). This suggests that *Z*-**90** may also occur through the same mechanism. We can assume the vinylene phenonium ion is likely destabilized by the fluorine substituent. While fluorine is stabilizing toward (sp^2) carbocations by p-donation into the empty p-orbital, in vinyl cations (sp) this effect is small, as a result fluorine is highly destabilizing by induction.^{90,91}



Scheme 3.19: Decompositions of vinyl (aryl)iodonium salts which lead to a single isomer

Fluorine has the ability to offer strong stabilization or strong destabilization to the molecules it is present in. Fluorine is strongly electronegative and therefore exhibits strong inductive effects; however it can also provide excellent stabilization as an electron donor. Fluorine offers excellent stabilization to carbocations (**100**), the short C-F bond length and small size of the fluorine atom results in good orbital overlap with the empty p-orbital (Scheme 3.20). Difluorocarbene (**101**) is another example of this interaction, a stable free carbene.

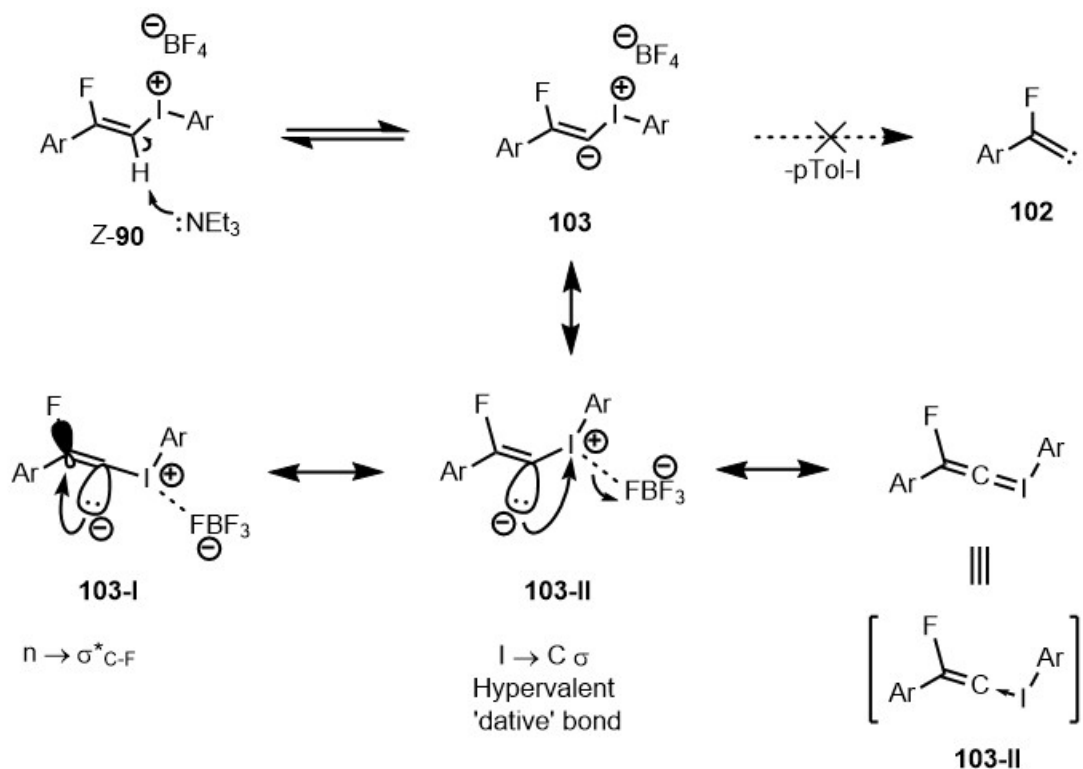


Scheme 3.21: Iodonium ylide resonance structures of Z-90

The anion produced after deprotonation also participates in interesting electronic effects. Since the vinyl anion (Scheme 3.22, **103**) is perpendicular to the π -system, it does not participate in conjugation. It is however anti-periplanar to the C-F bond, and can participate in negative hyperconjugation with the C-F σ^* orbital (**103-I**) and provides a significant stabilization (40.5 kcal/mol).⁹¹ This interaction could provide an energy barrier against further decomposition by α -elimination. Hypervalent iodine compounds necessitate that each of their ligands are sufficiently electronegative to stabilize the negative charge of two electrons from iodine, acting as dative bonds (**103-II**). In most cases, carbon is not electronegative enough to support this. In some hypervalent iodine compounds known as iodonium ylides,²² the carbon ligand possesses electron-withdrawing groups capable of delocalizing the negative charge, for a total of 4 bonding electrons with iodine.

It is possible that the 2-fluorovinyl(aryl)iodonium salt anion **103** exists in equilibrium with a stable vinylidene iodonium ylide (**103-II**) in solution as a part of an acid/base equilibrium. The negative charge is delocalized by hyperconjugation with the C-F σ^* orbital (**103-I**), which might be enough sufficiently stabilize the charge for the ylide/anion form to exist. This would explain why the iodonium salt could maintain stability in the presence of base without immediately decomposing into a fluorovinylidene carbene (**102**) and producing byproducts. If this species

exists, it could serve as a stable variety of the free fluorovinylidene carbene, and also participate in visible light activated chemistry characteristic of iodonium ylides. In the future, this effect could be examined in better detail using ^1H NMR and ^{19}F NMR studies. By treating **Z-90** with a base, we can monitor the disappearance of the α -proton using ^1H NMR, and we would then expect to see an up-field shift in the ^{19}F NMR as a result of the increased shielding of the fluorine nucleus.



Scheme 3.22: Electronic structure and reactivity of **Z-90 2-fluorovinyl (aryl)iodonium salt**

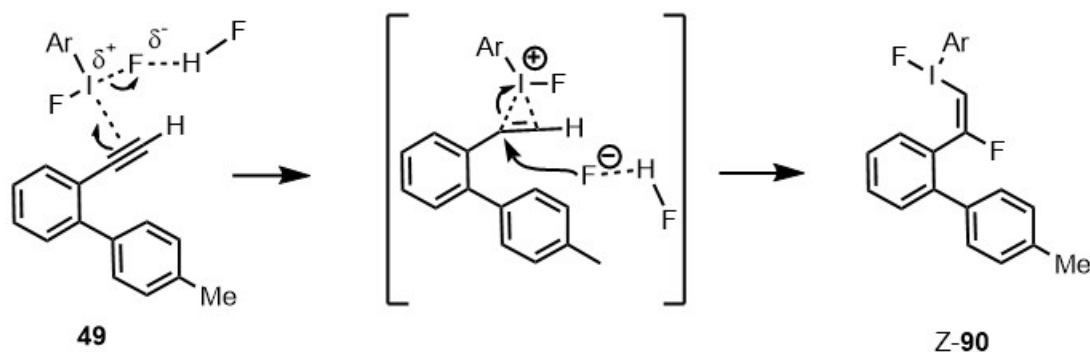
3.5 Future directions

We demonstrated that alkynyl trifluoroborates **88** are excellent precursors in this transformation, but alternatives still merit investigation. While our investigations regarding the terminal alkyne **49** were initially not fruitful, there remains to be an abundance of potential routes to be reinvestigated. For example, preparation of trifluoroacetate iodonium salt **89** from terminal alkyne **49** proceeded handily and in high yields (Scheme 3.13). As well as being operationally

simple and not requiring any additional additives, it is a promising methodology. However, to date its utility remains mostly unexplored. The direct preparation of 2-fluorovinyl iodonium **Z-90** from terminal alkyne **49** also remains mostly uninvestigated. Our attempts relied mostly on the published literature methods for the application to aliphatic alkynes. One of the only methods that reported a direct conversion of an aromatic alkyne, phenylacetylene, to the 2-fluorovinyl-iodonium salt, is that of Hara.^{92, 93} The authors reported that when ToIIF_2 was prepared electrolytically by the use of $\text{Et}_3\text{N}\cdot 5\text{HF}$, and then reacted directly with phenylacetylene, the *E*-2-fluorovinyl (aryl)iodonium salt was obtained in good yield. The authors reported the product was obtained when $\text{Et}_3\text{N}\cdot 5\text{HF}$ was used in excess as the solvent or as a solvent mixture, but that when $\text{Et}_3\text{N}\cdot 3\text{HF}$ was used instead, no product was obtained. This can be explained by the strong hydrogen bonding associated with liquid solutions containing hydrogen fluoride. As a result, the many possible $\text{Et}_3\text{N}\cdot \text{XHF}$ complexes possess different properties. With triethylamine, $\text{Et}_3\text{N}\cdot 2\text{HF}$, $\text{Et}_3\text{N}\cdot 3\text{HF}$ and $\text{Et}_3\text{N}\cdot 5\text{HF}$ have been reported, of these $\text{Et}_3\text{N}\cdot 2\text{HF}$ is the most nucleophilic and basic, and $\text{Et}_3\text{N}\cdot 5\text{HF}$ the least nucleophilic and basic. The decrease is explained by the hydrogen bonding interactions, which become stronger and more numerous as the relative concentration of HF to triethylamine increases. Nucleophilicity and basicity of the fluoride decrease as the fluoride nucleophile is increasing solvated. $\text{Et}_3\text{N}\cdot 3\text{HF}$ can be modified to give different reactivity, such as increasing nucleophilicity by *in situ* preparation of $\text{Et}_3\text{N}\cdot 2\text{HF}$ with the addition of triethylamine.⁹⁴ In the case of alkynyl iodonium salts, it appears the less nucleophilic $\text{Et}_3\text{N}\cdot 5\text{HF}$ is more suitable for this reaction.

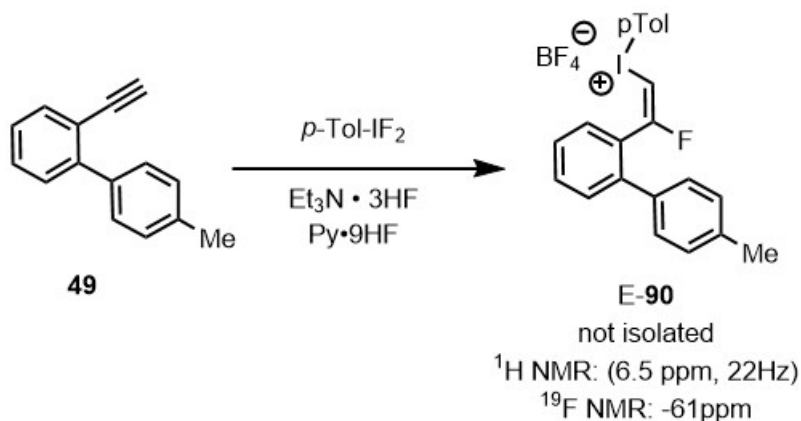
Bases like trimethylamine and fluoride are known to decompose vinyl (aryl)iodonium salts through α -elimination to generate a vinylidene carbene. However, the 2-fluorovinyl (aryl)iodonium salt **Z-90** we synthesized is very stable in comparison to the other vinyl

(aryl)iodonium salts we investigated, which decomposed at room temperature. Instead, it might be that the increased hydrogen bonding strength of $\text{Et}_3\text{N}\cdot 5\text{HF}$ is necessary to activate the iodotoluene difluoride and stabilize the vinylene iodonium fluoride intermediate **77** so that the final product can form.



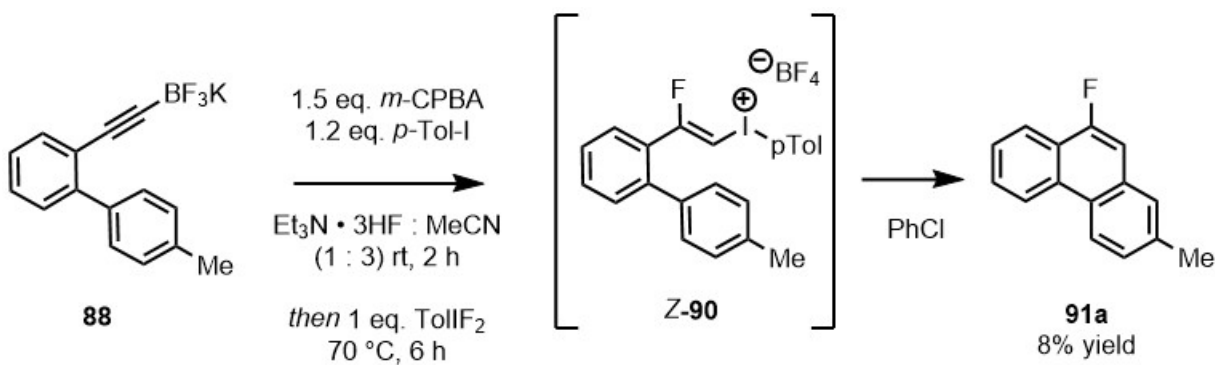
Scheme 3.23: Role of H-F hydrogen bonding in $\text{Et}_3\text{N}\cdot 5\text{HF}$ for the synthesis of *E*-90 from **49**

It is then possible that we could develop a process using $\text{Et}_3\text{N}\cdot 5\text{HF}$ to convert the readily accessible terminal alkyne **49** to the iodonium salt *E*-90, and the fluorinated phenanthrene (Scheme 3.26, **91a**). Since the $\text{Et}_3\text{N}\cdot 5\text{HF}$ used in the literature is not commercially available, we attempted to increase the concentration of HF with the combination of $\text{Et}_3\text{N}\cdot 3\text{HF}$ and Olah's reagent ($\text{Py}\cdot 9\text{HF}$). Analysis by NMR spectroscopy of the crude reaction mixture displayed the peaks ^1H NMR: 6.5 ppm, 22Hz, ^{19}F NMR: -61ppm. In comparison to *Z*-90, (6.5 ppm, 31 Hz), the 22 Hz doublet corresponds to the expected coupling for a $^2J_{\text{H-F}}$ coupling. This preliminary result is promising. Further optimization of $\text{Et}_3\text{N}\cdot 3\text{HF}$ and $\text{Py}\cdot 9\text{HF}$ concentrations, or the use of commercial $\text{Et}_3\text{N}\cdot 5\text{HF}$, could lead to a practical direct synthesis of the iodonium salt *Z*-90 from basic alkyne precursor (Scheme 3.24, **49**).



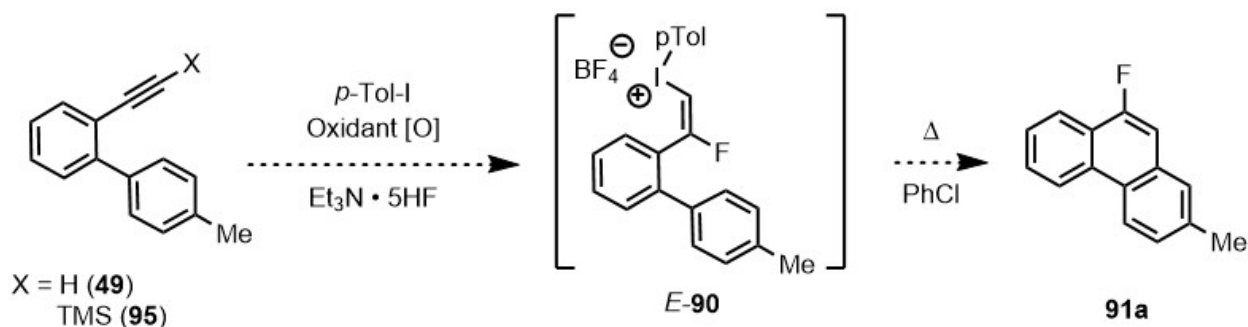
Scheme 3.24: Preliminary result in the direct synthesis of *E*-90 from 49

A single experiment was carried out in which the hypervalent iodine reagent (ToIIF_2) was prepared *in situ* from iodotoluene and *m*-CPBA in a solution of acetonitrile and triethylamine trihydrofluoride ($\text{Et}_3\text{N} \cdot 3\text{HF}$). After pre-stirring the reaction, the alkyne trifluoroborate **88** was added under an air atmosphere and heated as according to the optimized conditions. After this time the reaction mixture was diluted with aq. NaBF_4 and extracted with dichloromethane. The organic extract was concentrated to a residue and 1 mL of chlorobenzene added and heated to reflux. Analysis of the reaction mixture indicated the fluorinated phenanthrene product **91a** was produced in 8% yield starting from the alkyne trifluoroborate **88**. This initial reaction is a proof of concept, demonstrating a pseudo one-pot, metal-free synthesis of fluorinated phenanthrenes with common commercially available reagents is feasible (Scheme 3.25).



Scheme 3.25: Demonstration of one-pot synthesis of 91a using *in situ* generated TlIF₂

We can further improve this chemistry by exploring other iodoarenes, such as 2-methoxyiodobenzene, which is known to stabilize vinyl(aryl)iodonium salts.⁹⁵ By creating the hypervalent species *in situ* with an external oxidant, or with the use of an electrolytic cell⁸³ we could develop this chemistry into a highly scalable, efficient, and green process.

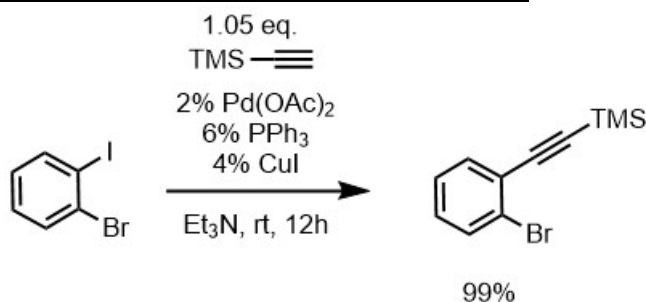


Scheme 3.26: Proposed scalable process for the synthesis of 91a

Future work on this reaction could be extended to heteroaromatic systems, applying the strategy to substrates that are well known for participating in an electrophilic cyclization, such as in the synthesis of benzofurans or indoles. It could then serve as a novel method to incorporate fluorine on sp^2 carbon atoms into medicinally desirable targets for the purposes of (¹⁸F) radiofluorination.

3.6 Experimental Procedures for Chapter 3

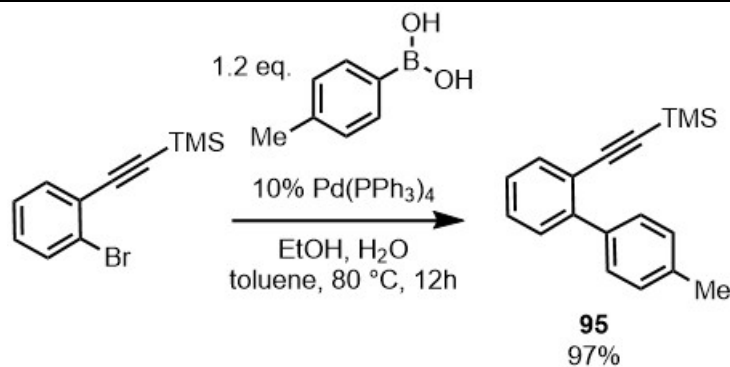
3.6.1 Synthesis of (2-bromophenyl)ethynyl trimethylsilane



To a dry 50 mL round bottom flask under an atmosphere of nitrogen was added palladium(II) acetate (43 mg, 0.2 mmol), triphenylphosphine (157 mg, 0.6 mmol), copper(I) iodide (77 mg, 0.4 mmol), and triethylamine (15 mL). The mixture was flushed with nitrogen and sealed with a septum, then stirred as a suspension for 5 minutes. Using a 10 mL syringe, 1-bromo-2-iodobenzene (2.83 g, 10 mmol, 1 eq.) was added, followed by 1-(trimethylsilyl)acetylene (1.01 g, 10.5 mmol). The reaction was stirred overnight at room temperature. The next day, to the reaction mixture was added ethyl acetate (100 mL) and saturated NH₄Cl (30 mL), and was stirred for 15 minutes. The mixture was extracted with ethyl acetate (3 x 30 mL) and washed with distilled water (2 x 50 mL) and with brine (50 mL). The organic solvent was dried over anhydrous MgSO₄, concentrated by rotary evaporation and purified through a short plug of silica (10% Et₂O / hexanes) to yield (2-Bromophenylethynyl)trimethylsilane (2.58 g, 99%) as a pale amber oil.

¹H-NMR (300 MHz; CDCl₃): δ 7.56 (d, *J* = 7.9 Hz, 1H), 7.48 (dd, *J* = 7.6, 1.7 Hz, 1H), 7.23 (td, *J* = 7.5, 1.2 Hz, 1H), 7.14 (td, *J* = 7.7, 1.7 Hz, 1H), 0.27 (s, 9H). Spectral data was consistent with those reported in the literature.⁸⁸

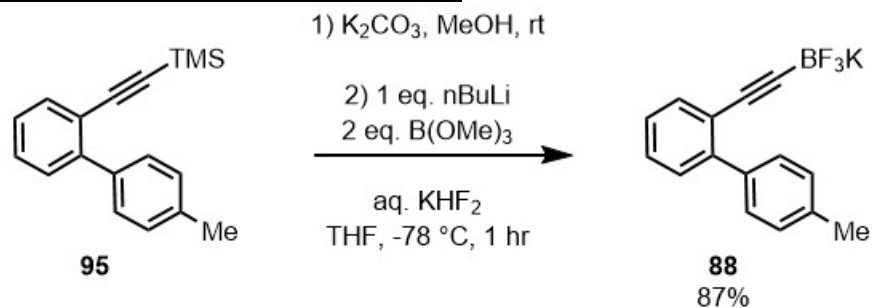
3.6.2 Synthesis of (4'-methyl-[1,1'-biphenyl]-2-yl)ethynyl trimethylsilane



To a dry 100 mL round bottom flask under an atmosphere of nitrogen was added 2-(Bromophenylethynyl)trimethylsilane (1013 mg, 4 mmol), potassium carbonate (1.64 g, 12 mmol), *p*-tolueneboronic acid (648 mg, 4.8 mmol), toluene (45 mL), H₂O (3 mL), and EtOH (3 mL). The mixture was stirred as a suspension for 5 minutes and flushed with nitrogen. Tetrakis(triphenylphosphine)palladium(0) (462 mg, 0.4 mmol) was added and the flask was promptly resealed and flushed with nitrogen. The reaction was then brought to reflux for 18 hours. The reaction mixture was filtered over celite, then diluted with ethyl acetate (100 mL), and water (100 mL). The mixture was extracted with ethyl acetate (3 x 30 mL) and washed with distilled water (2 x 50 mL) and with brine (50 mL). The organic solvent was dried over anhydrous MgSO₄, concentrated by rotary evaporation and purified through a short plug of silica (10% Et₂O/hexanes) to give (2-(4-tolyl)phenylethynyl)trimethylsilane (**95**) (1030 mg, 97%) as a pale amber oil.

¹H-NMR (300 MHz; CDCl₃): δ 7.59-7.51 (m, 3H), 7.39-7.35 (m, 2H), 7.29-7.20 (m, 3H), 2.39 (s, 3H), 0.16 (s, 9H). Spectral data was consistent with those reported in the literature.⁹⁶

3.6.3 Synthesis of alkynyl trifluoroborate (88)



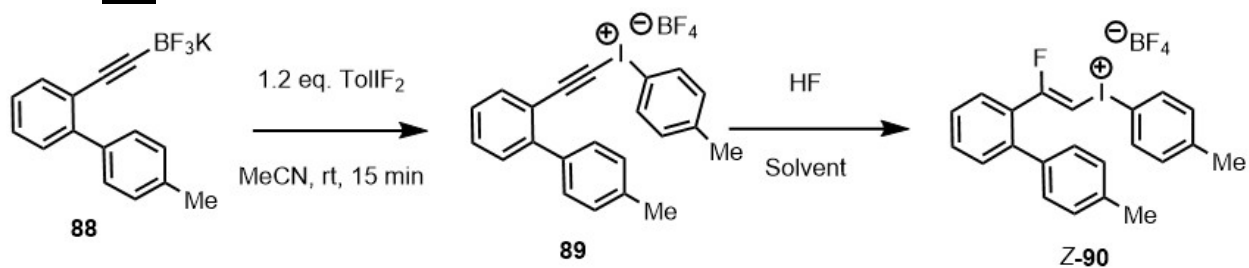
Step 1. To a 50 mL round bottom flask was added 2-(2-(4-tolyl)phenylethynyl)-1-trimethylsilane (**73**) (620 mg, 2.34 mmol), potassium carbonate (647mg, 4.68 mmol) and MeOH (20 mL). The reaction was stirred for 2 hours at room temperature. The reaction mixture was concentrated under reduced pressure by rotary evaporation, diluted with water (50 mL) and extracted with ethyl acetate (3 x 50 mL). The organic extracts were combined and washed with brine (50 mL), and dried over anhydrous $MgSO_4$. The organic solvent was removed by rotary evaporation to yield **49** (450 mg, 99%) as a yellow oil. This oil was used directly in the next step without further purification.

Step 2: The oil collected in the previous step (450 mg, crude) was added to a dry 50 mL round bottom flask, dissolved in anhydrous THF (20 mL) and cooled to $-78\text{ }^\circ\text{C}$ under a nitrogen atmosphere. A solution of n-butyllithium (2.5 M) in hexanes (0.94 mL, 2.34 mmol) was added dropwise by syringe over 10 minutes. The reaction was allowed to stir at $-78\text{ }^\circ\text{C}$ for 15 minutes. In a separate 50 mL round bottom flask, triethyl borate (683 mg, 4.68 mmol) was dissolved in anhydrous THF (10 mL) and cooled to $-78\text{ }^\circ\text{C}$ under an atmosphere of nitrogen. The flask containing the acetylide solution was transferred to the triethyl borate solution dropwise by cannula over 10 minutes. After complete addition the reaction was allowed to stir for 1 hour at $-78\text{ }^\circ\text{C}$, and then removed from the bath and allowed to warm slowly. When the reaction had warmed to $0\text{ }^\circ\text{C}$, a saturated aqueous solution of KHF_2 (1.1 g, 18.72 mmol) was added and the reaction was stirred

vigorously as a heterogenous solution for 30 minutes. The reaction mixture was concentrated under reduced pressure by rotary evaporation, and under high vacuum for 30 minutes in order to remove as much water as possible. To the flask was added 20 mL of dry acetone and heated to reflux with a heat gun to dissolve the precipitates. The hot acetone extract was filtered over celite, and washed with hot acetone (2 x 10 mL). The extracts were concentrated by rotary evaporation to one third of its original volume. Diethyl ether (20 mL) was layered on top of the extract and placed in the freezer for 24 hours. The alkynyl trifluoroborate (**88**) was isolated by vacuum filtration as a white solid (575 mg, 87%).

M.p. 232-234 °C, $^1\text{H NMR}$ (300 MHz, CD_3CN) δ 7.57 – 7.47 (m, 3H), 7.34 – 7.21 (m, 5H), 2.40 (s, 3H). $^{13}\text{C NMR}$ (75 MHz; CD_3CN): δ 143.7, 139.0, 138.1, 134.5, 130.36, 130.19, 129.5, 128.3, 127.8, 124.4, 118.4, 118.19, 118.14, 21.2 $^{19}\text{F NMR}$ (300 MHz, CD_3CN) δ -135.0.

3.6.4 General procedure for synthesis of (Z)-(2-fluoro-2-(4'-methyl-[1,1'-biphenyl]-2-yl)vinyl)-(p-tolyl) iodonium tetrafluoroborate (Z-90) from alkynyl trifluoroborate (88)

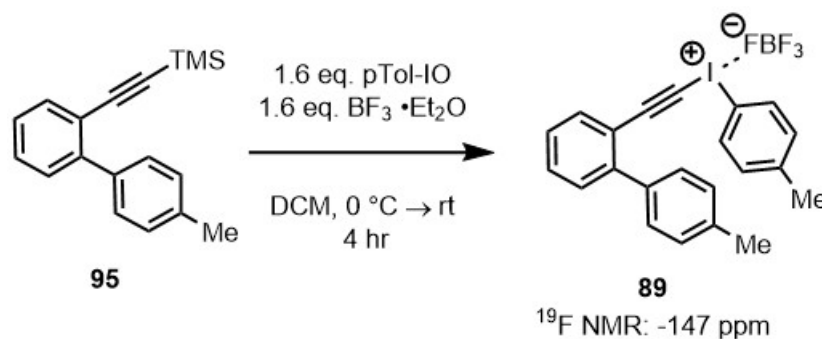


To a 5 mL PFA vial with a Teflon stir bar is added trifluoroborate (**88**) (26 mg, 0.09 mmol) and iodotoluene difluoride (28 mg, 0.11 mmol) under a nitrogen atmosphere. To the reaction was added 2 mL anhydrous MeCN (0.05 M) and the reaction was stirred for 15 minutes at room temperature. The vial was uncapped and 1.0 mL of Et₃N•3HF was added, the vial was sealed and heated to 70 °C in an oil bath for 6 hours. The reaction mixture was poured directly into a separatory funnel containing 50 mL of 5% NaBF₄ solution and mixed gently. The mixture was

extracted with CH₂Cl₂ (3 x 10 mL), and the organic extracts were dried with MgSO₄ and concentrated under reduced pressure to yield a yellow oil (66% NMR yield). The oil was dissolved in CHCl₃ (1 mL) and layered with diethyl ether (3 mL) and placed in a -20 °C for 24 hours. The product **Z-90** was isolated by trituration with hexanes as colourless needle-like crystals (30 mg, 64%)

m.p. 91-93 °C, ¹H-NMR (500 MHz; CDCl₃): δ 7.80 (d, *J* = 8.4 Hz, 2H), 7.67 (d, *J* = 7.8 Hz, 1H), 7.55 (t, *J* = 7.5 Hz, 1H), 7.42 (t, *J* = 7.8 Hz, 1H), 7.37 (d, *J* = 7.6 Hz, 1H), 7.28 (t, *J* = 6.2 Hz, 3H), 7.09 (d, *J* = 7.9 Hz, 2H), 7.03 (d, *J* = 7.9 Hz, 2H), 6.58 (d, ³*J*_{H-F} = 31.9 Hz, 1H), 2.48 (s, 3H), 2.37 (s, 3H). ¹³C NMR (126 MHz; CDCl₃): δ 170.7, 168.5, 143.9, 141.9, 137.7, 136.6, 135.6, 133.0, 132.5, 130.9, 129.4, 128.1, 107.3, 77.3, 77.1, 76.8, 21.2. ¹⁹F NMR (471 MHz; CDCl₃): δ -59.5, -148.5

3.6.5 General procedure for conversion of vinyl iodonium salt to phenanthrene (91a)

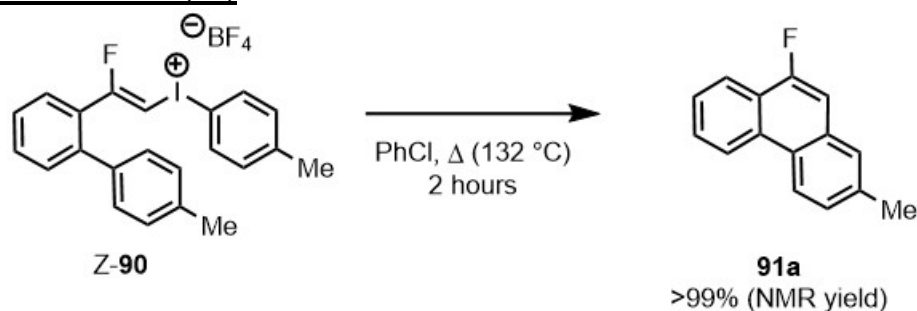


The crystals of **Z-90** containing triethylamine as an impurity were used as is. To a dry 10 mL round bottom flask was added **Z-90** (20 mg, 0.039 mmol) and chlorobenzene (1 mL) and stirred under an atmosphere of nitrogen. The flask was heated to reflux for 2 hours. The solvent was

removed by rotary evaporation, and the crude analyzed by NMR. Spectral data was consistent with those reported in the literature.⁷⁰

¹H-NMR (300 MHz; CDCl₃): δ 8.63 (d, *J* = 7.7 Hz, 1H), 8.51 (d, *J* = 8.6 Hz, 1H), 8.16 (d, *J* = 7.8 Hz, 1H), 7.70-7.54 (m, 4H), 6.92 (d, *J* = 7.7 Hz, 1H), 2.54 (s, 3H).

3.6.6 Synthesis of (4'-methyl-[1,1'-biphenyl]-2-yl)ethynyl(p-tolyl)iodonium tetrafluoroborate (89)



To a dry 25 mL round bottom flask was added ((4'-methyl-[1,1'-biphenyl]-2-yl)ethynyl)trimethylsilane (180 mg, 0.68 mmol) and 4-methyl-iodosylbenzene (255 mg, 1.08 mmol) and 6 mL anhydrous CH₂Cl₂ under a nitrogen atmosphere. The stirred suspension was cooled to 0 °C in an ice bath, and freshly distilled boron trifluoride diethyl etherate (136 μL, 1.08 mmol) was added dropwise by syringe over 5 minutes. The reaction was allowed to warm to room temperature and stirred for 3 hours. To the reaction was added 5% aq. NaBF₄ (10 mL) and the mixture was transferred to a separatory funnel and extracted with CH₂Cl₂ (3x 10 mL). The extracts were dried over MgSO₄, and concentrated under reduced pressure by rotary evaporation to yield an amber oil. The oil was dissolved in CHCl₃ (1 mL) and layered with diethyl ether (3 mL) and placed in a -20 °C freezer for 24 hours. The precipitated solid was isolated by decantation and trituration with hexanes, to yield **71** as a waxy red solid (210 mg, 62% crude).

¹H NMR (300 MHz, CHCl₃) δ 7.62 (*J* = 8.0 Hz, 1H), 6.46 (d, ³*J*_{H-F} = 31.0 Hz, 1H), 7.41 – 7.36 (m, 2H), 7.32 – 7.22 (m, 3H), 2.40 (s, 3H). **¹³C NMR** (300 MHz, CHCl₃) δ 141.4, **¹⁹F NMR** (300 MHz, CHCl₃) δ -147.0.

References

- (1) Zhao, Z.; Britt, L. H.; Murphy, G. K., *Chemistry—A European Journal* **2018**, *24*, 17002.
- (2) Kovács, A.; Vasas, A.; Hohmann, J., *Phytochemistry* **2008**, *69*, 1084.
- (3) Burtoloso, A.; Bertonha, A.; Rosset, I., *Current Topics in Medicinal Chemistry* **2013**, *14*.
- (4) He, X.; Eguchi, R.; Goto, H.; Uesugi, E.; Hamao, S.; Takabayashi, Y.; Kubozono, Y., *Organic Electronics* **2013**, *14*, 1673.
- (5) Wu, T.-L.; Chou, H.-H.; Huang, P.-Y.; Cheng, C.-H.; Liu, R.-S., *The Journal of Organic Chemistry* **2014**, *79*, 267.
- (6) Artioli, G. A.; Hammerath, F.; Mozzati, M. C.; Carretta, P.; Corana, F.; Mannucci, B.; Margadonna, S.; Malavasi, L., *Chemical Communications* **2015**, *51*, 1092.
- (7) Halton, B.; Maidment, A.; Officer, D.; Warnes, J., *Australian Journal of Chemistry* **1984**, *37*, 2119.
- (8) Flammang-Barbieux, M.; Nasielski, J.; Martin, R., *Tetrahedron Letters* **1967**, *8*, 743.
- (9) McMurry, J. E., *Accounts of Chemical Research* **1983**, *16*, 405.
- (10) McAtee, C. C.; Riehl, P. S.; Schindler, C. S., *Journal of the American Chemical Society* **2017**, *139*, 2960.
- (11) Yan, J.; Yoshikai, N., *Organic Letters* **2017**, *19*, 6630.
- (12) Saunthwal, R. K.; Danodia, A. K.; Saini, K. M.; Verma, A. K., *Organic & Biomolecular Chemistry* **2017**, *15*, 6934.
- (13) Xia, Y.; Liu, Z.; Xiao, Q.; Qu, P.; Ge, R.; Zhang, Y.; Wang, J., *Angewandte Chemie International Edition* **2012**, *51*, 5714.
- (14) Iuliano, A.; Piccioli, P.; Fabbri, D., *Organic Letters* **2004**, *6*, 3711.
- (15) Bates, R., *Organic synthesis using transition metals*. John Wiley & Sons: 2012.
- (16) Yoshimura, A.; Zhdankin, V. V., *Chemical Reviews* **2016**, *116*, 3328.
- (17) Maertens, G.; L'homme, C.; Canesi, S., *Frontiers in chemistry* **2015**, *2*, 115.
- (18) Willgerodt, C., *Journal für Praktische Chemie* **1886**, *33*, 154.
- (19) Moriarty, R. M.; Vaid, R. K., *Synthesis* **1990**, *1990*, 431.
- (20) Zhong, W.; Yang, J.; Meng, X.; Li, Z., *The Journal of Organic Chemistry* **2011**, *76*, 9997.
- (21) Pinto de Magalhães, H.; Lüthi, H. P.; Togni, A., *Organic Letters* **2012**, *14*, 3830.
- (22) Yusubov, M. S.; Maskae, A. V.; Zhdankin, V. V., *ARKIVOC: Online Journal of Organic Chemistry* **2011**.
- (23) Kozmin, S. A.; Rawal, V. H., *Journal of the American Chemical Society* **1998**, *120*, 13523.
- (24) Zhdankin, V. V., *Hypervalent iodine chemistry: preparation, structure, and synthetic applications of polyvalent iodine compounds*. John Wiley & Sons: 2013.
- (25) Zhou, B.; Hou, W.; Yang, Y.; Feng, H.; Li, Y., *Organic Letters* **2014**, *16*, 1322.
- (26) Fischer, D. R.; Williamson, B. L.; Stang, P. J., *Synlett* **1992**, *1992*, 535.
- (27) Ochiai, M.; Sumi, K.; Nagao, Y.; Fujita, E., *Tetrahedron Letters* **1985**, *26*, 2351.
- (28) Ochiai, M.; Toyonari, M.; Nagaoka, T.; Chen, D.-W.; Kida, M., *Tetrahedron Letters* **1997**, *38*, 6709.
- (29) Hinkle, R. J.; Stang, P. J., *Synthesis* **1994**, *1994*, 313.
- (30) Kita, Y.; Gyoten, M.; Ohtsubo, M.; Tohma, H.; Takada, T., *Chemical Communications* **1996**, 1481.
- (31) Tohma, H.; Iwata, M.; Maegawa, T.; Kita, Y., *Tetrahedron Letters* **2002**, *43*, 9241.
- (32) Depken, C.; Kraetzschmar, F.; Breder, A., *Organic Chemistry Frontiers* **2016**, *3*, 314.
- (33) Okuyama, T.; Ochiai, M., *Journal of the American Chemical Society* **1997**, *119*, 4785.
- (34) Okuyama, T.; Oka, H.; Ochiai, M., *Bulletin of the Chemical Society of Japan* **1998**, *71*, 1915.
- (35) Ochiai, M., *Journal of Organometallic Chemistry* **2000**, *611*, 494.
- (36) Okuyama, T., *Accounts of Chemical Research* **2002**, *35*, 12.
- (37) Gronheid, R.; Lodder, G.; Ochiai, M.; Sueda, T.; Okuyama, T., *Journal of the American Chemical Society* **2001**, *123*, 8760.
- (38) Okuyama, T.; Ishida, Y.; Ochiai, M., *Bulletin of the Chemical Society of Japan* **1999**, *72*, 163.

- (39) Hinkle, R. J.; Thomas, D. B., *The Journal of Organic Chemistry* **1997**, *62*, 7534.
- (40) McNeil, A. J.; Hinkle, R. J.; Rouse, E. A.; Thomas, Q. A.; Thomas, D. B., *The Journal of Organic Chemistry* **2001**, *66*, 5556.
- (41) Stang, P. J.; Dueber, T. E., *Journal of the American Chemical Society* **1977**, *99*, 2602.
- (42) Wirth, T.; Hirt, U. H., *Synthesis* **1999**, *1999*, 1271.
- (43) Seayad, J.; Seayad, A. M.; Chai, C. L., *Organic Letters* **2010**, *12*, 1412.
- (44) Emmanuvel, L.; Shaikh, T. M. A.; Sudalai, A., *Organic Letters* **2005**, *7*, 5071.
- (45) Kitamura, T.; Muta, K.; Oyamada, J., *The Journal of Organic Chemistry* **2015**, *80*, 10431.
- (46) Zupan, M.; Pollak, A., *Chemical Communications* **1975**, 715.
- (47) Ochiai, M.; Oshima, K.; Masaki, Y., *Chemical Communications* **1991**, 869.
- (48) Lucchini, V.; Modena, G.; Pasquato, L., *Journal of the American Chemical Society* **1995**, *117*, 2297.
- (49) Ochiai, M.; Oshima, K.; Masaki, Y., *Journal of the American Chemical Society* **1991**, *113*, 7059.
- (50) Seidel, A.; Luch, A.; Platt, K. L.; Oesch, F.; Glatt, H., *Polycyclic Aromatic Compounds* **1994**, *6*, 191.
- (51) Li, C.; Li, X.-Q.; Zhang, C., *Journal of Chemical Research* **2008**, *2008*, 525.
- (52) Corey, E.; Fuchs, P., *Tetrahedron Letters* **1972**, *13*, 3769.
- (53) Roth, G. J.; Liepold, B.; Mueller, S. G.; Bestmann, H. J., *Synthesis* **2004**, *2004*, 59.
- (54) Li, J.; Hua, R.; Liu, T., *The Journal of Organic Chemistry* **2010**, *75*, 2966.
- (55) Brown, C. A.; Ahuja, V. K., *Chemical Communications* **1973**, 553.
- (56) Yu, J.; Gaunt, M. J.; Spencer, J. B., *The Journal of Organic Chemistry* **2002**, *67*, 4627.
- (57) Lappert, M.; Prokai, B., *Journal of Organometallic Chemistry* **1964**, *1*, 384.
- (58) Wang, C.; Tobrman, T.; Xu, Z.; Negishi, E.-i., *Organic Letters* **2009**, *11*, 4092.
- (59) Sato, M.; Yamamoto, Y.; Hara, S.; Suzuki, A., *Tetrahedron Letters* **1993**, *34*, 7071.
- (60) Mohamed, R. K.; Mondal, S.; Guerrero, J. V.; Eaton, T. M.; Albrecht-Schmitt, T. E.; Shatruck, M.; Alabugin, I. V., *Angewandte Chemie International Edition* **2016**, *55*, 12054.
- (61) Alfaro, R.; Parra, A.; Alemán, J.; García Ruano, J. L.; Tortosa, M., *Journal of the American Chemical Society* **2012**, *134*, 15165.
- (62) Yoshida, M.; Osafune, K.; Hara, S., *Synthesis* **2007**, *2007*, 1542.
- (63) Ang, N. W.; Buettner, C. S.; Docherty, S.; Bismuto, A.; Carney, J. R.; Docherty, J. H.; Cowley, M. J.; Thomas, S. P., *Synthesis* **2018**, *50*, 803.
- (64) Wakabayashi, R.; Kurahashi, T.; Matsubara, S., *Synlett* **2013**, *24*, 2297.
- (65) Colomer, I.; Chamberlain, A. E.; Haughey, M. B.; Donohoe, T. J., *Nature Reviews Chemistry* **2017**, *1*, 1.
- (66) Li, Y.; Wu, Y.; Liu, P.; Prostran, Z.; Gardner, S.; Ong, B. S., *Chemistry of materials* **2007**, *19*, 418.
- (67) Elbs, K.; Larsen, E., *Berichte der Deutschen Chemischen Gesellschaft* **1884**, *17*, 2847.
- (68) Roy, D.; Maekawa, H.; Murai, M.; Takai, K., *Chemistry—An Asian Journal* **2015**, *10*, 2518.
- (69) Okamoto, H.; Eguchi, R.; Hamao, S.; Goto, H.; Gotoh, K.; Sakai, Y.; Izumi, M.; Takaguchi, Y.; Gohda, S.; Kubozono, Y., *Scientific Reports* **2014**, *4*, 5330.
- (70) Fuchibe, K.; Morikawa, T.; Ueda, R.; Okauchi, T.; Ichikawa, J., *Journal of Fluorine Chemistry* **2015**, *179*, 106.
- (71) Kasumov, T. M.; Pirculiyev, N. S.; Brel, V. K.; Grishin, Y. K.; Zefirov, N. S.; Stang, P. J., *Tetrahedron* **1997**, *53*, 13139.
- (72) Ochiai, M.; Hirobe, M.; Yoshimura, A.; Nishi, Y.; Miyamoto, K.; Shiro, M., *Organic Letters* **2007**, *9*, 3335.
- (73) Ochiai, M.; Uemura, K.; Oshima, K.; Masaki, Y.; Kunishima, M.; Tani, S., *Tetrahedron Letters* **1991**, *32*, 4753.
- (74) Hyatt, I. D.; Croatt, M. P., *Angewandte Chemie* **2012**, *124*, 7629.
- (75) Saito, A.; Taniguchi, A.; Kambara, Y.; Hanzawa, Y., *Organic Letters* **2013**, *15*, 2672.
- (76) Kitamura, T.; Furuki, R.; Taniguchi, H.; Stang, P. J., *Tetrahedron Letters* **1990**, *31*, 703.

- (77) Tóth, B. z. L.; Béke, F.; Egyed, O.; Bényei, A.; Stirling, A. s.; Novák, Z., *ACS Omega* **2019**, *4*, 9188.
- (78) Kitamura, T.; Kotani, M.; Fujiwara, Y., *Synthesis* **1998**, *1998*, 1416.
- (79) Zawia, E.; Moran, W. J., *Molecules* **2016**, *21*, 1073.
- (80) Ochiai, M.; Kunishima, M.; Tani, S.; Nagao, Y., *Journal of the American Chemical Society* **1991**, *113*, 3135.
- (81) Ochiai, M.; Nishi, Y.; Mori, T.; Tada, N.; Suefuji, T.; Frohn, H. J., *Journal of the American Chemical Society* **2005**, *127*, 10460.
- (82) Yoshida, M.; Kawakami, K.; Hara, S., *Synthesis* **2004**, 2821.
- (83) Hara, S.; Yamamoto, K.; Yoshida, M.; Fukuhara, T.; Yoneda, N., *Tetrahedron Letters* **1999**, *40*, 7815.
- (84) Yoshida, M.; Komata, A.; Hara, S., *Tetrahedron* **2006**, *62*, 8636.
- (85) Nguyen, T.-H.; Abarbri, M.; Guilloteau, D.; Mavel, S.; Emond, P., *Tetrahedron* **2011**, *67*, 3434.
- (86) Dixon, L. I.; Carroll, M. A.; Gregson, T. J.; Ellames, G. J.; Harrington, R. W.; Clegg, W., *European Journal of Organic Chemistry* **2013**, *2013*, 2334.
- (87) Ochiai, M.; Kunishima, M.; Sumi, K.; Nagao, Y.; Fujita, E.; Arimoto, M.; Yamaguchi, H., *Tetrahedron Letters* **1985**, *26*, 4501.
- (88) Kondoh, A.; Ozawa, R.; Aoki, T.; Terada, M., *Organic & Biomolecular Chemistry* **2017**, *15*, 7277.
- (89) Ochiai, M.; Takaoka, Y.; Nagao, Y., *Journal of the American Chemical Society* **1988**, *110*, 6565.
- (90) O'Hagan, D., *Chemical Society Reviews* **2008**, *37*, 308.
- (91) Alabugin, I. V., *A Bridge Between Structure and Reactivity* **2016**.
- (92) Hara, S.; Yoshida, M.; Fukuhara, T.; Yoneda, N., *Chemical Communications* **1998**, 965.
- (93) Herszman, J. D.; Berger, M.; Waldvogel, S. R., *Organic Letters* **2019**.
- (94) Giudicelli, M.; Picq, D.; Veyron, B., *Tetrahedron Letters* **1990**, *31*, 6527.
- (95) Hamnett, D. J.; Moran, W. J., *Organic & Biomolecular Chemistry* **2014**, *12*, 4156.
- (96) Bochis, R. J.; Wyratt, M. J.; Schoen, W. R., Benzo-fused lactams promote release of growth hormone. Google Patents: 1994.

Appendix I – X Ray Crystal Structures

3.6.7 Vinyl (aryl)iodonium trifluoroacetate (92)

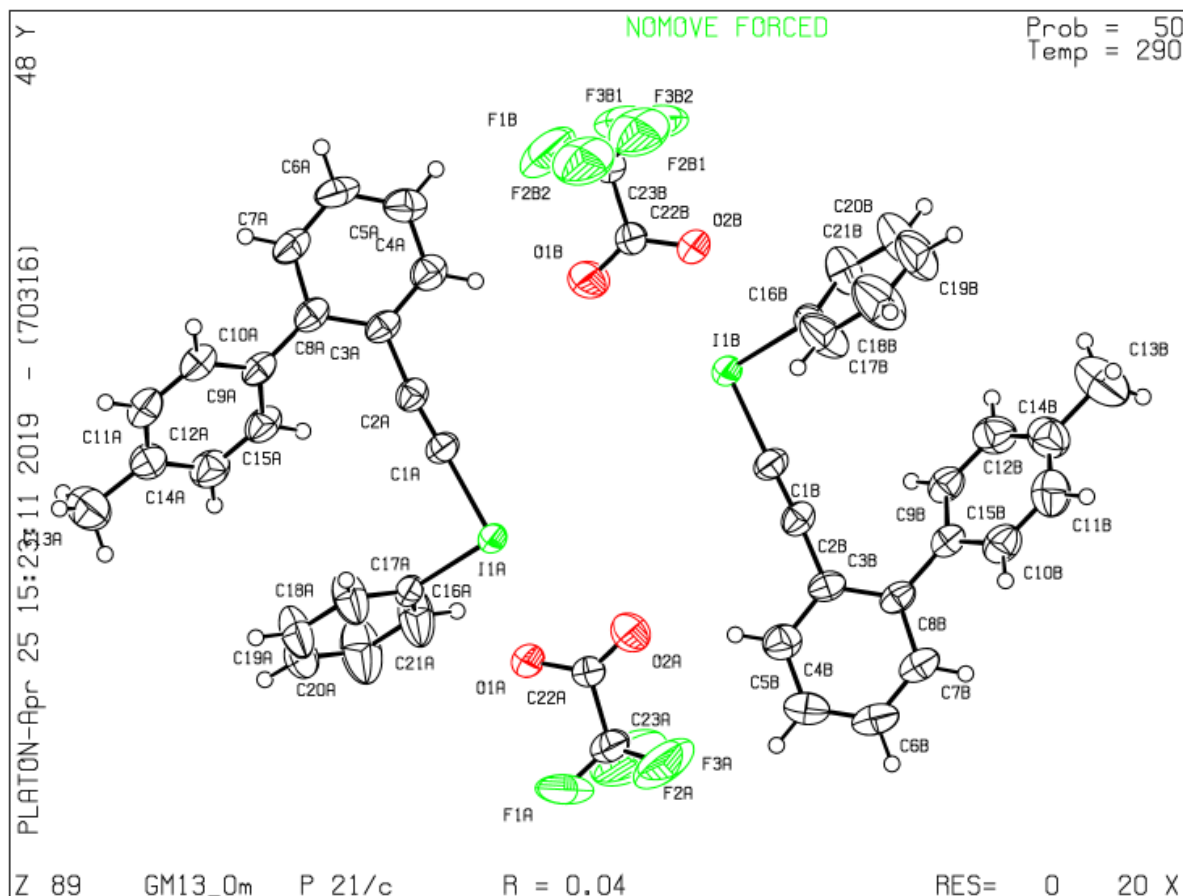


Table 1. Crystal data and structure refinement for GM13_0m.

Empirical formula	C ₂₃ H ₁₆ F ₃ I O ₂
Formula weight	508.26
Temperature	290(2) K
Wavelength	0.71073 Å
Crystal system	Monoclinic
Space group	<i>P</i> ₂ / <i>c</i>
Unit cell dimensions	<i>a</i> = 10.5678(3) Å, <i>b</i> = 18.0957(6) Å, <i>c</i> = 22.4547(8) Å, β = 103.2913(8)°
Volume	4179.0(2) Å ³
Z	8

Density (calculated)	1.616 g/cm ³
Absorption coefficient	1.574 mm ⁻¹
F(000)	2000
Crystal size	0.360 x 0.220 x 0.060 mm ³
Theta range for data collection	1.461 to 25.997°.
Index ranges	-13<=h<=13, -22<=k<=22, -27<=l<=27
Reflections collected	65029
Independent reflections	8205 [R(int) = 0.0304]
Completeness to theta = 25.242°	100.0 %
Absorption correction	Semi-empirical from equivalents
Max. and min. transmission	0.7460 and 0.5973
Refinement method	Full-matrix least-squares on F ²
Data / restraints / parameters	8205 / 12 / 534
Goodness-of-fit on F ²	1.160
Final R indices [I>2sigma(I)]	R1 = 0.0358, wR2 = 0.0972
R indices (all data)	R1 = 0.0621, wR2 = 0.1321
Extinction coefficient	n/a
Largest diff. peak and hole	0.878 and -0.803 e.Å ⁻³

Table 2. Atomic coordinates ($\times 10^4$) and equivalent isotropic displacement parameters ($\text{\AA}^2 \times 10^3$) for GM13_0m.

	x	y	z	U(eq)
I(1A)	8834(1)	3890(1)	4377(1)	39(1)
O(1A)	10112(4)	4560(2)	3747(2)	68(1)
O(2A)	10601(6)	5443(3)	4433(2)	99(2)
C(1A)	7681(5)	3178(3)	4713(2)	45(1)
C(2A)	7078(4)	2740(2)	4933(2)	42(1)
C(3A)	6351(4)	2271(2)	5255(2)	42(1)
C(4A)	5838(5)	2607(3)	5703(2)	52(1)
C(5A)	5211(5)	2185(3)	6063(2)	60(1)
C(6A)	5105(5)	1440(3)	5985(2)	61(2)
C(7A)	5590(5)	1106(3)	5529(2)	54(1)
C(8A)	6204(4)	1502(3)	5142(2)	43(1)
C(9A)	6580(4)	1111(2)	4629(2)	44(1)
C(10A)	7038(5)	384(3)	4699(2)	49(1)
C(11A)	7231(5)	-15(3)	4207(3)	54(1)
C(12A)	6978(5)	274(3)	3623(3)	55(1)
C(13A)	7125(7)	-180(4)	3083(3)	84(2)
C(14A)	6556(6)	1006(3)	3557(3)	62(2)
C(15A)	6364(5)	1411(3)	4044(2)	54(1)
C(16A)	8442(4)	3295(2)	3544(2)	39(1)
C(17A)	9006(7)	2625(3)	3526(3)	76(2)
C(18A)	8739(7)	2238(4)	2977(3)	83(2)
C(19A)	7940(6)	2516(3)	2475(3)	68(2)
C(20A)	7417(9)	3194(4)	2504(3)	108(3)
C(21A)	7647(8)	3591(4)	3046(3)	93(3)
C(22A)	10573(5)	5165(3)	3949(2)	48(1)
C(23A)	11136(7)	5605(4)	3494(3)	72(2)
F(1A)	11686(9)	5221(3)	3161(4)	227(5)
F(2A)	10248(7)	5982(4)	3124(3)	168(3)
F(3A)	11927(7)	6120(3)	3732(3)	158(3)
I(1B)	6162(1)	6064(1)	5617(1)	43(1)
O(1B)	4595(5)	4485(3)	5599(2)	94(2)

O(2B)	4826(5)	5418(2)	6249(2)	76(1)
C(1B)	7358(5)	6716(3)	5254(2)	47(1)
C(2B)	7993(4)	7123(2)	5023(2)	43(1)
C(3B)	8771(4)	7578(3)	4723(2)	42(1)
C(4B)	9223(5)	7268(3)	4242(2)	56(1)
C(5B)	10001(5)	7675(4)	3942(2)	62(1)
C(6B)	10337(5)	8382(3)	4122(3)	62(2)
C(7B)	9917(5)	8689(3)	4598(3)	55(1)
C(8B)	9129(4)	8305(2)	4913(2)	42(1)
C(9B)	8723(4)	8666(3)	5433(2)	43(1)
C(10B)	9593(5)	9113(3)	5836(3)	59(1)
C(11B)	9228(6)	9472(3)	6307(3)	72(2)
C(12B)	7981(7)	9409(3)	6400(3)	70(2)
C(13B)	7583(9)	9802(5)	6923(3)	113(3)
C(14B)	7125(6)	8970(3)	5999(3)	64(2)
C(15B)	7469(5)	8609(3)	5527(2)	50(1)
C(16B)	6630(5)	6647(2)	6456(2)	44(1)
C(17B)	7877(6)	6671(4)	6774(3)	84(2)
C(18B)	8148(7)	7068(5)	7316(3)	108(3)
C(19B)	7189(8)	7420(4)	7524(3)	90(2)
C(20B)	5940(8)	7356(4)	7204(3)	91(2)
C(21B)	5626(6)	6958(3)	6666(3)	68(2)
C(22B)	4510(5)	4784(3)	6066(2)	48(1)
C(23B)	3976(8)	4324(3)	6514(3)	75(2)
F(1B)	3521(8)	3707(4)	6333(3)	183(3)
F(2B1)	4495(16)	4432(10)	7084(6)	119(3)
F(2B2)	5029(11)	3887(6)	6855(4)	119(3)
F(3B1)	3814(15)	4688(7)	6989(8)	123(3)
F(3B2)	2738(11)	4515(6)	6532(5)	123(3)
H(4A)	5915	3115	5763	63
H(5A)	4860	2412	6360	71
H(6A)	4710	1156	6236	73
H(7A)	5502	597	5478	65
H(10A)	7215	167	5084	59
H(11A)	7542	-496	4269	65
H(13A)	7440	127	2799	126

H(13B)	6298	-385	2884	126
H(13C)	7733	-573	3219	126
H(14A)	6399	1224	3172	74
H(15A)	6084	1898	3982	65
H(17A)	9559	2429	3873	92
H(18A)	9120	1778	2957	100
H(19A)	7749	2247	2112	82
H(20A)	6891	3397	2152	130
H(21A)	7262	4050	3065	112
H(4B)	9001	6785	4121	67
H(5B)	10292	7466	3620	75
H(6B)	10855	8656	3920	74
H(7B)	10164	9171	4716	66
H(10B)	10436	9169	5785	71
H(11B)	9832	9765	6570	86
H(13D)	6815	9574	6999	169
H(13E)	7407	10312	6817	169
H(13F)	8274	9770	7284	169
H(14B)	6282	8917	6052	77
H(15B)	6856	8320	5264	61
H(17B)	8531	6430	6635	101
H(18B)	9001	7095	7544	130
H(19B)	7392	7700	7881	108
H(20B)	5283	7584	7350	109
H(21B)	4766	6901	6454	82

$U(\text{eq})$ is defined as one third of the trace of the orthogonalized U^{ij} tensor.

Table 3. Bond lengths [Å] and angles [°] for GM13_0m.

I(1A)-C(1A)	2.035(4)
I(1A)-C(16A)	2.115(4)
I(1A)-O(1A)	2.484(3)
O(1A)-C(22A)	1.241(6)
O(2A)-C(22A)	1.193(6)
C(1A)-C(2A)	1.192(6)
C(2A)-C(3A)	1.445(6)
C(3A)-C(4A)	1.388(7)
C(3A)-C(8A)	1.418(6)
C(4A)-C(5A)	1.387(7)
C(4A)-H(4A)	0.9300
C(5A)-C(6A)	1.361(8)
C(5A)-H(5A)	0.9300
C(6A)-C(7A)	1.385(8)
C(6A)-H(6A)	0.9300
C(7A)-C(8A)	1.395(6)
C(7A)-H(7A)	0.9300
C(8A)-C(9A)	1.480(7)
C(9A)-C(15A)	1.392(7)
C(9A)-C(10A)	1.398(6)
C(10A)-C(11A)	1.374(7)
C(10A)-H(10A)	0.9300
C(11A)-C(12A)	1.379(7)
C(11A)-H(11A)	0.9300
C(12A)-C(14A)	1.394(8)
C(12A)-C(13A)	1.503(8)
C(13A)-H(13A)	0.9600
C(13A)-H(13B)	0.9600
C(13A)-H(13C)	0.9600
C(14A)-C(15A)	1.371(7)
C(14A)-H(14A)	0.9300
C(15A)-H(15A)	0.9300
C(16A)-C(21A)	1.346(7)
C(16A)-C(17A)	1.356(7)

C(17A)-C(18A)	1.390(8)
C(17A)-H(17A)	0.9300
C(18A)-C(19A)	1.341(9)
C(18A)-H(18A)	0.9300
C(19A)-C(20A)	1.353(9)
C(19A)-H(19A)	0.9300
C(20A)-C(21A)	1.387(8)
C(20A)-H(20A)	0.9300
C(21A)-H(21A)	0.9300
C(22A)-C(23A)	1.521(7)
C(23A)-F(1A)	1.255(8)
C(23A)-F(3A)	1.284(8)
C(23A)-F(2A)	1.295(9)
I(1B)-C(1B)	2.032(4)
I(1B)-C(16B)	2.115(4)
O(1B)-C(22B)	1.201(6)
O(2B)-C(22B)	1.238(6)
C(1B)-C(2B)	1.192(6)
C(2B)-C(3B)	1.436(6)
C(3B)-C(4B)	1.396(7)
C(3B)-C(8B)	1.408(6)
C(4B)-C(5B)	1.386(7)
C(4B)-H(4B)	0.9300
C(5B)-C(6B)	1.364(8)
C(5B)-H(5B)	0.9300
C(6B)-C(7B)	1.368(8)
C(6B)-H(6B)	0.9300
C(7B)-C(8B)	1.396(6)
C(7B)-H(7B)	0.9300
C(8B)-C(9B)	1.485(7)
C(9B)-C(10B)	1.392(7)
C(9B)-C(15B)	1.393(6)
C(10B)-C(11B)	1.370(8)
C(10B)-H(10B)	0.9300
C(11B)-C(12B)	1.386(9)
C(11B)-H(11B)	0.9300

C(12B)-C(14B)	1.372(8)
C(12B)-C(13B)	1.513(9)
C(13B)-H(13D)	0.9600
C(13B)-H(13E)	0.9600
C(13B)-H(13F)	0.9600
C(14B)-C(15B)	1.364(7)
C(14B)-H(14B)	0.9300
C(15B)-H(15B)	0.9300
C(16B)-C(17B)	1.347(8)
C(16B)-C(21B)	1.377(7)
C(17B)-C(18B)	1.387(8)
C(17B)-H(17B)	0.9300
C(18B)-C(19B)	1.366(10)
C(18B)-H(18B)	0.9300
C(19B)-C(20B)	1.355(10)
C(19B)-H(19B)	0.9300
C(20B)-C(21B)	1.380(8)
C(20B)-H(20B)	0.9300
C(21B)-H(21B)	0.9300
C(22B)-C(23B)	1.513(7)
C(23B)-F(1B)	1.246(8)
C(23B)-F(2B1)	1.286(15)
C(23B)-F(3B1)	1.298(16)
C(23B)-F(3B2)	1.364(12)
C(23B)-F(2B2)	1.435(12)
F(1B)-F(2B2)	1.778(12)
F(2B1)-F(3B1)	0.841(17)
C(1A)-I(1A)-C(16A)	89.64(17)
C(1A)-I(1A)-O(1A)	166.11(16)
C(16A)-I(1A)-O(1A)	76.49(14)
C(22A)-O(1A)-I(1A)	116.2(3)
C(2A)-C(1A)-I(1A)	175.7(4)
C(1A)-C(2A)-C(3A)	173.3(5)
C(4A)-C(3A)-C(8A)	121.0(4)
C(4A)-C(3A)-C(2A)	116.6(4)

C(8A)-C(3A)-C(2A)	122.4(4)
C(5A)-C(4A)-C(3A)	120.0(5)
C(5A)-C(4A)-H(4A)	120.0
C(3A)-C(4A)-H(4A)	120.0
C(6A)-C(5A)-C(4A)	120.4(5)
C(6A)-C(5A)-H(5A)	119.8
C(4A)-C(5A)-H(5A)	119.8
C(5A)-C(6A)-C(7A)	119.6(5)
C(5A)-C(6A)-H(6A)	120.2
C(7A)-C(6A)-H(6A)	120.2
C(6A)-C(7A)-C(8A)	122.8(5)
C(6A)-C(7A)-H(7A)	118.6
C(8A)-C(7A)-H(7A)	118.6
C(7A)-C(8A)-C(3A)	116.1(5)
C(7A)-C(8A)-C(9A)	119.0(4)
C(3A)-C(8A)-C(9A)	124.8(4)
C(15A)-C(9A)-C(10A)	116.7(5)
C(15A)-C(9A)-C(8A)	122.2(4)
C(10A)-C(9A)-C(8A)	120.7(4)
C(11A)-C(10A)-C(9A)	121.1(5)
C(11A)-C(10A)-H(10A)	119.4
C(9A)-C(10A)-H(10A)	119.4
C(10A)-C(11A)-C(12A)	122.2(5)
C(10A)-C(11A)-H(11A)	118.9
C(12A)-C(11A)-H(11A)	118.9
C(11A)-C(12A)-C(14A)	116.6(5)
C(11A)-C(12A)-C(13A)	121.8(5)
C(14A)-C(12A)-C(13A)	121.6(6)
C(12A)-C(13A)-H(13A)	109.5
C(12A)-C(13A)-H(13B)	109.5
H(13A)-C(13A)-H(13B)	109.5
C(12A)-C(13A)-H(13C)	109.5
H(13A)-C(13A)-H(13C)	109.5
H(13B)-C(13A)-H(13C)	109.5
C(15A)-C(14A)-C(12A)	121.7(5)
C(15A)-C(14A)-H(14A)	119.1

C(12A)-C(14A)-H(14A)	119.1
C(14A)-C(15A)-C(9A)	121.5(5)
C(14A)-C(15A)-H(15A)	119.2
C(9A)-C(15A)-H(15A)	119.2
C(21A)-C(16A)-C(17A)	121.8(5)
C(21A)-C(16A)-I(1A)	119.3(4)
C(17A)-C(16A)-I(1A)	118.9(4)
C(16A)-C(17A)-C(18A)	118.4(5)
C(16A)-C(17A)-H(17A)	120.8
C(18A)-C(17A)-H(17A)	120.8
C(19A)-C(18A)-C(17A)	121.2(6)
C(19A)-C(18A)-H(18A)	119.4
C(17A)-C(18A)-H(18A)	119.4
C(18A)-C(19A)-C(20A)	119.0(5)
C(18A)-C(19A)-H(19A)	120.5
C(20A)-C(19A)-H(19A)	120.5
C(19A)-C(20A)-C(21A)	121.4(6)
C(19A)-C(20A)-H(20A)	119.3
C(21A)-C(20A)-H(20A)	119.3
C(16A)-C(21A)-C(20A)	118.2(6)
C(16A)-C(21A)-H(21A)	120.9
C(20A)-C(21A)-H(21A)	120.9
O(2A)-C(22A)-O(1A)	129.1(5)
O(2A)-C(22A)-C(23A)	117.4(5)
O(1A)-C(22A)-C(23A)	113.5(4)
F(1A)-C(23A)-F(3A)	107.7(7)
F(1A)-C(23A)-F(2A)	106.1(7)
F(3A)-C(23A)-F(2A)	101.0(6)
F(1A)-C(23A)-C(22A)	114.5(6)
F(3A)-C(23A)-C(22A)	114.7(6)
F(2A)-C(23A)-C(22A)	111.6(6)
C(1B)-I(1B)-C(16B)	91.55(19)
C(2B)-C(1B)-I(1B)	175.9(5)
C(1B)-C(2B)-C(3B)	176.8(5)
C(4B)-C(3B)-C(8B)	119.5(4)
C(4B)-C(3B)-C(2B)	117.9(5)

C(8B)-C(3B)-C(2B)	122.5(4)
C(5B)-C(4B)-C(3B)	120.6(5)
C(5B)-C(4B)-H(4B)	119.7
C(3B)-C(4B)-H(4B)	119.7
C(6B)-C(5B)-C(4B)	119.9(5)
C(6B)-C(5B)-H(5B)	120.1
C(4B)-C(5B)-H(5B)	120.1
C(5B)-C(6B)-C(7B)	120.2(5)
C(5B)-C(6B)-H(6B)	119.9
C(7B)-C(6B)-H(6B)	119.9
C(6B)-C(7B)-C(8B)	122.1(5)
C(6B)-C(7B)-H(7B)	118.9
C(8B)-C(7B)-H(7B)	118.9
C(7B)-C(8B)-C(3B)	117.6(5)
C(7B)-C(8B)-C(9B)	119.5(4)
C(3B)-C(8B)-C(9B)	122.9(4)
C(10B)-C(9B)-C(15B)	117.0(5)
C(10B)-C(9B)-C(8B)	120.0(4)
C(15B)-C(9B)-C(8B)	122.9(4)
C(11B)-C(10B)-C(9B)	121.1(5)
C(11B)-C(10B)-H(10B)	119.4
C(9B)-C(10B)-H(10B)	119.4
C(10B)-C(11B)-C(12B)	121.6(6)
C(10B)-C(11B)-H(11B)	119.2
C(12B)-C(11B)-H(11B)	119.2
C(14B)-C(12B)-C(11B)	117.0(6)
C(14B)-C(12B)-C(13B)	121.5(7)
C(11B)-C(12B)-C(13B)	121.5(7)
C(12B)-C(13B)-H(13D)	109.5
C(12B)-C(13B)-H(13E)	109.5
H(13D)-C(13B)-H(13E)	109.5
C(12B)-C(13B)-H(13F)	109.5
H(13D)-C(13B)-H(13F)	109.5
H(13E)-C(13B)-H(13F)	109.5
C(15B)-C(14B)-C(12B)	122.3(6)
C(15B)-C(14B)-H(14B)	118.9

C(12B)-C(14B)-H(14B)	118.9
C(14B)-C(15B)-C(9B)	121.0(5)
C(14B)-C(15B)-H(15B)	119.5
C(9B)-C(15B)-H(15B)	119.5
C(17B)-C(16B)-C(21B)	122.8(5)
C(17B)-C(16B)-I(1B)	119.2(4)
C(21B)-C(16B)-I(1B)	117.9(4)
C(16B)-C(17B)-C(18B)	117.5(6)
C(16B)-C(17B)-H(17B)	121.3
C(18B)-C(17B)-H(17B)	121.3
C(19B)-C(18B)-C(17B)	121.5(7)
C(19B)-C(18B)-H(18B)	119.3
C(17B)-C(18B)-H(18B)	119.3
C(20B)-C(19B)-C(18B)	119.2(6)
C(20B)-C(19B)-H(19B)	120.4
C(18B)-C(19B)-H(19B)	120.4
C(19B)-C(20B)-C(21B)	121.2(6)
C(19B)-C(20B)-H(20B)	119.4
C(21B)-C(20B)-H(20B)	119.4
C(16B)-C(21B)-C(20B)	117.7(6)
C(16B)-C(21B)-H(21B)	121.1
C(20B)-C(21B)-H(21B)	121.1
O(1B)-C(22B)-O(2B)	129.8(5)
O(1B)-C(22B)-C(23B)	116.5(5)
O(2B)-C(22B)-C(23B)	113.7(4)
F(1B)-C(23B)-F(2B1)	120.3(9)
F(1B)-C(23B)-F(3B1)	127.5(8)
F(2B1)-C(23B)-F(3B1)	38.0(8)
F(1B)-C(23B)-F(3B2)	86.4(8)
F(1B)-C(23B)-F(2B2)	82.8(7)
F(3B2)-C(23B)-F(2B2)	139.2(7)
F(1B)-C(23B)-C(22B)	116.9(5)
F(2B1)-C(23B)-C(22B)	116.0(8)
F(3B1)-C(23B)-C(22B)	114.0(7)
F(3B2)-C(23B)-C(22B)	112.7(7)
F(2B2)-C(23B)-C(22B)	107.3(7)

C(23B)-F(1B)-F(2B2)	53.2(6)
F(3B1)-F(2B1)-C(23B)	71.8(17)
C(23B)-F(2B2)-F(1B)	44.0(4)
F(2B1)-F(3B1)-C(23B)	70.2(17)

Symmetry transformations used to generate equivalent atoms:

Table 4. Anisotropic displacement parameters ($\text{\AA}^2 \times 10^3$) for GM13_0m.

	U^{11}	U^{22}	U^{33}	U^{23}	U^{13}	U^{12}
I(1A)	49(1)	34(1)	37(1)	-2(1)	13(1)	-9(1)
O(1A)	93(3)	53(2)	69(3)	-18(2)	44(2)	-31(2)
O(2A)	165(5)	87(3)	58(3)	-30(2)	54(3)	-46(3)
C(1A)	53(3)	41(2)	43(3)	3(2)	14(2)	-10(2)
C(2A)	44(3)	38(2)	40(2)	5(2)	5(2)	-2(2)
C(3A)	40(2)	43(2)	39(2)	10(2)	2(2)	-7(2)
C(4A)	56(3)	51(3)	49(3)	5(2)	9(2)	-6(2)
C(5A)	58(3)	76(4)	46(3)	5(3)	15(2)	-8(3)
C(6A)	61(3)	77(4)	45(3)	12(3)	14(3)	-25(3)
C(7A)	54(3)	52(3)	52(3)	9(2)	6(2)	-19(2)
C(8A)	36(2)	45(2)	44(3)	8(2)	-1(2)	-9(2)
C(9A)	39(3)	41(3)	49(3)	6(2)	5(2)	-12(2)
C(10A)	47(3)	44(3)	54(3)	11(2)	5(2)	-6(2)
C(11A)	46(3)	43(3)	70(4)	6(2)	9(3)	-5(2)
C(12A)	44(3)	58(3)	66(3)	-7(3)	18(2)	-11(2)
C(13A)	85(5)	88(5)	85(5)	-15(4)	33(4)	-3(4)
C(14A)	75(4)	60(3)	48(3)	7(2)	10(3)	-12(3)
C(15A)	65(3)	45(3)	50(3)	13(2)	8(3)	-8(2)
C(16A)	48(3)	31(2)	40(2)	0(2)	11(2)	-8(2)
C(17A)	104(5)	58(3)	56(3)	-10(3)	-5(3)	29(3)
C(18A)	109(5)	61(4)	76(4)	-22(3)	16(4)	23(4)
C(19A)	90(4)	65(4)	50(3)	-20(3)	16(3)	-16(3)
C(20A)	161(8)	83(5)	55(4)	-18(3)	-30(4)	22(5)
C(21A)	146(7)	58(4)	56(4)	-11(3)	-19(4)	27(4)
C(22A)	57(3)	45(3)	45(3)	-2(2)	21(2)	-9(2)
C(23A)	104(5)	63(4)	59(4)	0(3)	37(4)	-29(4)
F(1A)	411(12)	112(4)	267(8)	9(5)	302(9)	-11(6)
F(2A)	183(6)	194(6)	113(4)	90(4)	4(4)	-39(5)
F(3A)	189(6)	148(5)	145(5)	0(4)	56(4)	-116(4)
I(1B)	56(1)	39(1)	39(1)	-4(1)	16(1)	-13(1)
O(1B)	148(4)	91(3)	54(3)	-28(2)	48(3)	-50(3)
O(2B)	114(3)	48(2)	83(3)	-16(2)	59(3)	-30(2)

C(1B)	51(3)	44(3)	47(3)	4(2)	14(2)	-12(2)
C(2B)	41(3)	42(2)	42(3)	4(2)	2(2)	-6(2)
C(3B)	38(2)	49(3)	38(2)	12(2)	6(2)	-1(2)
C(4B)	57(3)	59(3)	50(3)	5(2)	12(2)	-4(2)
C(5B)	62(3)	81(4)	47(3)	10(3)	21(3)	3(3)
C(6B)	50(3)	74(4)	67(4)	24(3)	24(3)	-1(3)
C(7B)	47(3)	53(3)	69(4)	19(3)	18(3)	-3(2)
C(8B)	32(2)	41(2)	51(3)	12(2)	8(2)	-1(2)
C(9B)	39(2)	40(2)	51(3)	9(2)	10(2)	-2(2)
C(10B)	48(3)	56(3)	72(4)	3(3)	13(3)	-8(2)
C(11B)	76(4)	64(4)	71(4)	-7(3)	6(3)	-1(3)
C(12B)	86(5)	68(4)	60(4)	5(3)	22(3)	15(3)
C(13B)	130(7)	134(7)	82(5)	-16(5)	40(5)	23(6)
C(14B)	50(3)	71(4)	73(4)	8(3)	21(3)	6(3)
C(15B)	41(3)	48(3)	63(3)	8(2)	11(2)	-3(2)
C(16B)	58(3)	41(2)	34(2)	-3(2)	11(2)	-4(2)
C(17B)	57(4)	129(6)	66(4)	-43(4)	16(3)	-9(4)
C(18B)	78(5)	161(8)	78(5)	-58(5)	2(4)	-14(5)
C(19B)	99(5)	106(6)	65(4)	-43(4)	15(4)	-7(4)
C(20B)	100(5)	96(5)	74(5)	-31(4)	17(4)	24(4)
C(21B)	69(4)	65(4)	65(4)	-16(3)	5(3)	18(3)
C(22B)	58(3)	45(3)	42(3)	-6(2)	16(2)	-11(2)
C(23B)	126(6)	51(3)	64(4)	-3(3)	52(4)	-10(4)
F(1B)	286(9)	126(5)	163(6)	-13(4)	107(6)	-122(6)
F(2B1)	153(8)	126(7)	75(5)	46(5)	21(4)	-3(6)
F(2B2)	153(8)	126(7)	75(5)	46(5)	21(4)	-3(6)
F(3B1)	126(7)	120(6)	157(9)	47(6)	106(6)	22(6)
F(3B2)	126(7)	120(6)	157(9)	47(6)	106(6)	22(6)

The anisotropic displacement factor exponent takes the form: $-2\pi^2[h^2 a^{*2}U^{11} + \dots + 2 h k a^* b^* U^{12}]$

3.6.8 Fluorovinyl (aryl)iodonium tetrafluoroborate (Z-90)

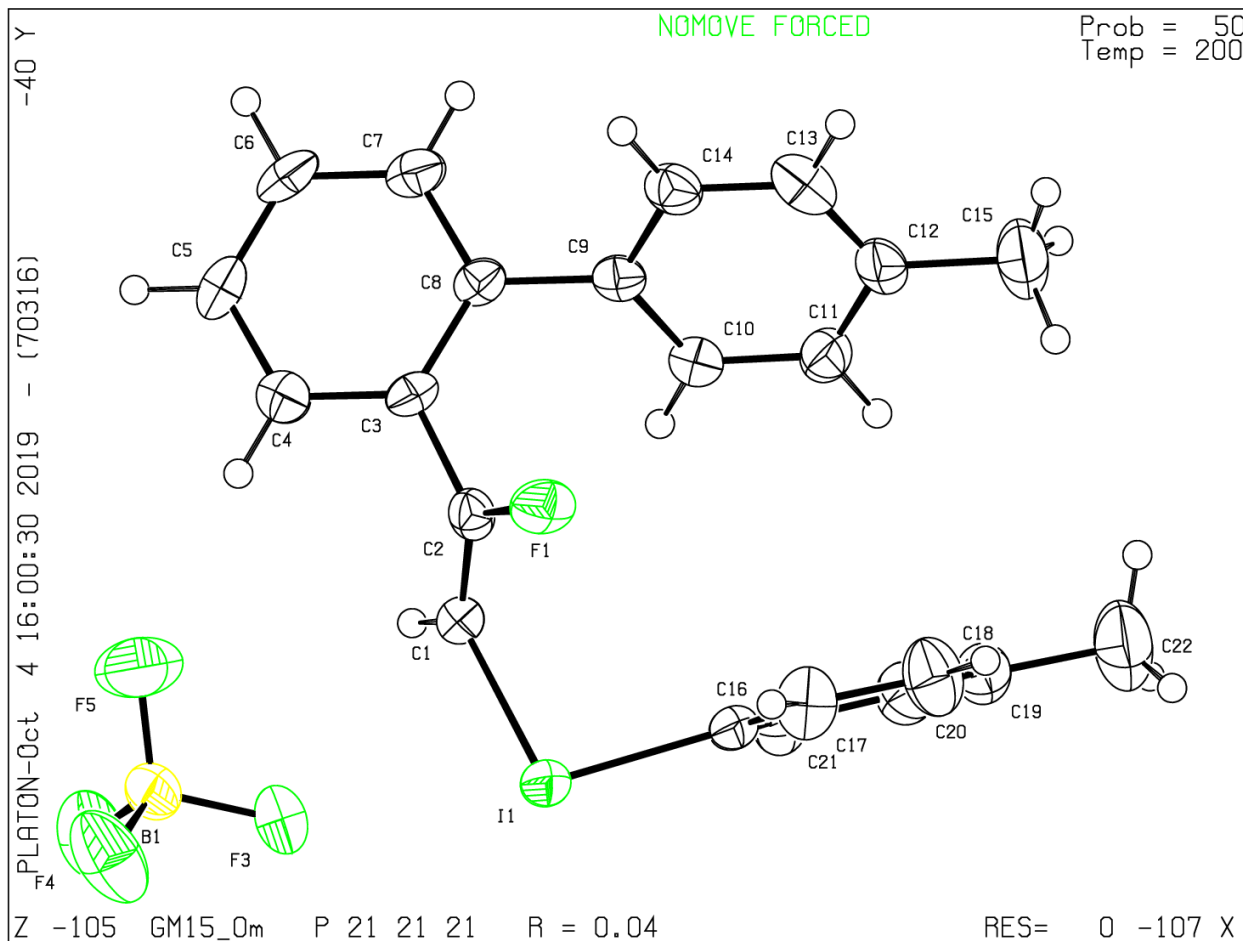


Table 1. Crystal data and structure refinement for [C₂₂H₁₉FI]⁺[BF₄]⁻

Empirical formula	[C ₂₂ H ₁₉ FI] ⁺ [BF ₄] ⁻
Formula weight	516.08
Temperature	200(2) K
Wavelength	0.71073 Å
Crystal system	Orthorhombic
Space group	<i>P</i> 2 ₁ 2 ₁ 2 ₁
Unit cell dimensions	<i>a</i> = 7.3924(10) Å, <i>b</i> = 11.0955(14) Å, <i>c</i> = 25.996(3) Å <i>α</i> = <i>β</i> = <i>γ</i> = 90°.
Volume	2132.3(5) Å ³
<i>Z</i>	4
Density (calculated)	1.608 g/cm ³

Absorption coefficient	1.549 mm ⁻¹
F(000)	1016
Crystal size	0.320 x 0.040 x 0.005 mm ³
Theta range for data collection	2.413 to 27.992°.
Index ranges	-9<=h<=9, -14<=k<=12, -32<=l<=34
Reflections collected	36864
Independent reflections	5146 [R(int) = 0.0814]
Completeness to theta = 25.242°	99.8 %
Absorption correction	Semi-empirical from equivalents
Max. and min. transmission	0.7460 and 0.6231
Refinement method	Full-matrix least-squares on F ²
Data / restraints / parameters	5146 / 0 / 265
Goodness-of-fit on F ²	1.171
Final R indices [I>2sigma(I)]	R1 = 0.0441, wR2 = 0.0683
R indices (all data)	R1 = 0.0655, wR2 = 0.0731
Absolute structure parameter	0.08(3)
Extinction coefficient	n/a
Largest diff. peak and hole	0.943 and -1.974 e.Å ⁻³

Table 2. Atomic coordinates ($\times 10^4$) and equivalent isotropic displacement parameters ($\text{\AA}^2 \times 10^3$) for $[\text{C}_{22}\text{H}_{19}\text{FI}]^+[\text{BF}_4]^-$

	x	y	z	U(eq)
I(1)	-369(1)	3601(1)	5728(1)	36(1)
F(1)	1673(4)	6076(3)	5692(2)	41(1)
C(1)	2208(8)	4085(6)	5487(2)	30(1)
C(2)	2751(8)	5205(6)	5503(2)	30(2)
C(3)	4558(11)	5634(5)	5329(2)	29(1)
C(4)	5122(9)	5276(6)	4840(2)	38(2)
C(5)	6802(9)	5639(7)	4653(3)	41(2)
C(6)	7877(8)	6381(8)	4952(2)	42(2)
C(7)	7315(8)	6743(6)	5439(3)	36(2)
C(8)	5667(6)	6358(6)	5637(2)	28(1)
C(9)	5131(8)	6695(5)	6175(2)	27(1)
C(10)	4614(9)	5803(6)	6520(2)	33(1)
C(11)	4205(8)	6094(7)	7027(2)	39(2)
C(12)	4304(8)	7264(7)	7202(2)	37(2)
C(13)	4787(10)	8156(6)	6852(3)	45(2)
C(14)	5219(9)	7877(6)	6343(2)	36(2)
C(15)	3898(11)	7552(8)	7757(3)	61(2)
C(16)	-16(7)	3970(6)	6519(2)	31(2)
C(17)	-915(9)	4948(7)	6721(3)	45(2)
C(18)	-809(10)	5138(7)	7249(3)	54(2)
C(19)	182(10)	4382(7)	7558(3)	45(2)
C(20)	1132(9)	3448(8)	7339(3)	47(2)
C(21)	1029(9)	3216(7)	6815(3)	44(2)
C(22)	266(15)	4601(8)	8141(3)	76(3)
B(1)	362(13)	3278(7)	4134(3)	41(2)
F(2)	-1166(6)	3534(6)	3848(2)	77(2)
F(3)	-152(8)	3145(4)	4651(2)	72(2)
F(4)	1048(6)	2179(5)	3972(2)	65(1)
F(5)	1596(7)	4158(5)	4094(2)	86(2)
H(1)	3007	3481	5362	36
H(4)	4360	4784	4634	46

H(5)	7205	5381	4324	50
H(6)	9013	6646	4824	51
H(7)	8066	7259	5638	43
H(10)	4541	4989	6409	39
H(11)	3849	5473	7258	47
H(13)	4823	8972	6962	54
H(14)	5572	8498	6112	43
H(15A)	4007	8423	7812	92
H(15B)	4759	7128	7980	92
H(15C)	2665	7293	7840	92
H(17)	-1588	5476	6506	54
H(18)	-1431	5801	7397	65
H(20)	1871	2952	7551	56
H(21)	1661	2557	6666	53
H(22A)	628	3855	8315	113
H(22B)	-928	4851	8265	113
H(22C)	1152	5235	8215	113

$U(\text{eq})$ is defined as one third of the trace of the orthogonalized U_{ij} tensor.

Table 3. Bond lengths [Å] and angles [°] for [C₂₂H₁₉FI]⁺[BF₄]⁻

I(1)-C(1)	2.076(6)
I(1)-C(16)	2.114(6)
F(1)-C(2)	1.346(7)
C(1)-C(2)	1.306(9)
C(1)-H(1)	0.9500
C(2)-C(3)	1.488(10)
C(3)-C(4)	1.397(8)
C(3)-C(8)	1.400(8)
C(4)-C(5)	1.393(9)
C(4)-H(4)	0.9500
C(5)-C(6)	1.383(10)
C(5)-H(5)	0.9500
C(6)-C(7)	1.390(9)
C(6)-H(6)	0.9500
C(7)-C(8)	1.391(8)
C(7)-H(7)	0.9500
C(8)-C(9)	1.501(8)
C(9)-C(14)	1.384(8)
C(9)-C(10)	1.388(8)
C(10)-C(11)	1.391(8)
C(10)-H(10)	0.9500
C(11)-C(12)	1.377(9)
C(11)-H(11)	0.9500
C(12)-C(13)	1.391(9)
C(12)-C(15)	1.509(9)
C(13)-C(14)	1.396(9)
C(13)-H(13)	0.9500
C(14)-H(14)	0.9500
C(15)-H(15A)	0.9800
C(15)-H(15B)	0.9800
C(15)-H(15C)	0.9800
C(16)-C(21)	1.374(9)
C(16)-C(17)	1.376(9)
C(17)-C(18)	1.390(10)

C(17)-H(17)	0.9500
C(18)-C(19)	1.374(10)
C(18)-H(18)	0.9500
C(19)-C(20)	1.375(10)
C(19)-C(22)	1.535(10)
C(20)-C(21)	1.390(9)
C(20)-H(20)	0.9500
C(21)-H(21)	0.9500
C(22)-H(22A)	0.9800
C(22)-H(22B)	0.9800
C(22)-H(22C)	0.9800
B(1)-F(5)	1.341(9)
B(1)-F(2)	1.382(9)
B(1)-F(4)	1.387(9)
B(1)-F(3)	1.404(9)
C(1)-I(1)-C(16)	97.5(2)
C(2)-C(1)-I(1)	121.2(5)
C(2)-C(1)-H(1)	119.4
I(1)-C(1)-H(1)	119.4
C(1)-C(2)-F(1)	120.8(6)
C(1)-C(2)-C(3)	124.8(6)
F(1)-C(2)-C(3)	114.4(5)
C(4)-C(3)-C(8)	120.6(6)
C(4)-C(3)-C(2)	117.0(6)
C(8)-C(3)-C(2)	122.4(5)
C(5)-C(4)-C(3)	120.1(6)
C(5)-C(4)-H(4)	119.9
C(3)-C(4)-H(4)	119.9
C(6)-C(5)-C(4)	119.2(6)
C(6)-C(5)-H(5)	120.4
C(4)-C(5)-H(5)	120.4
C(5)-C(6)-C(7)	120.8(6)
C(5)-C(6)-H(6)	119.6
C(7)-C(6)-H(6)	119.6
C(6)-C(7)-C(8)	120.7(6)

C(6)-C(7)-H(7)	119.7
C(8)-C(7)-H(7)	119.7
C(7)-C(8)-C(3)	118.5(5)
C(7)-C(8)-C(9)	120.1(5)
C(3)-C(8)-C(9)	121.4(5)
C(14)-C(9)-C(10)	119.0(5)
C(14)-C(9)-C(8)	121.1(5)
C(10)-C(9)-C(8)	119.8(5)
C(9)-C(10)-C(11)	120.4(6)
C(9)-C(10)-H(10)	119.8
C(11)-C(10)-H(10)	119.8
C(12)-C(11)-C(10)	121.3(6)
C(12)-C(11)-H(11)	119.3
C(10)-C(11)-H(11)	119.3
C(11)-C(12)-C(13)	117.9(6)
C(11)-C(12)-C(15)	120.3(7)
C(13)-C(12)-C(15)	121.7(7)
C(12)-C(13)-C(14)	121.4(6)
C(12)-C(13)-H(13)	119.3
C(14)-C(13)-H(13)	119.3
C(9)-C(14)-C(13)	119.8(6)
C(9)-C(14)-H(14)	120.1
C(13)-C(14)-H(14)	120.1
C(12)-C(15)-H(15A)	109.5
C(12)-C(15)-H(15B)	109.5
H(15A)-C(15)-H(15B)	109.5
C(12)-C(15)-H(15C)	109.5
H(15A)-C(15)-H(15C)	109.5
H(15B)-C(15)-H(15C)	109.5
C(21)-C(16)-C(17)	122.6(6)
C(21)-C(16)-I(1)	119.7(5)
C(17)-C(16)-I(1)	117.6(5)
C(16)-C(17)-C(18)	117.9(6)
C(16)-C(17)-H(17)	121.1
C(18)-C(17)-H(17)	121.1
C(19)-C(18)-C(17)	121.1(7)

C(19)-C(18)-H(18)	119.5
C(17)-C(18)-H(18)	119.5
C(18)-C(19)-C(20)	119.3(7)
C(18)-C(19)-C(22)	120.2(7)
C(20)-C(19)-C(22)	120.5(7)
C(19)-C(20)-C(21)	121.2(7)
C(19)-C(20)-H(20)	119.4
C(21)-C(20)-H(20)	119.4
C(16)-C(21)-C(20)	117.8(7)
C(16)-C(21)-H(21)	121.1
C(20)-C(21)-H(21)	121.1
C(19)-C(22)-H(22A)	109.5
C(19)-C(22)-H(22B)	109.5
H(22A)-C(22)-H(22B)	109.5
C(19)-C(22)-H(22C)	109.5
H(22A)-C(22)-H(22C)	109.5
H(22B)-C(22)-H(22C)	109.5
F(5)-B(1)-F(2)	111.4(6)
F(5)-B(1)-F(4)	111.6(7)
F(2)-B(1)-F(4)	108.4(6)
F(5)-B(1)-F(3)	109.6(6)
F(2)-B(1)-F(3)	108.4(7)
F(4)-B(1)-F(3)	107.4(6)

Symmetry transformations used to generate equivalent atoms:

Table 4. Anisotropic displacement parameters ($\text{\AA}^2 \times 10^3$) for $[\text{C}_{22}\text{H}_{19}\text{FI}]^+[\text{BF}_4]^-$

	U_{11}	U_{22}	U_{33}	U_{23}	U_{13}	U_{12}
I(1)	32(1)	46(1)	30(1)	0(1)	0(1)	-12(1)
F(1)	26(2)	41(2)	57(2)	-7(2)	6(2)	2(1)
C(1)	30(3)	31(4)	28(3)	-1(3)	3(3)	-4(3)
C(2)	25(3)	38(4)	26(3)	-4(3)	-1(2)	2(3)
C(3)	27(3)	26(3)	34(3)	5(3)	5(3)	-4(3)
C(4)	36(4)	41(4)	37(3)	-5(3)	1(3)	-5(3)
C(5)	42(4)	50(5)	32(4)	7(3)	14(3)	0(4)
C(6)	30(3)	49(4)	47(4)	13(4)	13(3)	-8(4)
C(7)	28(3)	39(5)	40(4)	9(3)	-2(3)	-6(3)
C(8)	20(3)	33(3)	30(3)	7(3)	-2(2)	1(3)
C(9)	18(3)	31(4)	32(3)	2(2)	-6(2)	2(3)
C(10)	32(3)	31(3)	35(3)	-1(3)	-2(3)	-2(3)
C(11)	32(4)	53(5)	31(3)	2(3)	0(3)	-6(3)
C(12)	20(4)	59(5)	33(3)	-10(3)	-5(3)	1(3)
C(13)	45(4)	41(4)	49(4)	-11(3)	-13(3)	2(3)
C(14)	35(4)	37(4)	36(3)	2(3)	-9(3)	-4(3)
C(15)	57(5)	93(7)	33(4)	-13(4)	0(3)	5(5)
C(16)	27(4)	39(4)	29(3)	1(3)	2(2)	-9(3)
C(17)	44(4)	48(5)	43(4)	4(4)	-1(3)	18(3)
C(18)	56(5)	57(5)	48(5)	-13(4)	1(4)	19(4)
C(19)	32(4)	64(5)	38(4)	-5(3)	1(3)	-1(4)
C(20)	43(4)	58(5)	40(4)	5(4)	-5(3)	-1(4)
C(21)	36(4)	57(5)	39(4)	-3(3)	2(3)	8(3)
C(22)	81(7)	104(7)	41(4)	-10(5)	-1(5)	8(7)
B(1)	36(4)	52(6)	35(4)	-2(3)	-7(4)	-4(5)
F(2)	57(3)	102(4)	71(3)	-31(4)	-29(2)	30(3)
F(3)	86(4)	95(4)	36(2)	-18(2)	6(2)	-33(3)
F(4)	65(3)	77(3)	53(3)	-7(3)	-10(2)	26(3)
F(5)	79(4)	99(4)	83(4)	18(3)	-9(3)	-46(3)

The anisotropic displacement factor exponent takes the form: $-2\pi^2[h^2 a^{*2}U_{11} + \dots + 2 h k a^* b^* U_{12}]$